Direct regulation of the interferon signaling pathway by the bromodomain containing protein 4

Dissertation

to obtain the academic degree
Doctor rerum naturalium
(Dr. rer. nat.)

submitted to the Department of Biology, Chemistry and Pharmacy
of Freie Universität Berlin
by
Andrea Wunderlich
from Berlin

Dezember 2012

Die vorliegende Arbeit wurde im Zeitraum von Oktober 2008 bis Dezember 2012 am Max-Planck-Institut für Molekulare Genetik in Berlin unter der Leitung von Herrn Prof. Dr. Hans Lehrach angefertigt.

1. Gutachter **Prof. Dr. Hans Lehrach**
Max-Planck-Institut für Molekulare Genetik
Ihnenstraße 63-73, 14195 Berlin
Tel. +49 30 8413 1220
E-Mail: lehrach@molgen.mpg.de

2. Gutachter **Prof. Dr. Rupert Mutzel**
Institut für Biologie
Freie Universität Berlin
Königin-Luise-Straße 12-16, 14195 Berlin
Tel. +49 30 838 53116
E-Mail: rmutzel@zedat.fu-berlin.de

Tag der Disputation: 13.03.2013

Eigenständigkeitserklärung

Hiermit versichere ich, dass ich die vorliegende Dissertation mit dem Titel "*Direct regulation of the interferon signaling pathway by the bromodomain containing protein 4*" eigenständig verfasst und keine weiteren als die angegebenen Hilfsmittel verwendet habe. In der Arbeit verwendete Aussagen anderer Autoren habe ich durch Quellenangaben kenntlich gemacht. Die vorliegende Arbeit wurde in keinem früheren Promotionsverfahren eingereicht oder als ungenügend beurteilt.

Berlin, den 20. Dezember 2012

(Andrea Wunderlich)

Contents

1 Introduction

1.1 Nuclear factor $\varkappa$B (NF$\varkappa$B), signal transducers and activators of transcription (STATs), inflammation and cancer

In 2011, Douglas Hanahan and Robert Weinberg published a tumor model which explains and summarizes the multi-step process of tumor formation. This process is triggered by genome instability, mutations and tumor-promoting inflammation, supporting the emergence of certain tumor characteristics ("hallmarks"). Tumor cells are capable of sustaining proliferative signaling (enhanced proliferation), resist to cell death (anti-apoptotic and pro-survival) and exhibit the ability of immortal replication. Additionally, they evade growth suppression as well as the destruction by immune cells. Inflammatory signaling, on the other side, enhances tumor formation by providing tumor promoting molecules. Tumor cells also induce the formation of aberrant blood vessels (angiogenesis), providing the tumor with necessary nutritions and subsequently reprogram their energy metabolism. In the end, they evolve the potential of invading the surrounding tissue with further metastasis formation (invasion) [1, 2].

The nuclear factor $\varkappa$B (NF$\varkappa$B) is a transcription factor which is involved in the response to a variety of different stimuli, including stress signals, cytokine signaling and also bacterial and viral antigens. NF$\varkappa$B is held in an inactive state in the cytoplasm by inhibitor proteins. Upon stimulation, these become degraded and the transcription factor translocates to the nucleus and regulates gene expressions. Due to its presence in an inactive condition, which can be mobilized very quickly, the complex presents one of the "rapid-acting" primary transcription factors. It is therefore known as a key player in diverse immune responses per se [3, 4]. NF$\varkappa$B mainly presents a complex of v-rel reticuloendotheliosis viral oncogene homolog A (avian) (RelA) and nuclear factor of kappa light polypeptide gene enhancer in B-cells 1 (NFKB1). Its induction occurs for example by bacterial lipopolysaccharides (LPS) and different cytokines, like tumor necrosis factor alpha (TNFα) and interleukine 1 beta (IL1β) [3] which leads to acute inflammatory responses and enhanced

production of further cytokines, such as TNFα, IL1β, and others. A de-regulation of NFκB is associated with auto-immune diseases and cancer [3, 5, 6]. Aberrant activation is frequently observed in many tumors and results in the upregulation of tumor promoting cytokines, like IL6 and TNFα, and the induction of pro-survival and anti-apoptotic genes that increase the survival of the malignant cells. Thus, the protein complex presents a critical link between inflammation and cancer [6]. The IL6 cytokine, for example, triggers a persistent activation of STAT3, which is a transcription factor acting in response to stimulation and induces the expression of genes involved in tumor proliferation, survival, angiogenesis, and also invasion [7, 8]. As a feedback loop it thus supports the aberrant activation of NFκB in malignant progression [9]. Therefore, NFκB is crucial for the development of a tumor promoting inflammatory environment and its maintenance. In the contrary, it is likewise indispensable for mediating the opposing immune responses and anti-tumor effects [10, 5, 11, 9]. This action is supported by the STAT1 protein, which is also a transcription factor acting in response to certain stimuli. In contrast to STAT3, STAT1 is activated by anti-tumor promoting cytokines, like interferon gamma (IFNγ) and interleukine 12 (IL12). It induces pro-apoptotic, anti-proliferative as well as anti-angiogenic genes [12, 7]. STAT1 therefore antagonizes the effects of STAT3. Figure 1 summarizes the effects mediated by STAT1 and STAT3 in regard to tumor progression.

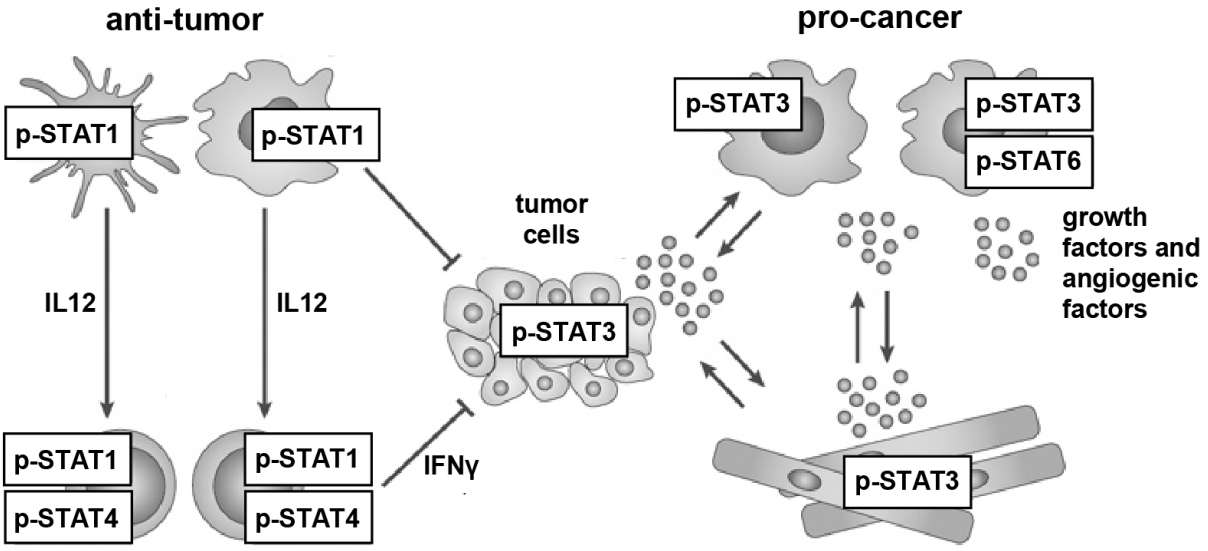

Figure 1: Tumor promoting and preventing inflammatory effects by STAT3 and STAT1. Schematic of anti-tumor and pro-cancer inflammatory effects mediated by phosphorylation activated STAT proteins (p-STAT1 and p-STAT3) through the tumor surrounding immune and tissue cells. STAT1 activation is associated with the expression of anti-tumor cytokines, such as IL12 and IFNγ. The activation of STAT3, on the other hand, leads to pro-tumor signaling and the production of growth factors and angiogenic factors (modified after Yu *et al.* 2009).

The signal transducer and activator of transcription (STAT) protein family consists of seven members (STAT1 to STAT4, STAT5A and B, as well as STAT6), which were originally identified in interferon (IFN) signaling. Interferons are secreted proteins which stimulate intracellular and intercellular networks of immune responses. They are involved in the regulation of innate and acquired immunity, the resistance to viral infections as well as the survival and death of normal and also tumor cells [13]. STAT proteins are the corresponding signaling mediators in the cell and present - like NFκB - rapidly acting primary transcription factors which reside inactive in the cytoplasm. Upon cytokine binding to the associated receptor and subsequent activation of the receptor associated kinases, they become phosphorylated, form homo- or hetero-dimers and translocate to the nucleus for the activation of gene expressions [13]. The STAT1 protein binds directly to the RelA component of the NFκB transcription factor complex and suppresses its activity and thereby decreases anti-apoptotic gene expression [14]. Notably, suppression of NFκB limits also the proliferation of cancer cells. Hence, methods of inhibiting NFκB signaling have potential therapeutic application in cancer as well as inflammatory diseases [15, 16].

In addition to STAT1, the RelA subunit of NFκB has been identified in a direct protein-protein interaction with the bromodomain containing protein 4 (Brd4). This binding results in a modulation of the transcription factor complex and subsequently affects NFκB target gene expressions [17]. The inhibition of Brd4 and its protein family members is accompanied by a general suppression of inflammation [18]. Therefore, these proteins potentially present suitable targets in the matter of NFκB as well as associated immune diseases. Additionally, the cellular protein Brd4 is already widely discussed in the literature as therapeutic target in regard to a variety of human cancers [19, 20, 21, 22, 23, 24].

1.2 Brd4 and the BET family of proteins

The bromodomain containing protein 4 (Brd4) belongs to the BET (bromodomains and extra terminal domain) family of proteins. The family includes members such as mammalian Brd2, Brd3, Brd4 and Brdt, *Drosophila melanogaster*'s Fsh, *Saccharomyces cerevisiae's* Bdf1 and Bdf2 and corresponding homologs in other species. All proteins are found ubiquitously expressed, only Brdt is exclusively present in testis and ovary [25, 26]. Interestingly, the human *Brd* genes are found in close genomic context to the four *Notch* genes. *Brd2* and *Notch4* lie next to each other on chromosome 6, *Brd3* close to

Notch1 on chromosome 9, *Brd4* and *Notch3* together on chromosome 19 and *Brdt* in the neighborhood of *Notch2* on chromosome 1 [27, 28]. This finding suggests a general relationship between the BET and Notch proteins, but a functional connection has not yet been described.

1.2.1 The structures of the BET proteins

All BET family members consist of two tandem bromodomains (BDI and BDII), an extra terminal (ET) domain, a motif B (B) as well as a SEED motif. Also present in most of the BET proteins is a motif A (A), which has not been identified in *S. cerevisiae* [29, 30]. Figure 2 gives an overview of the structures of the known BET proteins and highlights similarities as well as differences between the family members.

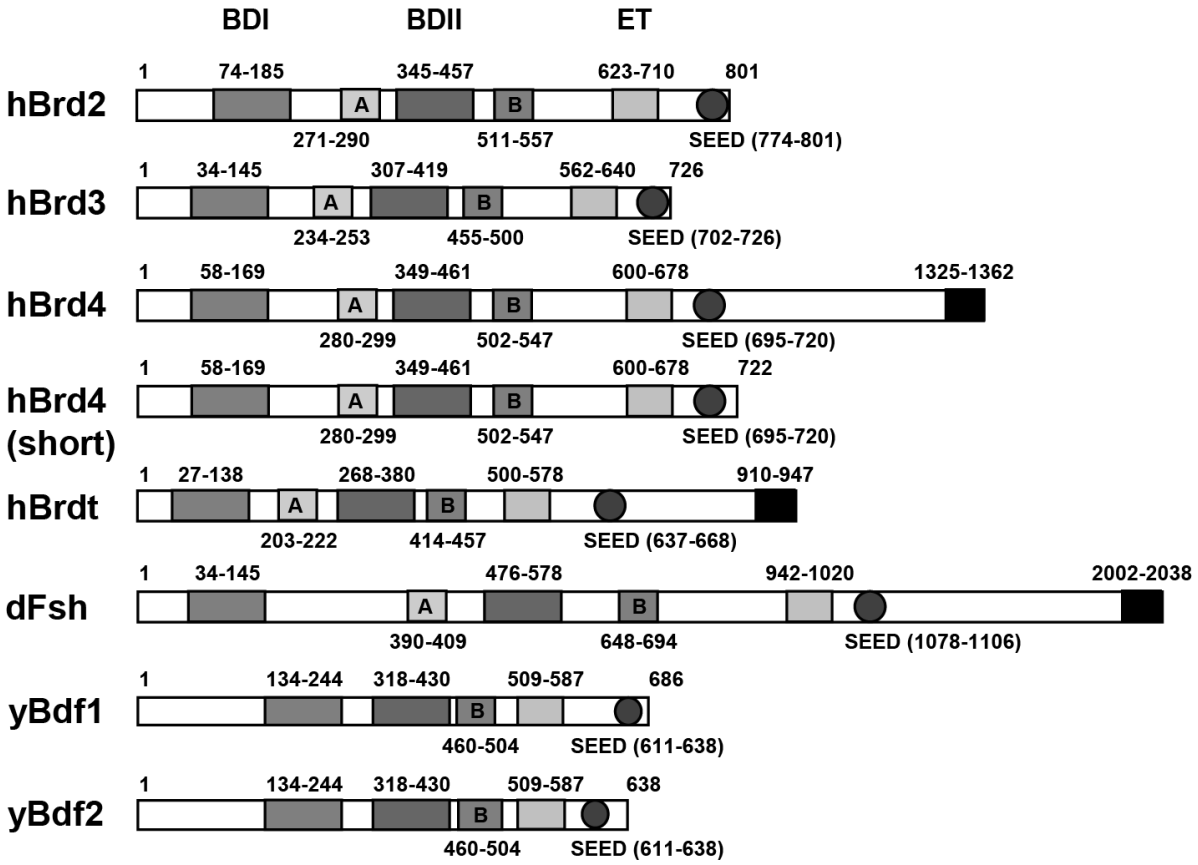

Figure 2: Schematic domain organization of the BET family proteins. Displayed are the known BET protein family members. These include the human proteins hBrd2, hBrd3 as well as hBrd4 and its shorter form hBrd4-short, the fruit fly protein dFsh and also the *S. cerevisiae* proteins yBdf1 and yBdf2. Additionally shown are their domain structures (h = *homo sapiens*, d = *Drosophila melanogaster*, y = *Saccharomyces cerevisiae*) (modified after Wu *et al.* 2007).

The two bromodomains are approximately 110 amino acids long and form four alpha-helices and two loops [31]. They share less sequence homology within one protein (44% identity) than with the corresponding domain in another BET family member (>75% identity) [32]. Bromodomains are known to bind acetyl-lysine residues, especially in histones H3 and H4, but also associate with other non-histone proteins. They help to read and decipher the epigenetic code and regulate important cellular activities such as transcription, DNA replication and cell cycle progression [31]. The extra terminal domain has recently been identified to be involved in protein-protein interactions [33]. Motif A, which is not present in the yeast homologs, and motif B were identified by sequence alignment. Additionally, motif A was recently characterized to contain the nuclear localization signals (NLS) of the BET proteins [34]. The SEED region contains a poly-serine (S) stretch interspersed with glutamic acids (E) and aspartic acid (D) and takes part in the recognition of regulatory elements in the DNA. The distinct carboxy-terminal region, which is only present in three of the displayed seven BET proteins - hBrd4, hBrdt and dFsh - is a platform for specific protein associations [35]. Brd4 and its different interaction partners as well as their functional relationships will be further illuminated in section 1.3.

1.3 The cellular Brd4 protein

Human Brd4 has two distinct isoforms with a predicted molecular mass (MW) of about MW = 80,000 Da for the short variant (often named HUNK1) and MW = 150,000 Da for the long form (also called MCAP) [36]. The structural differences are highlighted in figure 2. The two isoforms vary in their C-terminus, leading to the absence of the carboxy-terminal 640 amino acids in the short variant. Both proteins are localized in the nucleus and ubiquitously expressed.

The bromodomain containing protein 4 is an essential protein. A knockout in mouse embryos leads to their death shortly after implantation [28], embryonic stem cells do not grow in culture without its presence [37] and a severe knockdown of Brd4 is accompanied by a significant reduction in the growth of cultured cells [38]. Interestingly, the inhibition of Brd4 causes a G2/M cell cycle arrest [35] and its overexpression in turn is associated with a G1/S arrest [39]. Taking these results together, they lead to the assumption of Brd4 as a regulator of the cell cycle and cell growth at various stages.

The bromodomains in Brd4 enable the protein to bind to acetylated histones H3 and H4. It specifically shows preferences for acetylated lysine 14 on histone H3 (H3K14) as well as lysines 5 and 12 on histone H4 (H4K5 and H4K12), respectively [37]. In contrast to general transcription factors Brd4 remains associated with chromosomes even throughout mitosis [39] which is even within the group of bromodomain containing proteins an atypical occurrence [40]. Interestingly, Brd4 heterozygous (+/-) cells exhibit less acetylation after anti-microtubule drug-induced mitotic arrest. Specifically lysine residues K14 on histone H3 as well as K5 and K12 on histone H4 are affected, which emphasizes a possible role for the protein in the maintenance of the global acetylation state of the chromatin in the cell [37]. This picture is further supported by its implementation in the maintenance of higher-order chromatin structure. Its depletion is accompanied by a large-scale chromatin unfolding as measured by an *in situ* single cell chromatin imaging and micrococcal nuclease (MNase) assay [41]. Histones, and particularly their tails, are modified at many sites. There are at least eight distinct types of modifications found on histones which includes, amongst others, acetylation, methylation and phosphorylation. The interplay of these modifications influences various fundamental biological processes such as transcription, DNA replication and chromatin condensation [42]. Therefore, Brd4 seems to take part, at least to some extent, in the perpetuation of the epigenetic code of the chromatin and influences the associated cellular functions.

1.3.1 Brd4 and its interaction partners

The Brd4 protein has been implemented in a variety of different networks in the cell by direct protein-protein interactions and assembled complexes. The combinations play a vital role in the regulation of the cell cycle and cell growth as well as DNA replication and transcription. The participation of Brd4 in transcriptional regulation and its consequences will be elucidated in section 1.3.2.

Early work on Brd4 identified the protein in direct protein-protein interactions with the papillomavirus (PV) regulatory protein E2 in tethering the viral genome to host mitotic chromosomes. The association builds the basis of the maintenance process of the viral infection in dividing cells [19]. The described mechanism for the maintenance of viral infections is also copied by the Kaposi's sarcoma associated human herpesvirus type 8 (KSHV) in binding Brd4 to latency associated-nuclear antigen 1 (LANA-1) as well as the Brd4 and Epstein-Barr virus (EBV) nuclear antigen 1 (EBNA1) interaction, which

also contributes to the distribution of the viral genomes to the daughter cells [43, 44, 45] (figure 3). Recently (Nov. 2012), Brd4 has been additionally identified to directly bind to the Merkel cell polyomavirus (MCV) protein large T antigen (LT), which is found in the majority of Merkel cell tumors [41, 46]. Although the publication does not state a mechanism for virus infection maintenance it seems most likely that the bromodomain containing protein 4 plays an essential part in it.

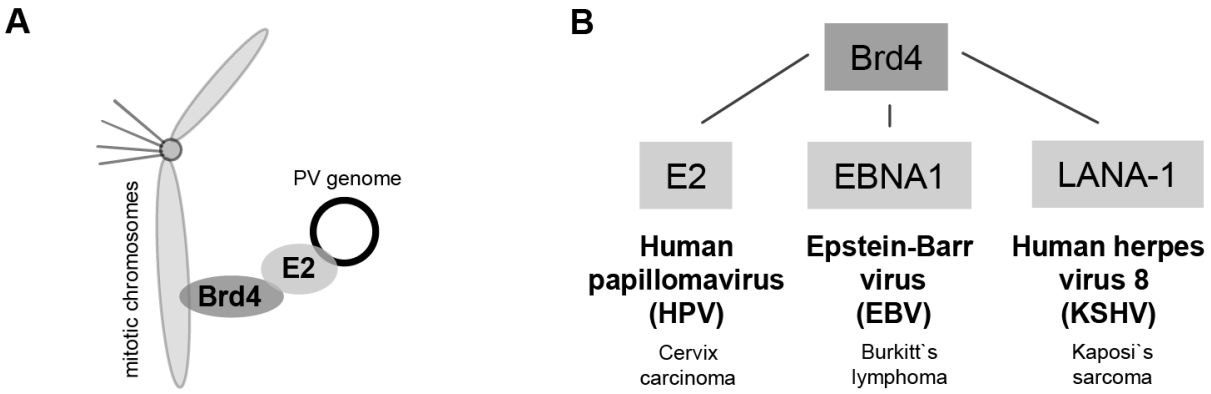

Figure 3: Tethering complexes for viral genome maintenance. (A) Schematics of the Brd4:E2 tethering complex with host mitotic chromosomes and papillomavirus (PV) genome. (B) Known Brd4 interactions with viral proteins which participate in the maintenance of persistent infections as well as their corresponding virus associated cancer.

The described associations, next to sustaining latent virus infections, additionally regulate viral and cellular transcription [47, 43]. The first connection between Brd4 and viral transcription has been identified for the transcriptional function of the papillomavirus E2 protein [47]. Later on, Brd4 and the papillomavirus E2 protein have also been shown to function in a complex repressing virus encoded oncogene *E6* and *E7* (transforming proteins) expression [48].

Besides interactions with proteins from other organisms, Brd4 also directly associates with cellular candidates such as the signal-induced proliferation-associated 1 (SIPA1). SIPA1 is a protein exhibiting a mitogen inducible GTPase activity for Rap1 and Rap2 (members of the oncogenic Ras family of GTPases) which leads to their inactivation [49] and subsequent regulation of their cellular functions, including proliferation and cell adhesion [50]. The identified direct protein-protein interaction via the second bromodomain of Brd4 is associated with the modulation of SIPA1 enzyme activity. An intracellular imbalance between Brd4 and SIPA1 (with SIPA1 overexpressed) is accompanied by an G2/M arrest which can be abolished by an elevation of Brd4 to a comparable level. This implies a necessity of an equal protein level of SIPA1 and Brd4 for normal cell cycle transition and

an impaired Brd4 regulatory function in the presence of a SIPA1 over-representation [51].

In addition to the association with SIPA1, Brd4 also interacts with the replication factor C (RFC) subunit RFC140 through the second bromodomain (BDII). This leads to a binding of Brd4 to the entire replication complex and its subsequent implementation in DNA replication. *In vitro* DNA replication experiments additionally state the dependency of the protein in this process. Its downregulation results in a G1/S cell cycle transition defect potentially caused by a Brd4-mediated repression of RFC function during DNA replication [52].

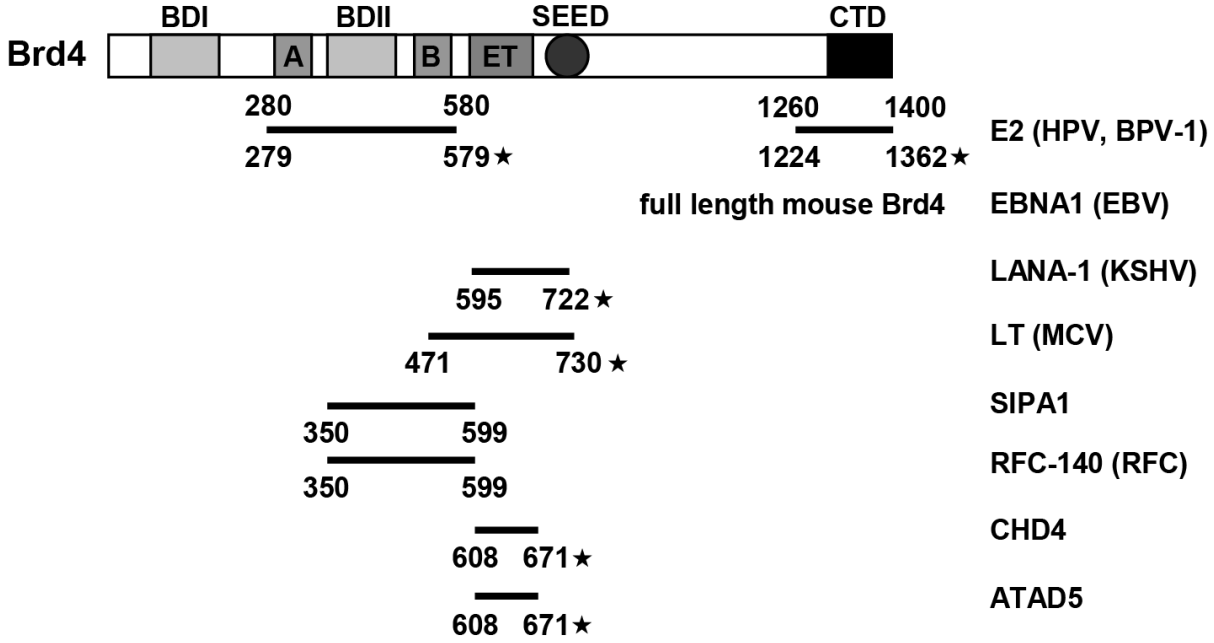

Figure 4: Overview of Brd4 interactions and the involved domains. Shown are the identified protein-protein interactions of the Brd4 protein with the involved domains under specification of the participating amino acids as well as the corresponding interaction partners. The studies performed with human Brd4 are marked with a star and the mouse protein analyses without (modified after Wu *et al.* 2007).

Furthermore, a proteome-wide binding study identified chromodomain helicase DNA binding protein 4 (CHD4) and ATPase family AAA domain containing 5 (ATAD5) to interact with the so far uncharacterized ET domain of Brd4. ATAD5 is discussed to be involved in ATM/ATR-mediated DNA damage response [53]. The identified direct interaction of the two proteins possibly highlights an attending role for Brd4 in the responses to DNA damage [33]. CHD4, on the other hand, is a component of the Mi-2/nucleosome remodeling and deacetylase (NuRD) complex. Its interaction to Brd4 could potentially be seen in

the light of the before described histone acetylation changes after anti-microtubule drug-induced mitotic arrest in Brd4 heterozygous (+/-) cells [37]. This could further support the role for Brd4 in the maintenance of higher-order chromatin structure [41].

Figure 4 summarizes the so far listed direct protein-protein interactions identified for Brd4 and its interaction partners and highlights the involved domains in the bromodomain protein.

1.3.2 The role of Brd4 in transcriptional regulation

Besides its involvement in viral infections, the regulation of gene expression by Brd4 is now well established. Transcription per se represents one of the most complex cellular processes to study. It involves the cooperation of numerous actors and depends on fine tuning mechanisms at various stages as well as specific molecular requirements for changing conditions.

The first study showing an involvement of Brd4 in transcriptional regulation through the binding to a transcription factor was done with the papillomavirus E2 protein [47]. Almost parallel, the group of K. Ozato identified the association of Brd4 with cyclin T1 (CCNT1), cyclin T2 (CCNT2) and cyclin-dependent kinase 9 (Cdk9) - constituting the positive transcription elongation factor b (pTEFb) [54, 55, 56]. The interaction of Brd4 and pTEFb via the bromodomains in Brd4 results in the release of an inhibitory subunit - composed of 7SK small nuclear RNA (7SK snRNA) and hexamethylene bis-acetamide inducible 1 (MAQ1/HEXIM1) - and subsequent activation of pTEFb [54, 57]. The active complex exhibits kinase activity and phosphorylates the C-terminal domain of the largest subunit of RNA polymerase II (RNA pol II). This action releases negative elongation factors and promotes the transfer of transcription from initiation to elongation [56, 58]. In 2012, the picture of transcriptional regulation is further extended by the identification of an atypical kinase activity of Brd4 which directly phosphorylates the RNA polymerase II at the C-terminal domain [59]. This finding greatly circumstantiates that RNA polymerase II-mediated transcription elongation is directly controlled by Brd4 next to its known function in activating and recruiting pTEFb. Several gene expressions dependent on Brd4 are described in the literature. You *et al.* pointed out a positive stimulation of the expression of Aurora kinase B (*AURKB*). A knockdown of Brd4 is accompanied by a decrease in *AURKB* expression which leads to segregation defects of chromosomes in mitosis [60]. Additionally, Brd4 activates the expression of certain

cell cycle G1 related genes, such as cyclins D1 and D2 (*CCND1*, *CCND2*), as well as origin recognition complex subunit 2 (*Orc2*) and minichromosome maintenance complex component 2 (*Mcm2*), which are necessary for proper cell cycle progression in late mitosis [61, 52, 62].

The positive transcription elongation factor b can also be recruited to promoters by other transcription factors and regulators than Brd4. This includes well known tumor associated proteins like NFκB, v-myc myelocytomatosis viral oncogene homolog (avian) (Myc) and retinoblastoma protein 1 (pRB) [63, 64, 65]. Through the activation of pTEFb, Brd4 is implemented in Myc transcriptional regulation. The oncogene itself has been identified as a Brd4 downstream target [54, 61, 22, 24, 66]. A schematic drawing of the pTEFb activation by Brd4 and the subsequent regulation of transcriptional elongation is presented in figure 5.

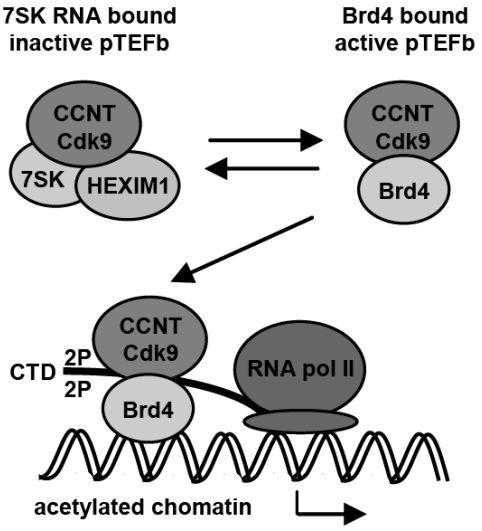

Figure 5: Schematic of the Brd4 and pTEFb interaction in promoting transcriptional elongation. The interaction between Brd4 and pTEFb leads to the release of an pTEFb inhibitor subunit and subsequent activation. This results in the phosphorylation of the C-terminus of RNA polymerase II and transcriptional elongation (modified after Jang *et al.* 2005).

Besides the regulation of Myc, Brd4 is also involved in the regulation of NFκB. NFκB mainly presents a complex of v-rel reticuloendotheliosis viral oncogene homolog A (avian) (RelA) and nuclear factor of kappa light polypeptide gene enhancer in B-cells 1 (NFKB1). It is not only associated with pTEFb, but also directly interacts with Brd4 via acetylated RelA [17]. The transcriptional activator NFκB is the mediating complex in a variety of stimuli, amongst others, the regulation of inflammatory responses (figure 1). Huang *et al.* showed that Brd4 positively stimulates the activity of NFκB. This results in the activation of inflammatory response genes after tumor necrosis factor alpha (TNFα) treatment. These responses are suppressed in a Brd4 knockdown which directly connects Brd4 to the regulation of the inflammation process [17]. In 2010, Nocodeme *et al.* generated a specific

inhibitor molecule, "I-BET", against the double bromodomains within the BET protein family members. Their results support the finding of Brd4's involvement in the tumor necrosis factor alpha response. The inhibition of BET binding to acetylated proteins is accompanied by a global suppression of primary response gene expressions after TNFα stimulation [18]. This is also seen for the direct downregulation of Brd4. Interestingly, the expression of *TNFα* itself, which leads to an enhanced response after stimulation through a positive feedback loop, is not abolished after "I-BET"-inhibition, but inhibited after Brd4 knockdown. This result implicates yet another role for Brd4 in the regulation of transcription through a bromodomain independent mechanism [18]. In general, inducible transcriptional programs consist of primary and secondary response genes (PRGs and SRGs). Recently, it has been shown that PRGs contain pre-assembled RNA polymerase II [67, 68]. Stimulation leads to positive histone modifications, including acetylations of H4K5, H4K8 and H4K12. Interestingly, these are the preferred Brd4 binding sites. Thus, stimulation is accompanied by rapid Brd4 and pTEFb recruitment and subsequent activation of transcriptional elongation of the primary response genes [67]. Therefore, Brd4 seems to play an important role in the course of inducible programs per se which most likely combines its transcriptional regulation function via acetylated histone binding but potentially also by independent mechanisms [67, 18].

Having illuminated the role for Brd4 in direct and indirect regulation of RNA polymerase II phosphorylation and subsequent transcriptional elongation, an additional role for Brd4 in the transcriptional process will be described. Next to the identification of protein-protein interactions with ATAD5 and CHD4 in 2011, the group of P. Howley showed a binding of Brd4 to the Wolf-Hirschhorn syndrome candidate 1-like 1 (NSD3), the jumonji domain containing 6 (JMJD6) as well as the glioma tumor suppressor candidate region gene 1 (GLTSCR1) [33]. NSD3 - also known as WHSC1L1 - is a histone methyltransferase which leads to epigenetic marks associated with transcriptional regulation [69]. JMJD6 exhibits histone demethylase activity [70]. Additionally, it was reported to be important for lysyl hydroxylation of the RNA splicing associated factor U2AF65 [71] and suggested to bind single-stranded RNA itself [72]. The function of GLTSCR1 is presently unknown. NSD3, GLTSCR1 as well as JMJD6 impairment by siRNA showed strong effects in regard to Brd4-mediated activation of specific target genes (*CCND1*, *PIM2* and *DCPS*) [33]. Interestingly, Brd4 and NSD3 were, in addition to their binding to promoter regions, also found at coding sequences within the target gene body of *PIM2* [33]. This demonstrates Brd4 and NSD3 involvement in transcription even throughout elongation. The novel protein-protein interactions reveal a mechanism of transcriptional activation of

Brd4 probably due to selective chromatin modifications. Additionally, the protein-protein interaction to JMJD6 potentially connects Brd4 with the splicing process [33]. Figure 6 summarizes the interactions of Brd4 which are implicated in transcriptional regulation and highlights the involved protein domains.

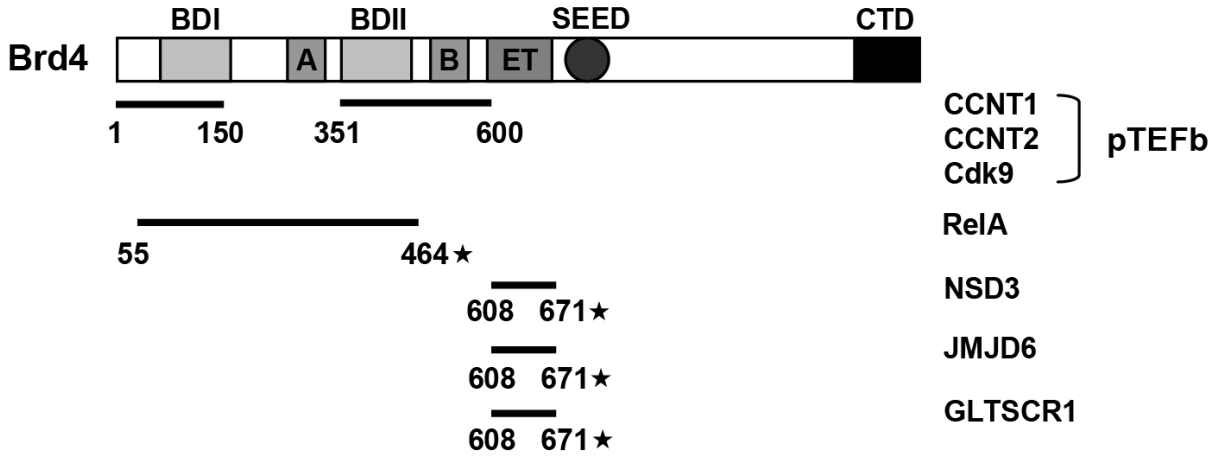

Figure 6: Overview of Brd4 interactions in transcriptional regulation. Shown are the identified protein-protein interactions with association to transcriptional regulation of the Brd4 protein. Additionally highlighted are the involved domains under specification of the participating amino acids as well as the corresponding interaction partners. The studies performed with human Brd4 are marked with a star and the mouse protein analyses without (modified after Wu *et al.* 2007).

1.4 Association of Brd4 with cancer

The bromodomain containing protein 4 is linked to human cancer 1) over its interaction partners, 2) identified genomic rearrangements, 3) its expression level, and 4) its regulatory functions in transcription.

1) Its binding to the papillomavirus E2 protein [19, 47] (section 1.3.1) implements the protein in cervical and anal cancer emerging from persistent virus infections. These cancers are associated with human papillomaviruses (HPV) which are present in over 90% of the cases [73]. A similar picture arises in regard to Kaposi's sarcomas (based on KSHV infection) and Epstein-Barr-virus-associated cancers like the Burkitt's lymphomas, where Brd4 is involved in the maintenance of viral infections via its interactions with virus encoded proteins [43, 44]. Recently, Brd4 has been additionally identified to directly bind to the Merkel cell polyomavirus (MCV) protein large T antigen (LT) which is found in 80% of all Merkel cell tumors, a rare and highly aggressive type of tumor [46, 41]. Thus,

Brd4 is well established in the connection of tumor viruses to their related cancers and presents a potent target for therapy by inhibition of the virus-host interactions.

2) A genomic rearrangement involving *Brd4* has been identified in a rare and lethal carcinoma arising in midline organs of young people. The characterized translocation appears between the *Brd4* and nuclear protein in testis (*Nut*) genes. It results in a fusion product of Brd4-Nut with a truncation of Brd4 after the extra terminal (ET) domain which is followed by almost the entire Nut sequence. A similar translocation has been seen in the same tumor entity for *Nut* and *Brd3*, which presents another member of the BET family of proteins [74]. The fusions impair normal Brd4 and Brd3 functions and lead to the expression of the testis protein apart from its origin tissue, thus subsequently resulting in *Nut* oncogene activation [75, 76, 74, 77]. Figure 7 shows the schematic of *Brd4*, *Brd3* and *Nut* as well as the Brd-Nut fusion proteins.

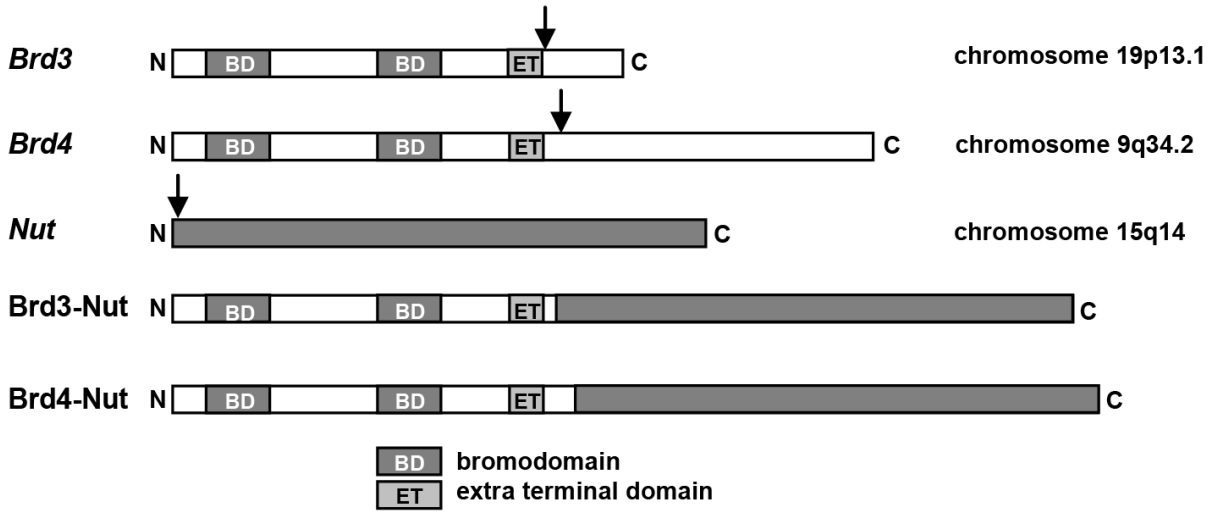

Figure 7: Schematic of *Brd4*, *Brd3*, *Nut*, and the Brd-Nut fusion proteins. The translocation between *Brd3* and *Brd4* as well as the *Nut* oncogene results in fusion proteins which compose of the Brd3 or Brd4 sequence up to the extra terminal domain (ET) followed by almost the entire sequence of Nut. The arrows indicate the breakpoints of each gene and BD the bromodomains of Brd3 and Brd4 (modified after French *et al.* 2011).

3) Next to its connection to viral infection mediated malignancies and chromosomal rearrangements, the expression of *Brd4* itself is found altered in specific tumors such as colon cancer and breast cancer. In 2012, Rodriguez *et al.* described a frequent downregulation of Brd4 in colon tumors [78]. This positively correlated with *Brd4* promoter hypermethylation and/or the enrichment in histone H3K9me3 methylation at the promoter, which presents a repressive mark [42]. In addition, a re-introduction of the bromodomain pro-

tein resulted *in vitro* and *in vivo* in a marked reduction of tumor growth, implying a potential tumor suppressor activity for Brd4 [78]. In breast tumors, the re-expression of Brd4's complete long isoform led to growth reduction and diminished metastatic potential. Higher Brd4-long levels additionally correlated with a better prognosis, indicating a prognostic potential for the long isoform of Brd4 [20]. However, for the prognostic value of Brd4 contradictory results exist. In the same tumor type the overexpression of Brd4-short, on the other hand, resulted in an increased metastasis forming capacity of the cells and correlation analysis showed a correlation with poor prognosis [21].

4) Although not found altered in expression, Brd4 has been identified as a therapeutic target in acute myeloid leukemia (AML) [22]. The group around C. R. Vakoc took advantage of another available cell-permeable small molecule inhibitor of the BET family of proteins, called "JQ1" (similar to "I-BET" [18]). It inhibits the binding of Brd4 to acetylated histones and subsequently their activating function in transcriptional elongation [79, 22]. Zuber *et al.* compared the effects resulting from the "JQ1"-block to an siRNA approach against Brd4 in mice. The downregulation of Brd4 as well as its inhibition was associated with delayed leukemia progression, survival benefits, loss of stem cell characteristics with self-renewal ability, and the reduction of Myc oncogene expression [22]. The same effect on Myc and its target genes was validated by C. J. Ott and colleagues, who used the BET inhibitor "JQ1" in B-cell acute lymphoblastic leukemia (B-ALL) cell lines and showed a potent reduction of cell viability [66]. The general mechanism for "JQ1" inhibition of BET proteins, including Brd4, is shown in figure 8.

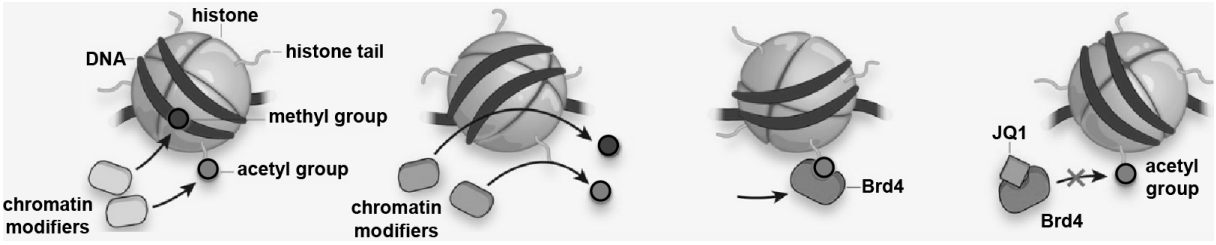

Figure 8: Mechanism of the BET protein inhibition by "JQ1". Histone tails can posttranscriptionally be modified by methyl and acetyl groups. Acetyl groups can be recognized by the bromodomains in the BET family of proteins. The inhibitor "JQ1" was specifically designed to prevent the binding of the BET proteins, and also Brd4, to the acetylated histone tails (modified after A. Maxmen 2012).

The positive effect of growth reduction of tumor cells by a Brd4 knockdown was further supported by the results from Toyoshima *et al.* and Kessler *et al.* in relation to Myc-driven cancers. Each group used an siRNA-based negative selection approach for the identification of essential tumor growth regulated genes. Both of them identified *Brd4* in common [24, 23].

Taken together, Brd4 seems to be a potential universal target for therapy in numerous human cancers and other diseases. However, for a detailed understanding of Brd4's function in transcription, a transcriptome-wide expression profile after its knockdown as well as the identification of its genome-wide binding sites are necessary. These analyses are still due.

The Next Generation Sequencing (NGS) technology by Illumina represents the starting point of this thesis, investigating the gene expression profile after Brd4 knockdown using mRNA sequencing (mRNA Seq). Chromatin immunoprecipitation followed by sequencing (ChIP Seq) finally complements the genomic profile of Brd4.

2 Research outline

The cellular bromodomain containing protein 4 (Brd4) is a transcriptional regulator. It interacts with transcription factors, transcriptional elongation complexes and acetylated histones and thus directly facilitates transcription, but also chromatin modifications. Brd4 plays a role in cellular responses to inflammatory signals and is essential for tumor growth maintenance. Although quite well established in transcriptional regulation events, transcriptome-wide analyses and genome-wide binding assays are still missing. To enlarge the picture of transcriptional dependencies on the Brd4 protein, I used mRNA sequencing experiments after Brd4 knockdown, validated the findings and investigated their functional relevance in cell culture experiments. Furthermore, I used Brd4 specific chromatin immunoprecipitations and sequencings to screen for direct associated target genes. The goal of this work was to broaden the knowledge of Brd4 and to try to understand the function of Brd4 as a master regulator of cancer development. Understanding the networks around Brd4 and the cellular functions depending on it may expand the comprehension of diseases and here tumors in particular with de-regulated Brd4-levels. This may potentially pave the way for novel therapeutic strategies and applications for Brd4 inhibitors.

3 Materials and Methods

3.1 Materials

3.1.1 Equipments and materials

Table 1: Equipment and materials. Collection of utilized equipments and materials with corresponding purchasing companies.

name	company
agarose gel system and combs	in house preparation
Bioruptor sonication system	Diagenode
bunsen burner	Bochem
canonical tubes (15ml, 50ml)	Greiner
cell scraper	TPP
centrifuge Avanti J-25 (canonical tubes)	Beckman Coulter
centrifuge 5810R (falcons)	Eppendorf
centrifuge 5425 (1.5ml reaction tubes)	Eppendorf
centrifuge 5417C (1.5ml reaction tubes)	Eppendorf
centrifuge PC-100 (strips)	FugeOne
clean-bench HeraSafe HSP12	Heraeus Instruments
clear optical reaction plate (384-well) ABI PRISM	Applied Biosystems
cryo container Mr. Frosty	NALGENE
cryo vial cryo.s	Greiner Bio-One
cuvettes Plastibrand - 759015	BRAND
dishes/plates/flasks (cell culture)	TPP
Fast Real-Time PCR system 7900HT	Applied Biosystems
freezer economic-****	Bosch
freezer -86C Freezer	Forma Scientific
gel documentation chamber AlphaImager	Alpha Innotech
head-over-heel-rotator Type REAX2	Heidolph
incubator Cytoperm2 (cell culture)	Heraeus Instruments
incubator Innova44 (shaking) (bacteria)	New Brunswick Scientific
incubator Kelvitron t (bacteria)	Heraeus Instruments
luciferase assay maschine Glomax Multi	Promega
light microscope DMIL HC	Leica
liquid nitrogen tank	Taylor-Wharton
magnetic particle concentrator Dynal MPC-S	Invitrogen
magnetic stirring/heating plate RH basic 2 IKAMAG	IKA

name	company
multi-pipet Research Pro	Eppendorf
optical 96-well reaction plate MicroAmp	Applied Biosystems
optical adhesive films MicroAmp	Applied Biosystems
Parafilm "M"	Pechiney Plastic Packaging
pasteur pipettes	BRAND
PCR SoftStrips (0.2ml)	Eppendorf
petri dishes	Greiner Bio-One
photographic film Super RX	Fujifilm Corporation
photographic film developer Curix 60	Agfa
photographic film developing case Hypercassette	Fujifilm Corporation
pipet tips TipOne RPT (10µl, 200µl, 1250µl)	STARLAB
pipet filter tips TipOne RPT (10µl, 20µl, 200µl, 1250µl)	STARLAB
pipetboy Pipetboy acu	IBS Integra biosciences
pipettes (sterile)	Sarstedt
power supply PowerPac 200	Bio-Rad
power supply PowerPac Basic	Bio-Rad
Qubit assay tubes	Invitrogen
Qubit fluorometer	Invitrogen
reaction tubes (0.5ml, 1.5ml, 2ml)	Eppendorf
refrigerator economic	Bosch
rocking shaker PMR-30	Grant-Bio
scale EMB 200-2	KERN
scanner Expression 1640 XL	Epson
spectrophotometer ND-1000	Nanodrop
spectrophotometer Ultrospec 3100 pro	Amersham Biosciences
surgical disposable scalpels	BRAUN
Mini-PROTEAN Tetra Electrophoresis System	Bio-Rad
thermal cycler PTC-100	MJ Research, Inc.
thermomixer compact 5350	Eppendorf
transfer membrane (PVDF) Immobilion-P	Millipore
transilluminator UVT-28M	Herolab
vortexer Vortex-Genie2	Scientific Industries
water bath WNB 7	Memmert
Whatman filter paper (3mm)	Whatman
white 96-well plate with clear flat bottom 3610	Costar

3.1.2 Chemicals and reagents

Table 2: Chemicals and reagents. Collection of utilized chemicals and reagents with corresponding order numbers and purchasing companies.

name	company (order number)
acrylamide/bis-acrylamide solution (30%)	Bio-Rad (#161-0154)
agarose standard	Roth (#3810.2)
ammonium persulfate (APS)	Merck (#2300-25GM)
ampicillin	AppliChem (#A0839,0010)
Agencourt AMPure XP 60ml kit	Beckman Coulter Genomics (#A63881)
bidest water	in house preparation
bovine serum albumin (BSA)	AppliChem (#A6588,0025)
Bradford reagent	Sigma (#B6916-500ML)
bromphenol blue	Sigma (#B-6131)
ChIP-Seq DNA Sample Prep Kit	Illumina (#IP-102-1001)
chloroform	Merck (#1.02445.1000)
deoxyribonuclease (DNase I)	Sigma (#D4527)
dimethyl sulfoxide (DMSO)	Sigma (#D8418-100ML)
disodium hydrogen phosphate (Na_2HPO_4)	Merck (#1.06585.5000)
dithiothreitol (DTT)	AppliChem (#A2948,0010)
dNTP set	Bioline (#BIO-39025)
Dual-Luciferase Reporter Assay System	Promega (#E1910)
Dulbecco's Modified Eagle's Medium (DMEM)	Biochrom (#F0415)
Dulbecco's phosphat buffered saline (DPBS)	Sigma (#D8537)
Dynalbeads-Protein G-Beads (magnetic)	Invitrogen (#100.03D)
ECL solutions	PerkinElmer (#NEL100)
EndoFree Plasmid Maxi Kit	QIAGEN (#12362)
ethanol	Merck (#1.00983.2500)
ethidium bromid solution	Roth (#2218.1)
ethylene diamine tetraacetic acid (EDTA)	Roth (#X986.1)
ethylene glycol tetraacetic acid (EGTA)	Sigma (#E-0396)
fetal bovine serum (FBS)	Biochrom (#S0113)
formaldehyde solution (37%)	Sigma (#F1635-500ML)
FuGENE6	Roche (#11-815-091-001)
GeneRuler 1 kb DNA ladder	Fermentas (#SMO319)
GeneRuler 100 bp DNA ladder	Fermentas (#SMO249)
GoTaq qPCR Master Mix	Promega (#A600A)
glycerol	Merck (#1.04093.1000)
glycine	Merck (#1.04201.1000)
heavy phase lock gel tubes	5PRIME (#2302830)
HEPES, free acid ULTROL	Calbiochem (#391338)
IFN-γ (human)	PeproTech, Inc. (#300-02)
isopropanol	Merck (#1.09634.2511)

name	company (order number)
LB agar medium	MP Biomedicals, LLC (#3002-232)
L-Broth	MP Biomedicals, LLC (#3001-032)
L-glutamine solution	Biochrom (#K0283)
LigaFast rapid DNA ligation system	Promega (#M8221)
linear polyacrylamide (LPA)	Sigma (#5-6575)
lithium acetate (LiAc)	Sigma-Aldrich (#517992)
lithium chloride (LiCl)	Merck (#1.05679.0250)
magnesium chloride ($MgCl_2$)	Merck (#1.05833.1000)
magnesium sulfate ($MgSO_4$)	Merck (#5886.5000)
MEM Earle's	Biochrom (#F0325)
methanol	Merck (#1.06009.2500)
MinElute Gel Extraction Kit	QIAGEN (#28604)
MinElute PCR Purification Kit	QIAGEN (#28004)
N-lauroylsarcosine	Sigma (#L-9150-250G)
Nonidet P40 (NP-40)	AppliChem (#A1694,0250)
nuclease free water	Promega (#P119E)
Page Ruler Plus Pre-stained Protein ladder	Fermentas (#26619)
penicillin/streptomycin solution	Biochrom (#A2213)
Phusion DNA polymerase kit	Biozym (#F-530L)
potassium clorid (KCl)	Merck (#1.04936.1000)
polysorbate 20 (Tween 20)	Sigma (#P9416-100ML)
Protease Inhibitor Cocktail (PIC) tablet	Roche (#11-836-170-001)
Proteinase K	Roche (#03-115-836-001)
QIAprep Spin Miniprep Kit (250)	QIAgen (#27106)
Quant-iT dsDNA HS Assay Kit	Invitrogen (#Q32851)
ribonuclease A (RNase A)	QIAgen (#1007885)
ribonuclease H (RNase H)	Promega (#M428A)
ribonuclease inhibitor (RNasin)	Promega (#N2511)
RNase-free DNase kit	QIAgen (#79254)
restriction enzyme HindIII (10U/µl)	Promega (#R6041)
restriction enzyme BglII (10U/µl)	Promega (#R6081)
SuperScript II Kit	Invitrogen (#18080-093)
sodium chloride (NaCl)	AppliChem (#A1149,5000)
sodium dihydrogen phosphate (NaH_2PO_4*H_2O)	Merck (#1.06346.1000)
sodium dodecyl sulfate (SDS)	Roth (#4360.1)

name	company (order number)
sodium deoxycholate	Merck (#1.06504.0100)
Taq DNA polymerase (1 U/µl)	in house preparation
Taq DNA polymerase buffer (10x)	in house preparation
tetramethylethylenediamine (TEMED)	Invitrogen (#15524-010)
tris(hydroxymethyl)aminomethan	Merck (#1.08382.0500)
trisodium citrat dihydrat	Merck (#1.06448.1000)
Triton X100	Sigma (#T8787-50ML)
TRIzol reagent	Invitrogen (#15596-018)
TrueSeq RNA Sample Preparation Kit	Illumina (#RS-122-2001)
TrypZean solution	Sigma (#T3449)
X-tremeGENE9	Roche (#06365779001)

3.1.3 Buffers and solutions

Blocking solution with milk powder: 5% fatless milk powder (w/v) in TBST

Blocking solution with BSA: 3% BSA (w/v) in TBST

BSA control solution: 0.1% BSA (w/v) in nuclease free water

ChIP lysis buffer 1: 50mM HEPES-KOH, pH 7.6, 140mM NaCl, 1mM EDTA, 10% (v/v) glycerol, 0.5% (v/v) NP-40, 0.25% (v/v) Triton X100, PIC tablet

ChIP lysis buffer 2: 10mM Tris-HCl, pH 8.0, 200mM NaCl, 1mM EDTA, 0.5mM EGTA, PIC tablet

ChIP lysis buffer 3: 10mM Tris-HCl, pH 7.4, 100mM NaCl, 1mM EDTA, 0.5mM EGTA, 0.1% (v/v) sodium deoxycholate, 0.5% (v/v) N-lauroylsarcosine, PIC tablet

ChIP blocking solution: 1x PBS, 0.5% (w/v) BSA

ChIP wash buffer: 50mM HEPES-KOH, pH 7.6, 500mM LiCl, 1mM EDTA, 1% (v/v) NP-40, 0.7% (v/v) sodium deoxycholate

ChIP elution buffer: 50mM Tris-HCl, pH 8.0, 10mM EDTA, 1% (w/v) SDS

Formaldehyde solution: 50mM HEPES-KOH, pH 7.6, 100mM NaCl, 1mM EDTA, 0.5mM EGTA, 11% formaldehyde

Lysis buffer A: 10mM HEPES, pH 7.4, 10mM NaCl, 3mM $MgCl_2$, 1mM DTT, PIC tablet

Lysis buffer B: 10mM HEPES, pH 7.4, 10mM NaCl, 3mM $MgCl_2$, 0.2U DNase I, 1mM DTT, PIC tablet

NaCl in TE: 500mM NaCl in 1x TE

10x PBS, pH 7.4: 1.37M NaCl, 27mM KCl, 80mM Na_2HPO_4, 18mM KH_2PO

Running gel buffer, pH 8.8: 10% acrylamide/bis-acrylamide solution, 375mM Tris-HCl (pH 8,8), 0.1% APS, 0.01% TEMED

6x SDS loading buffer: 300mM Tris-HCl (pH 6.8), 12% (w/v) SDS, 0.6% (w/v) bromphenol blue, 60% (v/v) glycerol

10x SDS running buffer: 250mM Tris, 2.5M glycine, 1% SDS

Stacking gel buffer, pH 6.8: 5% acrylamide/bis-acrylamide solution, 125mM Tris-HCl (pH 6,8), 0.1% APS, 0.01% TEMED

50x TAE buffer, pH 8.0: 50mM Tris, 25mM glacial acetic acid, 2.5mM EDTA

10x TE, pH 7.5: 10mM Tris-HCl, 1mM EDTA

Transfer buffer: 25mM Tris, 192mM glycine

Tris buffered saline (TBS): 20mM Tris-HCl (pH 7.4), 500mM NaCl

Tris buffered saline with Tween20 (TBST): 20mM Tris-HCl (pH 7.4), 500mM NaCl, 0.05% (v/v) Tween 20

3.1.4 Media

3.1.4.1 Bacteria media

The bacteria strains used in this thesis were cultured and grown in the following media.

LB (Luria Bertani) liquid medium, pH 7.0: 0.5% NaCl, 1% Bacto-Pepton, 0.5% Yeast extract

LB (Luria Bertani) solid medium, pH 7.0: 0.5% NaCl, 1% Bacto-Pepton, 0.5% Yeast extract, 1.7% Bacto-Agar

3.1.4.2 Cell culture media

The utilized human cell lines were cultured and stored in the following media.

DMEM **Dulbecco's Modified Eagle's Medium (regular glucose = 1g/l D-glucose):** 10% (v/v) FBS, 1% (v/v) L-glutamine, 1% (v/v) Pen/Strep

DMEM **Dulbecco's Modified Eagle's Medium (high glucose = 4g/l D-glucose):** 10% (v/v) FBS, 1% (v/v) L-glutamine, 1% (v/v) Pen/Strep

MEM **Earle's (regular glucose = 1g/l D-glucose):** 10% (v/v) FBS, 1% (v/v) L-glutamine, 1% (v/v) Pen/Strep

freezing **DMEM and MEM medium:** 20% (v/v) FBS, 1% (v/v) L-glutamine, 1% (v/v) Pen/Strep, 20% (v/v) DMSO

3.1.5 Bacteria strains

Different *E.coli* strains with specific characteristics were used for cloning experiments, plasmid amplification and the generation of unmethylated plasmid DNA for Dual-Luciferase Reporter Assay System ("Promega").

Table 3: Bacteria strains. Used *E.coli* strains with their corresponding genotype and experimental application.

name	genotype	application
DH5α	F- dlacZ DeltaM15 Delta(lacZYA-argF) U169 recA1 endA1 hsdR17(rK-mK+) supE44 thi-1gyrA96 relA1	cloning/plasmid amplification
GM2929	F- dam-13::Tn 9 dcm-6 hsdR2 recF143 mcrA0 mcrB9999 galK2 galT22 ara-14 lacY1 xyl-5 thi-1 tonA31 rpsL136 hisG4 tsx-78 mtl-1 supE44 leuB6 rfbD fhuA13	generating unmethylated plasmids

3.1.6 Human cell lines

The experiments in this thesis were performed with the specified human cell lines.

Table 4: Human cell culture cell lines. Utilized human cell lines with background information on the tissue origin and corresponding ATCC identification number [80].

cell line	organ and site of extraction	ATCC number
Wi38	normal lung cells	CCL-75
Hek293T	normal kidney cells	CRL-11268
MCF10A	normal breast cells	CRL-10317
MCF-7	breast adenocarcinoma cells derived from pleural effusion metastatic site	HTB-22
SK-BR-3	breast adenocarcinoma cells derived from pleural effusion metastatic site	HTB-30

3.1.7 Oligonucleotides

3.1.7.1 Primer sequences for cloning into the pGl3-Enhancer vector

Table 5: Primer sequences for pGL3-Enhancer vector cloning. Displayed are the *STAT1* and *LGALS3BP* promoter fragment cloning primers with incorporated restriction sites (bold). The forward and reverse primer sequences are presented in 5' to 3' direction for cloning into the luciferase reporter vector pGl3-Enhancer.

gene promoter	sequence (5'-3') with restriction site
***STAT1_1* forward**	TTT**AAGCTT**GCTCAGCCAATTAGACGC
***STAT1_1* reverse**	TTT**AGATCT**GACGTCGCCAAATCTGTC
***STAT1_2* forward**	TTT**AAGCTT**CACCCGGAACCTCAC
***STAT1_2* reverse**	TTT**AGATCT**CAGGTCTTTATTAGCAGCG

gene promoter	sequence (5‘-3‘) with restriction site
***LGALS3BP* forward**	TTT**AAGCTT**CTATGTGCAAACAGGGAGG
***LGALS3BP* reverse**	TTT**AGATCT**TAGGAGAGTGGCCACAG

3.1.7.2 qPCR primer sequences

Table 6: Primer sequences for qPCR analyses. Displayed are the primer pairs for each mRNA analyzed in the qPCR expression experiments. The forward and reverse primer sequences are presented in 5’ to 3’ direction.

mRNA of gene	forward sequence (5‘-3‘)	reverse sequence (5‘-3‘)
Brd4-both	AACCTGGCGTTTCCACGGTA	GCCTGCACAGGAGGAGGATT
Brd4-long	GAAATGAAGCCTGTGGATGTCG	TCGGCTCCTGTTTCTGTTTGTC
IFITM1	CCCTCTTCTTGAACTGGTGCT	CCAACCATCTTCCTGTCCCTA
IFI6	CTGGTCTGCGATCCTGAATG	TTACCTATGACGACGCTGCTG
IFITM2	GTCCCTGTTCAACACCCTCTT	CCAACCATCTTCCTGTCCCTA
IFITM3	GCTCATCGTCATCCCAGTGCT	GGGATACAGGTCATGGGCAGA
PARP10	TTGGACACAGGCCTTGAAGA	TGGTCACCACCTGTACTGTCTG
HSPA13	TGCCAATGCTGTCATTTCTGT	TGCTGCTGTGGGTTCATTTAT
SLC7A11	GAGGAGCTGCTGCTTTCAAAT	GCAACAAAGATCGGAACTGCT
YOD1	GTGCCTGGATCTCAGCAATG	GCCTGGTTTGGTCTTCTTCAA
HMGCS1	TATGGTTCCCTTGCATCTGTTC	GCAGCCAAACCAGAACCATA
FAR1	AGCCTGGTATTCCGGAGTTAAT	CCCAGTGGAAAGGATTAGTGC
LGALS3BP	AGAGAGACGCTGGTGTGGTCT	GCTGGCTGTCAAAGATCTGG
STAT1	GCATGAAATCAAGAGCCTGGAA	CCACACCATTGGTCTCGTGTT
STAT2	CAGCCAACTGAAAGACCAGCA	TTCTGCTCTTTGGTCTGATGG
STAT3	GCAGCTGGAACAGATGCTCAC	TGCACGTACTCCATCGCTGAC
IRF1	ATGCAGGACTTGGAGGTGGAG	GTCCGGCACAACTTCCACTG
IRF9	TGGAGTTTCTGCTTCCTCCAGA	CAATCCAGGCTTTGCACCTG
ERBB2	GCTGCTGGGGAGAGAGTTCTG	CTCATGGCAGCAGTCAGTGG
MYD88	TTTACAGGTGGCCGCTG	TCTCCTGCACAAACTGGATG
HPRT1	AGGAAAGCAAAGTCTGCATTG	GGTGGAGATGATCTCTCAACT

3.1.8 Vectors, constructs and vector maps

Table 7: Vector names and characteristics. Summary of the utilized vector systems with the size of the vector and fused expression tag as well as information for their purchase.

name	size	tag	company (order number)
pSUPER.retro.puro	6349bp	none	OligoEngine, Inc. (VEC-PRT-0002)
pcDNA4C-HisMax	5257bp	XPRESS, 6xHis	Invitrogen (V864-20)

name	size	tag	company (order number)
pRL-TK	4045bp	sea pansy luciferase	Promega (E2241)
pGL3-Enhancer	5064bp	firefly luciferase	Promega (E1771)

pSUPER.retro.puro was used for the cloning of Brd4 and GFP specific shRNAs for knockdown experiments in cultured human cells. The resulting constructs "shC2", "shE1" (Brd4) and "shGFP" (GFP) were already available in our work group.

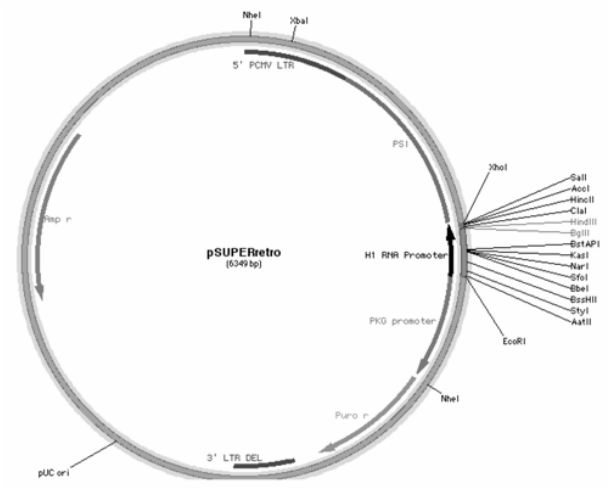

Figure 9: Vector map of pSUPER.retro.puro. The vector pSUPER.retro.puro (OligoEngine, Inc. - VEC-PRT-0002) is used for the expression of mRNA interfering short hairpin RNAs (shRNAs) in human cultured cells. Its backbone is 6349bp long and the multiple cloning site of the vector exhibits the restriction sites for BglII and HindIII, which are used for insertion of shRNAs. In Addition, it carries the genes for *ampicillin* and *puromycine*, enabling a selection in bacteria and cultured cells.

pcDNA4C-HisMax was used for the cloning of Brd4-long for overexpression experiments in cultured human cells. The Brd4-long construct was already available in our work group.

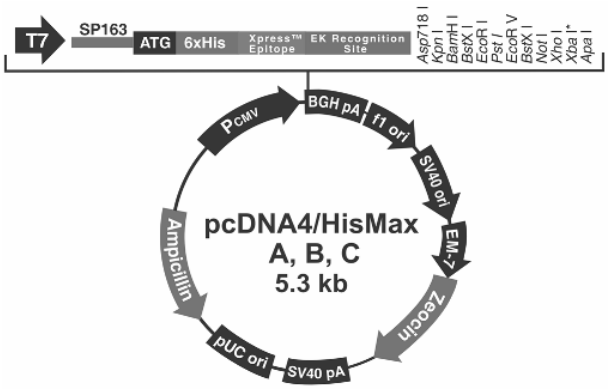

Figure 10: Vector map of pcDNA4C-HisMax. The vector pcDNA4C-HisMax (Invitrogen - V864-20) is used for the over expression of a gene in human cultured cells. Its backbone is 5257bp long, the expression driven by a CMV promoter and the gene expressed as a fusion protein with a XPRESS and 6xHis tag. The multiple cloning site of the vector exhibits the restriction sites for BamHI and NotI, which are used for insertion of a cDNA. In Addition, it carries the genes for *ampicillin* and *zeocin*, enabling a selection in bacteria and cultured cells.

pRL-TK was used as a normalization plasmid in the Dual-Luciferase Reporter Assay System ("Promega"). It was kindly provided by the collaborating group of Dr. Sylvia Krobitsch.

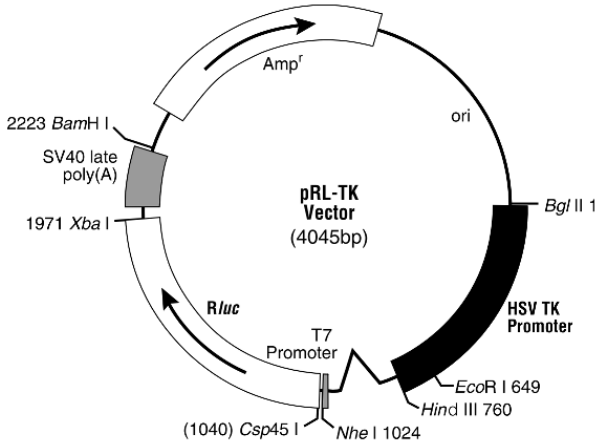

Figure 11: Vector map of pRL-TK. The vector pRL-TK (Promega - E2241) carries the *Renilla reniformis* (sea pansy) *luciferase* gene for its expression in human cultured cells. It is 4045bp long and used for normalization in the Dual-Luciferase Reporter Assay System (Promega). In Addition, it exhibits the *ampicillin* gene for specific selection in bacteria.

pGL3-Enhancer was used for the cloning of the *STAT1* and *LGALS3BP* gene promoter fragments for the Dual-Luciferase Reporter Assay System ("Promega").

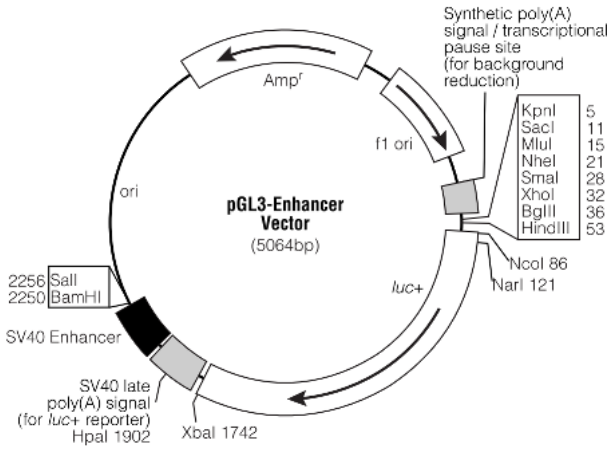

Figure 12: Vector map of pGL3-Enhancer. The vector pGL3-Enhancer (Promega - E1771) is used for the activity analysis of a promoter fragment in human cultured cells. Its backbone is 5064bp long and includes the *Photynus pyralis* (firefly) *luciferase* gene for Dual-Luciferase Reporter Assay System (Promega) experiments. Its expression is driven by the cloned promoter fragment. The multiple cloning site of the vector exhibits the restriction sites for BglII and HindIII, which are used for insertion of a promoter fragment. In Addition, it carries the *ampicillin* gene for specific selection in bacteria.

3.1.9 Antibodies

3.1.9.1 Primary antibodies

Antibodies are designed and generated for the detection of specific proteins or their fused tags. The provided list summarizes the used primary antibodies.

Table 8: Primary antibodies. Summary of used primary antibodies, the corresponding concentrations as well as the purchasing companies.

antibody	company	concentration
Brd4	Abcam (ab46199) - no longer available	1mg/ml
Brd4	Abcam (ab75898)	1mg/ml
RNA Polymerase II	Santa Cruz Biotechnology (sc-9001X)	2.0mg/ml
Gamma globulin	Jackson ImmunoResearch (011-000-002)	11.2mg/ml
STAT1	Cell Signaling Technology (#9172)	—
LGALS3BP	Sigma (HPA000554)	—
XPRESS	Invitrogen (R910-25)	1.14 mg/ml
GAPDH	Ambion (AM4300)	—
TUBA	Sigma (T9026)	—

3.1.9.2 Secondary antibodies

Secondary antibodies are generated for the binding to primary antibodies in a species specific manner and conjugated with an enzyme for chemiluminescence detection or colorimetric staining.

Table 9: Secondary antibodies. Summary of used secondary antibodies, the corresponding concentrations as well as the purchasing companies.

anti	company (article number)	concentration
mouse IgG	Jackson ImmunoResearch (115-035-146)	0.8mg/ml
rabbit IgG	Jackson ImmunoResearch (111-035-144)	0.8mg/ml

3.2 Methods

3.2.1 Polymerase chain reaction (PCR)

The polymerase chain reaction is an *in vitro* method to amplify DNA fragments of interest using specific forward and reverse primers. Genomic, plasmid or complementary DNA (cDNA) serves as template and is replicated during cycling steps consisting of denaturation of the template, annealing of the primers and elongation of the newly synthesized strand. The reaction conditions were determined for each application depending on the used primers (the length and content of guanine (G) and cytosine (C) bases were crucial) as

well as the fragment size. The resulting DNA was utilized for cloning after purification as well as cloning confirmation (colony PCR) (see 3.2.2 and 3.2.3.1).

Material:

- Phusion polymerase (2U/µl)
- 5x Phusion HF reaction buffer
- Taq polymerase (1U/µl)
- 10x Taq reaction buffer
- dNTPs (40mM)
- nuclease free water (H_2O)
- cDNA, plasmid DNA, bacteria colony
- 10µM primer (forward/reverse)
- PCR cycler PTC-100

Protocol: The Taq DNA polymerase, without proof reading capability, was applied for general testing such as cloning verification (colony PCR) while the Phusion DNA polymerase, including proof reading ability, was used for cloning experiments. The reaction conditions and pipetting schemes for the different polymerases can be extracted from table 10.

Table 10: PCR reaction conditions for different DNA polymerases. The PCR reactions were prepared as presented. The Phusion DNA polymerase was used for cloning experiments and the Taq DNA polymerase for general testing (e.g. colony PCR).

	DNA polymerase	
	Phusion	**Taq**
reaction buffer	10µl	2.0µl
dNTPs	1.5µl	0.4µl
forward primer	0.75µl	0.5µl
reverse primer	0.75µl	0.5µl
polymerase	0.5µl	2.0µl
template	10-100ng	colony
H_2O	**add to 50µl**	**add to 20µl**

The primers for cloning experiments were designed with annealing temperatures varying from 52°C to 60°C, a guanine/cytosine (GC) content of 40-60% and a length between 18 and 24 nucleotides, matching the start and end point of the desired region. The elongation time depended on the fragment size and the pace of the employed DNA polymerase. The cycling instructions for different PCR reactions are listed in table 11.

Table 11: PCR cycling instructions for different polymerases. PCR reactions are performed following the presented denaturing, annealing and elongation steps.

step	Phusion	Taq
1. Denaturing	98°C → 30sec	95°C → 2min
	34 cycles of steps 2 - 4	
2. Denaturing	98°C → 10sec	95°C → 30s
3. Annealing	52-58°C → 30sec	60°C → 30s
4. Elongation	72°C → 30s/kb	72°C → 60s/kb
5. Elongation	72°C → 5min	72°C → 10min

3.2.2 Agarose gel electrophoresis

Negatively charged DNA or RNA molecules can be separated according to their size in agarose gels using an electric current at which smaller fragments can pass through the gel faster than larger ones.

Material:

- agarose
- 1x TAE buffer
- electrophoresis chamber
- power supply PowerPac 200

Protocol: The amount of agarose for fragment separation was dissolved in 1x TAE and chosen according to the fragment size of interest. Table 12 gives an overview on established proportions.

agarose concentration (w/v)	fragment size (bp)
$< 0.8\%$	> 1000
~ 1.0%	~ 1000
$> 1.5\%$	< 1000

Table 12: Agarose gel electrophoresis. The concentration of the agarose gel depended on the fragment size of interest.

3.2.3 Purification of linear DNA molecules

Linear PCR products as well as restriction enzyme digested DNA molecules with a length greater than 70 base pairs can be either purified by cutting from an agarose gel using a gel extraction kit or directly from the PCR reaction with a PCR purification kit.

3.2.3.1 Agarose gel extraction

The Gel Extraction Kit by QIAGEN relies on silica-gel-membranes which bind DNA in high-salt buffer and elute it with low-salt buffer or water.

Material:

- excised gel fragment
- scale EMB 200-2
- QIAquick Gel Extraction Kit
- thermomixer compact 5350
- isopropanol
- MinElute Gel Extraction Kit
- centrifuge 5425

Protocol: The purification was performed following the manufacturer's instructions. The excised gel fragment was weighed, three volumes of buffer QG added to the gel slice and the gel dissolved for 10min at 50°C. The solution was mixed with one gel volume of isopropanol and the DNA immobilized on a QIAquick spin column or MinElute spin column. These were used for DNA elution with low buffer volumes. In addition, the application of QG buffer prior to the washing step enhanced the binding affinity of the DNA to the silica-gel-membranes. A washing step using buffer PE and a drying step were performed before an elution with 30µl or 10µl of EB elution buffer, respectively.

3.2.3.2 DNA purification from PCR reactions

DNA fragment purification directly from the PCR reaction mixture is also silica-gel-membrane-based and follows a similar protocol as described above (part 3.2.3.1).

Material:

- PCR reaction
- QIAquick PCR Purification Kit
- MinElute PCR Purification Kit
- centrifuge 5425

Protocol: The DNA purification was performed following the manufacturer's guidelines. The PCR reaction was mixed with five times the reaction volume of PB binding buffer and subsequently bound to a provided QIAquick spin column or MinElute spin column

by centrifugation. The washing (buffer PE) and drying steps were performed at room temperature and the DNA eluted in 50 - 30µl or 10µl EB elution buffer, respectively.

The purified DNA was further used in experiments such as restriction enzyme digestion or ligation (parts 3.2.5 and 3.2.6).

3.2.4 Determination of nucleic acid concentrations

3.2.4.1 NanoDrop Spectrophotometer

The NanoDrop2000 ("Thermo Scientific") uses the UV-absorbance method based on the natural absorption of light of DNA and RNA molecules at 260nm and proteins at 280nm. The higher the DNA or RNA concentrations, the more light is absorbed. It allows a low volume measurement in the concentration range of 2ng/µl to 15,000ng/µl for double-stranded DNA without further dilutions and equipments.

Material:

- 1-2µl DNA or RNA in solution
- spectrophotometer NanoDrop2000
- solvent of the nucleic acid (control fluid)

Protocol: The NanoDrop2000 was calibrated on the control fluid, 1-2µl of sample were pipetted on the designated platform, the absorption was measured at 260nm and 280nm, respectively, and the concentration was displayed in ng/µl. The ratio of absorption at 260nm and 280nm stated the purity of the tested sample (1.8 is accepted as "pure" for DNA and a 2.0 ratio for RNA).

3.2.4.2 Qubit Fluorometer

The Qubit fluorometer ("Life Technologies") can be used to quantify DNA, RNA and proteins. It relies on the incorporation of a fluorescent dye (leading to a change in its fluorescence) which resembles the concentration of a sample. The "Qubit dsDNA HS Assay Kit" (HS = high sensitivity) detects ranges from 10pg/µl to 100ng/µl. The company offers precise and reliable measurements in that specific range and supports the analysis

of DNA from experimental set-ups such as the chromatin immunoprecipitation (ChIP) (part 3.2.17) with relatively low concentrations.

Material:

- double-stranded (ds) ChIP-DNA
- Quant-iT dsDNA HS Assay Kit
- Qubit assay tubes
- Qubit fluorometer

Protocol: The Qubit working solution was prepared containing HS reagent diluted 1:200 in HS buffer. The two DNA standards (Components A and B) as well as the samples were mixed 1:20 and 1:100 to a final volume of 200µl in the set up working solution, respectively, and incubated for 2min at room temperature. The fluorescence of the dye was afterwards measured using the Qubit fluorometer and the DNA concentration calculated as described below:

concentration of the sample in ng/ml = the value given by the fluorometer * (200/2)

3.2.5 Restriction enzyme digestion

Restriction enzymes (endonucleases) recognize palindromic sequences in DNA molecules and produce "blunt ends" or "sticky ends" (overhang) by cutting the DNA at specific sites. They are used to generate matching sites in vectors and inserts for cloning experiments as well as the examination of positive cloning results.

Material:

- plasmid DNA (cloned construct/empty vector)
- linear PCR product (insert)
- restriction enzyme BglII (10U/µl)
- restriction enzyme HindIII (10U/µl)
- 10x reaction buffer
- nuclease free water
- thermomixer compact 5350

Protocol: Between 50ng and 1000ng of DNA were mixed with 1x reaction buffer, 10U of each restriction enzyme, respectively, and filled up with nuclease free water to a final volume of 20µl. The reaction was performed for 1h (general examination) or over night

(12-16h) (cloning) at 37°C. The restriction enzymes BglII and HindIII were used for the promoter fragment cloning of STAT1 and LGALS3BP into the pGL3-Enhancer vector.

3.2.6 Ligation of restricted DNA fragments

Ligation reactions are used for the connection of linearized DNA fragments (inserts) with linearized vector molecules to generate constructs for gene expression analyses, knockdown experiments and Sanger sequencings.

The ligation approach performed in this thesis required pre-digested DNA fragments and vector molecules (part 3.2.5).

Material:

- restricted vector
- restricted insert
- 2x Quick ligation buffer
- T4 DNA ligase (400U/µl)
- nuclease free water

Protocol: The desired insert and vector were mixed in a molar ratio of 1:5. Usually, 25ng of the vector were used as starting point. The corresponding amount of insert was calculated according to the following formula:

m = 125ng * insert length (bp)/vector length (bp)

For the ligation reaction, the amount of insert and vector were combined with 2µl of 10x ligation buffer and 1µl of T4 DNA ligase in a total volume of 20µl. The reaction was performed for 15min at room temperature and the mixture then applied to an *E.coli* transformation.

3.2.7 Transformation of heat shock competent *E.coli* strains

Heat shock competent *E.coli* are generated for an uncomplicated admission of plasmid DNA from the surrounding into the cells following a specific heat and chill cycle.

Material:

- plasmid DNA (Miniprep, Maxiprep, ligation reaction)
- heat shock competent *E.coli*
- thermomixer compact 5350
- LB liquid medium without antibiotics
- incubator Innova44
- LB agar plate with antibiotic
- incubator Kelvitron t

Protocol: For the transformation, 30µl of *E.coli* were mixed with 1-5µl of plasmid DNA and incubated for 30min on ice. The heat shock cycle was performed for 45sec at 42°C and 30sec at 4°C. Afterwards, 800µl of LB medium without antibiotics were added and the bacteria incubated for 30 to 60min at 37°C and 160rpm shaking. Depending on the DNA used for transformation, either 20µl of the bacteria-medium mix (Miniprep or Maxiprep) or the entire transformation reaction (ligation reaction) (centrifuged for 5min at 5,000*g and RT and discarded the supernatant) were plated on a LB agar plate containing a selective antibiotic. The bacteria plates were incubated over night at 37°C.

3.2.8 Plasmid DNA preparation

Plasmid DNA becomes highly amplified in *E.coli* cells and can be used, after purification, for a broad range of experiments such as transformation of other *E.coli* strains, Sanger sequencing and the transfection of cultured human cells.

3.2.8.1 Miniprep

The Miniprep Kit by QIAGEN is based on the anion-exchange principle where negatively charged DNA is coupled to positively charged silica-membranes and proteins as well as cell debris are washed out.

Material:

- bacteria culture (3ml)
- QIAprep Spin Miniprep Kit
- centrifuge 5425

Protocol: Following the manufacturer's protocol, one bacteria colony was inoculated in 3ml LB medium containing a selective antibiotic and grown for 16h at 37°C and 160rpm shaking. The bacteria were pelleted for 1min at 13,000*g at room temperature, resuspended in buffer P1, lysed with buffer P2 and the reaction neutralized using buffer N3. The cellular debris was separated by centrifugation for 10min at 13,000*g at RT and plasmid DNA immobilized on a provided spin column. The column was washed once with buffer PE and the remaining DNA eluted with 30-50µl of buffer EB.

3.2.8.2 Maxiprep

The EndoFree Plasmid Maxi Kit by QIAGEN is built on the same principal as the above described Miniprep Kit (part 3.2.8.1) and yields endotoxin free plasmid DNA, suitable for transfection experiments of cultured human cells.

Material:

- bacteria culture (100ml)
- EndoFree Plasmid Maxi Kit
- isopropanol
- centrifuge Avanti J-25

Protocol: The plasmid DNA purification was performed as specified by the manufacturer. Briefly, one bacteria colony was inoculated in a 5ml starter culture (LB medium with a selective antibiotic), grown for 8-10h at 37°C and 160rpm shaking and afterwards diluted 1:750 in 100ml LB medium with a selective antibiotic for an over night culture. The bacteria were harvested by centrifugation for 15min at 6000*g and 4°C, resuspended in buffer P1, lysed with buffer P2 and the reaction neutralized using buffer P3. The cellular debris was removed using a provided filter cartridge and a plunger and the endotoxins in the mixture eliminated by adding buffer ER. The plasmid DNA was immobilized on a column, two washing steps with buffer QC followed and then an elution with buffer QN by gravity flow at room temperature. Addition of isopropanol as well as centrifugation for 30min at 17,000*g and 4°C precipitated the DNA contained in the solution and after washing (endotoxin-free 70% ethanol) and air-drying at RT the pellet was resuspended in a suitable volume of endotoxin-free buffer TE. The DNA concentration was determined on a NanoDrop.

3.2.9 Sanger sequencing

Sanger sequencing is a method to determine the nucleotide sequence in DNA molecules using the specific amplification by a DNA polymerase and an incorporation of dideoxynucleotides, that terminate the strand elongation. All generated constructs were validated by Sanger sequencing by the company Eurofins/MWG Operon.

3.2.10 Cryo-preservation of human cell lines

Human cells can be stored in liquid nitrogen after culturing and manipulation. Freezing medium containing DMSO prevents water crystallization and subsequent cell lysis during thawing. This allows long term storage for future experiments.

Material:

- cultured cells in T75 flask
- Dulbecco's PBS (DPBS)
- Trypzean (trypsin) solution
- centrifuge Avanti J-25
- freezing medium
- cryo container Mr. Frosty
- liquid nitrogen tank

Protocol: Human cells were grown to approximately 80% confluence, washed once with DPBS and detached by trypsin solution with subsequent inactivation by medium administration. A centrifugation step at 300*g for 5min and 4°C pelleted the cells which were afterwards gathered in 2ml of freezing medium. The cell solution was allocated á 1ml in cryo vials and cooled in a cryo container for 24h in a -80°C freezer (cooling frequency of 1°C per hour) prior to their long term storage in a liquid nitrogen tank.

3.2.11 Thawing, culturing and seeding of human cell lines

The application of cryo-preserved human cells allows consistent cellular conditions for experimental set-ups over a long period of time. The thawing, culturing and handling of the cells is relatively simple and enables a variety of manipulations. These include for

example transfections (part 3.2.12) and stimulations (part 3.2.24) with the possibility of gene expression analyses under specified conditions of interest.

Material:

- human cell lines
- culturing medium
- centrifuge Avanti J-25
- Dulbecco's PBS (DPBS)
- Trypzean (trypsin) solution
- incubator Cytoperm2

Protocol: The thawing of cryo-preserved cells required their quick collection in 5ml of pre-warmed appropriate culturing medium which was followed by a centrifugation step for 5min at 300*g and room temperature to remove all residual DMSO. Afterwards the cells were resuspended in 5ml of culturing medium containing additional 10% FBS and transferred to a T25 flask. The cells were incubated for 24h in an incubator set to 37°C, 95% O_2, 5% CO_2 and 5% humidity. On the next day, the cells were washed once with DPBS and overlayed with 1ml of trypsin solution until they detached from the surface. Following resuspension in 13ml of culturing medium with a total of 20% FBS, they were next transferred to a fresh T75 flask and kept in the incubator until they reached approximately 80% confluence. After full recovery from the cryo-preservation and the thawing process, the cells were splitted to an 1:4 ratio about twice a week for continuative culturing, thereby repeating the above mentioned DPBS washing, trypsin detachment and medium resuspension steps. The medium was subsequently switched to standard substance amounts (part 3.1.4.2).

Table 13: Cell numbers and culturing formats for seeding human cell lines. The number of seeded cells was adapted for each cell line and culturing format. It depended on the cell size as well as the growth rate.

cell line	plating format	density	plating volume
Hek293T	15mm dish	5,000,000	20ml
	60mm dish	2,000,000	5ml
	6-well plate	200,000	2ml
	24-well plate	80,000	500µl
	96-well plate	10,000	100µl
Wi38	60mm dish	1,000,000	5ml
SK-BR-3	6-well plate	200,00	2ml
	24-well plate	80,000	500µl

The seeding of cells for experimental set-ups included again the defined washing, detachment and resuspension steps. This time, after resuspension in growth medium, the cells were counted using a Neubauer counting chamber, diluted to the desired cell number, seeded in an appropriate dish and cultured in the incubator until further treatment. The proportions of seeding for each of the handled cell lines and plates are highlighted in table 13. The experimentally used MCF10A and MCF-7 cells were cultured and kindly provided by the collaborating group of Dr. Bodo Lange.

3.2.12 Transfection of cell lines

Transfection is the process of introducing extrinsic DNA or RNA into eukaryotic cells. The method used in this thesis relies on the production of liposomal structures around the applied DNA or RNA molecules by the transfection reagent, the fusion of these structures with the cell membrane and the final release of its content into the cell. It is used for different experimental set-ups such as the downregulation and upregulation of specific gene expressions. This is achieved by cloning the cDNA of a gene or a short hairpin RNA (shRNA) against a specific messenger RNA (mRNA) into a vector system and transfection of the resulting plasmid DNA into the cells.

3.2.12.1 Transfection of plasmid DNA using transfection reagent Attractene

The transfection reagent Attractene ("QIAGEN") shows relatively low cytotoxic side effects. It is suitable for the transfection of plasmid DNA into the Wi38 fibroblast cell line and provides here an efficiency of more than 80%.

Material:

- maxiprep plasmid DNA
- Attractene
- MEM medium
- MEM medium without additional substances
- seeded Wi38 cells
- incubator Cytoperm2

Protocol: The Wi38 cells were seeded as specified in table 13 and retained in the incubator for 24h. Plasmid DNA (2µg) was diluted in 175µl of MEM medium without any additional substances and mixed afterwards with 7.5µl of Attractene. To accomplish

liposomal complex formation the mixture was incubated for 15min at room temperature and added afterwards drop-wise onto the seeded cells. After gently swirling for uniform distribution the cells were placed back in the incubator until harvest. This protocol was performed for the various shRNA knockdowns of Brd4 and the corresponding GFP control. The cells were harvested 72h after transfection.

3.2.12.2 Transfection of plasmid DNA using transfection reagent Fugene6 and X-tremeGENE9

X-tremeGENE9 (former known as FuGENE6) ("Roche") additionally presents a liposomal complex forming transfection reagent. It also exhibits low cytotoxic effects on the cells and a high transfection efficiency of more than 90% in the Hek293T and SK-BR-3 cell lines.

Material:

- maxiprep plasmid DNA
- X-tremeGENE9/FuGENE6
- DMEM medium without antibiotics
- DMEM medium without additional substances
- seeded Hek293T/SK-BR-3 cells
- incubator Cytoperm2

Protocol: The Hek293T and SK-BR-3 cells were seeded following the instructions listed in table 13 and further cultured for 24h. Prior to transfection, the plating DMEM medium was replaced by the corresponding medium without antibiotics and the cells were further stored in the incubator until the actual treatment. Table 14 summarizes the applied components depending on the seeded format.

Table 14: Transfection with X-tremeGENE9/FuGENE6. The amount of applied components was adjusted to the growth area of the dish.

	plating format				
	60mm	**6-well**	**12-well**	**24-well**	**96-well**
DMEM without antibiotics [µl]	4,600	2,000	792	410	66.7
DMEM without additives [µl]	223	97	38.4	19.9	3.23
DNA [ng]	2,300	1,000	396	205	33.3
X-tremeGENE9/FuGENE6 [µl]	6.9	3.0	1.19	0.62	0.1

Briefly, DNA as well as X-tremeGENE9 were diluted in separate vessels in medium without any additional substances and incubated for 5min at room temperature. Afterwards, the prepared mixes were combined, shortly vortexed, and incubated at room temperature for another 20min. The reaction was added drop-wise onto the cells and swirled for uniform dispersion. The cells were incubated until harvest in the incubator. Usually, 72h for knockdown experiments and 48h for overexpression analyses were sufficient.

3.2.13 RNA extraction from cultured cells

Total RNA presents a mix of ribosomal RNA, messenger RNA and different kinds of small as well as non-coding RNAs. It contains the information on gene expression patterns under specific conditions, that can be analyzed and quantified via real time PCR (qPCR) experiments (parts 3.2.15 and 3.2.16).

3.2.13.1 RNA extraction using TRIzol

The TRIzol ("Invitrogen") reagent contains the substance phenol which ensures cell lysis and RNA integrity maintenance during RNA preparation. The general protocol using this reagent includes the following steps in order: cell lysis, phase separation, RNA precipitation, washing and dissolving.

Material:

- cultured cells
- PBS
- cell scraper
- TRIzol
- chloroform
- centrifuge 5417C
- isopropanol
- linear polyacrylamide (LPA)
- ethanol (>99% and 70%)
- nuclease free water
- RNase-Free DNase Set
- heavy phase lock gel tubes
- phenol:chloroform:isoamyl alcohol (25:24:1)
- 3M sodium acetate

Protocol: The cells were washed once in PBS and harvested in the same using a cell scraper. After pelleting the cells for 5min at 500*g and 4°C they were resuspended in a suitable amount of TRIzol (e.g., 300µl TRIzol for a 6-well), incubated for 5min at RT and combined with one fifth volume of chloroform. For phase separation, the solution was mixed by flipping, incubated for 2-3min at RT and afterwards centrifuged for 15min at 12,000*g and 4°C. The upper aqueous phase was transferred to a new vial, 1 µl of LPA was added for visibility of the pellet, and the RNA precipitated with one additional volume of isopropanol and subsequently storage for 30min at -80°C. A centrifugation step for 10min at 12,000*g and 4°C followed after cooling. The resulting pellet was washed once with 70% ethanol and dried for 5min at 37°C or 10min at RT. For digestion of the remaining DNA, the pellet was resuspended in 87.5µl nuclease free water, 10µl of 10x RDD buffer were added and subsequently mixed with 2.5µl DNase I. After incubation for 10min at RT, the RNA was again purified. Therefore, the mix was filled up with nuclease free water to a total volume of 200µl, chloroform was added in the same amount and the solution afterwards transferred to a pre-spun heavy phase lock gel tube. Phase separation was performed using a centrifuge for 5min at maximum speed and RT. The upper phase was transferred to a new tube containing 17µl of 3M sodium acetate, 1µl of LPA and 500µl of ethanol. Following an incubation for 40min at -80°C, the RNA was precipitated for 30min at maximum speed and 4°C. The pellet washed once with 70% ethanol and air dried for 15min at RT or 10min at 37°C. Eventually, the pellet was resuspended in a suitable volume of nuclease free water. The total RNA concentration was measured on a NanoDrop (part 3.2.4.1) and its integrity checked on an 1% agarose gel (part 3.2.2). The total RNA solution was further used for Next Generation Sequencing library preparation (part 3.2.18.2), reverse transcription (highlighted in 3.2.15) and qPCR analyses (part 3.2.16).

3.2.13.2 RNA extraction using Quick-RNA MicroPrep

The Quick-RNA MicroPrep Kit ("ZYMO RESEARCH") enables total RNA preparation in ten minutes from tissue cultures using small cell numbers. The extraction protocol is performed at room temperature via Fast-Spin columns and without further use of organic solvents, beta-mercaptoethanol and proteases.

Material:

- cultured cells
- PBS
- cell scraper
- Quick-RNA MicroPrep Kit
- centrifuge 5417C
- ethanol (>99%)
- RNase-Free DNase Set

Protocol: The protocol was performed following the manufacturer's instructions. The cells were washed once in PBS and harvested in the same using a cell scraper. After pelleting the cells for 5min at 500*g and 4°C they were lysed by resuspension in 400µl RNA lysis buffer and afterwards spun for 1min at 13,000*g. The lysate was passed over the first provided spin column (Zymo-Spin IIIC) using a centrifuge for 30sec at 8,000*g and the flow-through was combined with twice the volume of ethanol for small RNA recovery. The mixture was next passed over the second provided spin column (Zymo-Spin IC) for 1min at 13,000*g and washed once with 400µl of RNA wash buffer. The remaining DNA was digested on the RNA bound column using DNase I. Therefore, 3µl of RNase-free DNase I were mixed with 3µl of 10x reaction buffer and 24µl of RNA wash buffer and added to the column. After an incubation for 15min at RT and a centrifugation for 30sec at 13,00*g, a washing steps with 400µl of RNA prep buffer was performed. Two additional washing steps with 800µl and 400µl of RNA wash buffer, respectively, followed. The elution was performed into a fresh tube using >6µl of nuclease free water. The concentration of the total RNA solution was determined by NanoDrop.

3.2.14 qPCR primer design

The qPCR primers were designed using the freely available software tool Primer3 [81] with the following parameter settings: 20-22 nucleotides long, 63-65°C annealing temperature, 40-60% GC content, a maximum of 2-3 PolyX positions and a resulting amplicon size of 70-120 nucleotides. Their additional feature of over spanning exon-exon junctions ensured the specific amplification of processed transcripts in qPCR expression analyses.

3.2.15 cDNA synthesis using reverse transcriptase (RT)

Reverse transcription relies on the activity of a RNA depending DNA polymerase which produces complementary DNA (cDNA) to a given RNA template. The resulting cDNA allows further gene expression detection in qPCR analyses and also serves as template for transcript cloning experiments.

Material:

- random hexamers (NNNNNN) (100µM)
- dNTPs (40mM)
- nuclease free water
- PCR cycler PTC-100
- 5x first strand buffer
- 0.1M DTT
- SuperScript II (200U/µl)
- RNase H (2U/µl)

Protocol: At first, 300ng of total RNA were mixed with 250ng of random hexamers, 10mM of dNTPs and filled up with nuclease free water to a final volume of 13µl. Then, the mixture was incubated for 5min at 65°C and cooled down on ice for 2min. Afterwards, 4µl of 5x first strand buffer, 1µl of 0.1M DTT and 1µl of SuperScript II were added. Subsequently, a three step reverse transcription reaction was performed. Therefore, an incubation of 5min at 25°C was followed by 60min at 50°C and 15min at 70°C. The template RNA was digested next using 1µl of RNase H and an incubation for 30min at 37°C. Finally, 20min at 65°C heat-inactivated the RNase H and the single stranded cDNA was diluted in nuclease free water to a final concentration of 5ng/µl for further analysis.

3.2.16 Quantitative real time PCR (qPCR)

Quantitative real time PCR (qPCR) presents a specific DNA amplification method which is based on the general principal of a polymerase chain reaction (section 3.2.1). Additionally, it features the ability of simultaneous quantification via a non-specific intercalating fluorescent dye that is detected after every cycling step.

Material:

- 5ng cDNA per reaction
- 2x SYBR green master mix with ROX (passive reference dye)
- qPCR primers (5µM each)
- nuclease free water
- optical 96-well reaction plate
- optical adhesive films
- 7900HT Fast Real-Time PCR system cycler
- SDS2.2.1 software

Protocol: Every 5ng of cDNA was mixed with specific forward and reverse primers (0.75µl each), 5µl of SYBR green master mix and filled up with nuclease free water to a total volume of 10µl. The SYBR green master mix already contained the amplification and detection needed fluorescent dye (ROX), DNA polymerase and dNTPs. The qPCR reaction was performed with absolute quantification (standard curve) and 9600 emulation settings in a 7900HT Fast Real-Time PCR system cycler as summarized in table 15.

step	duration	temperature
1.	2min	50°C
2.	10min	95°C
	40 cycles of steps 3 - 4	
3.	15sec	95°C
4.	1min	60°C
	dissociation curve	
5.	15sec	95°C
6.	15sec	60°C
7.	15sec	95°C

Table 15: QPCR cycling conditions. QPCR reactions were performed following the presented cycling and dissociation curve steps.

ΔΔ Ct method:

For the interpretation of the qPCR results - captured by the provided SDS2.2.1 software - the "ΔΔ Ct method" was used:

1. **Calculation of the ΔCt (correction to control):**
   (gene in sample (Ct)) − (gene in control sample (Ct))
   This correction was performed for each gene individually.

2. **Calculation of the ΔΔCt (internal correction to a housekeeping gene):**
   (**Δ**Ct of gene) − (**Δ**Ct of *HPRT1*)
   This was done for each gene accordingly.

3. **Calculation of the relative expression level in the sample vs. the control:**
   2^(−(**ΔΔ**Ct of a gene))

4. The mean for the relative expression of each gene was taken and followed by the calculation of the standard deviation.

Calculation of Brd4-short proportion:

The calculation of the specific proportion of the short Brd4 isoform was accomplished after the "**ΔΔ** Ct method" was performed for each primer set, "Brd4-both" and "Brd4-long", individually. The first set of primers was used to determine the expression of both Brd4 isoforms at the same time and the second pair specifically provided the information of the long variant in the same sample. The following formula combines the results acquired by both primer sets and subsequently calculates the proportion of the short isoform in the sample:

(2^(−(**ΔΔ**Ct of Brd4-both))∗2) − (2^(−(**ΔΔ**Ct of Brd4-long))

Exclusive internal normalization to a housekeeping gene:

If an analyzed sample set does not include a negative control or if the results of a sample set should be pictured including all samples (also the corresponding negative control), the qPCR results were calculated only in matters of an internal normalization to a housekeeping gene.

1. **Internal correction to a housekeeping gene = calculation of the ΔCt**
   (gene in sample (Ct)) − (arithmetic average of *HPRT1* in the sample (Cts))
   This correction was performed for each gene individually.

2. **Calculation of the relative expression level in the sample:**
   2^(−(**Δ**Ct of a gene))
   This was done for each gene accordingly.

3. **Calculation of the relative expression level in the sample vs. control = setting control value to 1:**
   The following calculation was exclusively performed, when a control was included in a sample set. Otherwise, the internal correction was completed with step 2 (after calculation of the mean and corresponding standard deviation).
   The relative expression of each gene in a sample was determined according to its expression

in the control sample.
(2^(−(ΔCt of a gene in sample)) / (arithmetic average of 2^(−(ΔCt of a gene in control))

4. The mean for the relative expression of each gene was taken and followed by the calculation of the standard deviation.

Internal normalization was in general performed to the housekeeping gene *HPRT1* in all experiments and cell lines used in this thesis.

3.2.17 Chromatin immunoprecipitation (ChIP)

Chromatin immunoprecipitation is a method to investigate specific protein and DNA interactions as well as their incurring associations, respectively. The DNA and attached proteins in a current cellular stage are therefor covalently linked (cross-linked). The use of an antibody against a specific protein of interest allows then the enrichment of the same as well as its bound/associated DNA sequences. These can be further analyzed in qPCR experiments and determined genome-wide using Next Generation Sequencing.

Material:

- cultured Hek293T cells
- formaldehyde solution
- 2.5M glycine
- PBS
- cell scraper
- centrifuge 5810R
- ChIP lysis buffer 1
- ChIP lysis buffer 2
- ChIP lysis buffer 3
- 10% (v/v) Triton X100
- „Bioruptor“ sonifier
- Brd4 antibody, RNA Pol II antibody, rabbit IgG (5µg each)
- Protein G magnetic Dynal beads
- head-over-heel-rotator Type REAX2
- ChIP blocking solution
- ChIP wash buffer
- NaCl in 1x TE
- centrifuge 5425
- 5M NaCl
- ChIP elution buffer
- 1x TE (pH 8.0)

- RNase A (0.2µg/ml final concentration)
- Proteinase K (0.2µg/ml final concentration)
- phenol:chloroform:isoamyl alcohol (25:24:1)
- heavy phase lock gel tubes
- linear polyacrylamide (LPA)
- ethanol (>99% and 80%)

Protocol: Hek293T cells were grown on five 150mm dishes (approximately 15x10^8cells) to 80% confluence and cross-linked with 1.1% formaldehyde solution for 10min at RT. The reaction was stopped with 125mM glycine for 5min at RT. A PBS washing step with 10ml was followed by the cell harvest in also 10ml of PBS using a cell scraper. The cells were transferred to a clean conical tube and pelleted for 5min at 350*g and 4°C. Afterwards, the cells were lysed in three steps to obtain their nuclear fraction. They first were resuspended in 5ml of ice cold ChIP buffer 1 and rocked for 10min at 4°C. After pelleting for 5min at 600*g and 4°C, they secondly were resuspended in 5ml ice cold ChIP lysis buffer 2 and rocked for 10min at RT. The mentioned pelletization was repeated and the cells subsequently collected in 3ml ice cold ChIP lysis buffer 3. Further disruption of the nuclear membrane and additional DNA fragmentation was performed using a "Bioruptor" sonifier. A DNA size range between 100 and 300bp after cross-link abrogation was achieved by repeating the following cycling steps for 1h at 200W: 30sec of sonication (without foam production) and 30sec of cooling time. Immediately after sonication the sample was split in two fresh reaction tubes and mixed with 0.5% (v/v) of Triton X100. An incubation for 5min on ice followed. Centrifugation for 10min at 10,000*g and 4°C separated the cellular debris and the sample was subsequently pooled again. Thereof, 50µl were saved as "Input" DNA and stored at -20°C until further handling. The remaining lysate was split in three clean reaction tubes and enriched for the protein of interest using 5µg of antibody and an overnight incubation (12-16h) at 4°C on a head-over-heel rotator. On the next day, 65µl of Protein G coupled magnetic beads per enrichment were washed once in ChIP wash buffer and blocked for 30min at 4°C on a slow wheel in ChIP blocking buffer. Afterwards, the beads were added to the immunoprecipitation and incubated rotating for another 4h. The beads were collected using a magnetic stand on ice and washed five times with ChIP wash buffer by repeating mixing by flipping and magnetic collection steps. An additional washing with 500µl of NaCl in TE followed and was completed with a short spin for 30sec at 960*g and 4°C and subsequent removal of all residual liquid. The precipitated protein and DNA complexes were eluted in 100µl of ChIP elution buffer for 15min at 65°C and 900rpm. The supernatant was transferred to a clean reaction tube and pooled with the same from a second repeated elution step. Afterwards, 8µl of 5M NaCl were added to the pooled elutions. The recovered "Input" DNA was filled up to

200µl with ChIP elution buffer and additionally combined with 7µl of 5M NaCl. Each sample was incubated overnight (12-16h) at 65°C for reverse cross-link. On the third day, the samples were diluted in clean TE (1:2), RNA was digested with RNase A for 2h at 37°C and the remaining proteins also with Proteinase K for 2h at 55°C. Afterwards, 400µl of phenol:chloroform:isoamyl alcohol were added to each sample and transferred to pre-spun heavy phase lock gel tubes. Phase separation was performed for 5min at 16,000*g and RT and the upper phase collected in a fresh reaction tube. Afterwards, 16µl of 5M NaCl, 1µl LPA and 800µl ethanol were added and subsequently cooled for 1h at -20°C. DNA precipitation was accomplished for 20min at 20,000*g and 4°C and followed by a washing step with 80% ethanol. The pellet was dried for 10min at 37°C and finally resuspended in 25µl of clean 1x TE. The DNA concentration was determined using a NanoDrop and Qubit assay and sonication efficiency checked on an 1.5% agarose gel. The chromatin immunoprecipitation samples were stored at -20°C until further Illumina library preparation and Next Generation Sequencing.

3.2.18 Illumina (Solexa) sequencing

Next Generation Sequencing presents a technique of determination of the nucleotide sequence in DNA molecules, meaning the exact order of the four bases – adenine, guanine, thymine and cytosine - one after the other. Solexa sequencing is based on reversible dye-terminators. The DNA is ligated with adapters to slides and amplified to form local clonal colonies. Afterwards, the four types of reversible fluorescent terminator bases are added, incorporated (unbounds are washed away) and photographed. This cycling process allows the uncovering of the nucleotide order in DNA one step after another.

3.2.18.1 Library preparation for ChIP sequencing

The library preparation protocol prepares the DNA of interest for the following Next Generation Sequencing process. The Illumina protocol contains steps of end repair (generates phosphorylated blunt ends), attachment of an adenine base to the 3' end (important for adapter ligation), ligation of specific adapter molecules (contain a thymine base for their attachment to the DNA and allow the hybridization to the sequencing slide), DNA size selection and specific amplification in a PCR reaction using primers matching the adapter sequences.

Material:

- 50ng of ChIP DNA
- ChIP-Seq Sample Prep Kit
- centrifuge 5810R
- QIAquick PCR Purification Kit
- MinElute PCR Purification Kit
- QIAquick Gel Extraction Kit
- MinElute Gel Extraction Kit
- PCR cycler PTC-100

Protocol: The library preparation and purification protocols were performed following the instructions by the manufacturers. The ChIP DNA was diluted to a total volume of 40µl in nuclease free water. The end repair reaction was prepared by adding 5µl of T4 DNA ligation buffer, 2µl of dNTPs, 1µl of T4 DNA polymerase, 1µl of Klenow DNA polymerase and 1µl of T4 PNK and performed for 30min at 20°C in a PCR cycler. Afterwards, the DNA was purified using the QIAquick PCR Purification Kit and 34µl of EB elution buffer (part 3.2.3.2). For the adenine attachment, the DNA was mixed with 5µl of Klenow buffer, 10µl of dATP and 1µl of Klenow exo (3' to 5' exo minus) and incubated for 30min at 37°C. DNA purification followed subsequently using the MinElute PCR Purification Kit and 10µl of EB elution buffer (part 3.2.3.2). The adapter ligation was performed with 15µl of DNA ligase buffer, 1µl of prepared adapter oligo mix and 4µl of DNA ligase for 15min at RT. The DNA clean-up was repeated with the MinElute PCR Purification Kit and 10µl of EB elution buffer (part 3.2.3.2). The DNA size range between 150 and 250bp was selected on an 2% agarose gel and extracted via the QIAquick Gel Extraction Kit and 36µl of EB elution buffer (part 3.2.3.1). In the end, the library was amplified as described in table 16 and terminatory purified using the MinElute Gel Extraction Kit and 15µl of EB elution buffer (part 3.2.3.1).

Table 16: PCR cycling conditions for ChIP library amplification. The PCR reaction was prepared as presented and performed following the displayed denaturing, annealing and elongation steps.

	volume	step	duration	temperature
ChIP DNA library	36µl	**1.**	30sec	98°C
5x Phusion buffer	10µl		**18 cycles of steps 2-4**	
dNTP mix	1.5µl	**2.**	10sec	98°C
PCR primer 1.1	1µl	**3.**	30sec	65°C
PCR primer 2.1	1µl	**4.**	30sec	72°C
Phusion polymerase	0.5µl	**5.**	5min	72°C
total	**50µl**	**6.**	hold at	4°C

The prepared ChIP DNA library for Next Generation Sequencing was analyzed on the Illumina Genome Analyzer IIx.

3.2.18.2 Library preparation for mRNA sequencing

Messenger RNA (mRNA) presents the portion of ribonucleic acid (RNA) which codes for proteins. Its constitution resembles gene expression patterns under specific cellular condition. Next Generation Sequencing provides the information of mRNA levels, which further enables the comparison of differences and commonalities between certain cellular states. The Illumina library preparation from total RNA for Next Generation sequencing includes enrichment steps of poly-adenylated mRNA, fragmentation of the enriched material, reverse transcription of the mRNA into single strand cDNA, second strand synthesis and DNA end repair performance. In the end, specific adapter sequences are ligated and the library amplified for further analysis.

Material:

- 5µg of total RNA
- TrueSeq RNA Sample Preparation Kit
- PCR cycler PTC-100
- magnetic stand Dynal MPC-S
- SuperScript II Kit
- AMPure XP kit
- 80% ethanol

Protocol: The library preparation and purification protocols were performed following the instructions by the manufacturers. The total RNA was filled up with nuclease free water to a final volume of 50µl. The poly-adenylated mRNA was enriched by adding 50µl of RNA Purification Beads (magnetic, oligo-dT). Denaturing for 5min at 65°C and subsequent cooling to 4°C were performed in a PCR cycler. An incubation for 5min at RT was followed by a bead separation on the magnetic stand. Separation was sufficient using 5min of incubation before the supernatant was discarded. The mRNA bound beads were washed once with 200µl of Bead Washing Buffer. The enriched mRNA was eluted with 50µl of Elution Buffer for 2min at 80°C and a cooling phase to 25°C. Application of another 50µl of Bead Binding Buffer and incubation for 5min at RT allowed the eluted mRNA to re-bind to the beads for a second time. Magnetic separation was again performed on the magnetic stand and the washing step with 200µl of Bead Washing Buffer was

repeated. The mRNA was subsequently eluted from the beads using 19.5µl of Elute, Prime, Fragment Mix. An incubation for 8min at 94°C and cooling to 4°C combined the elution, fragmentation and priming of the mRNA for the first strand synthesis in one. After magnetic bead separation, 17µl of the supernatant were transferred to a clean reaction tube and mixed with 7µl of First Strand Buffer and 1µl of SuperScript II. The reverse transcription reaction was performed in a PCR cycler programmed to 10min at 25°C, 50min at 42°C, 15min at 70°C and 4°C afterwards. The second strand synthesis followed subsequently with 25µl of Second Strand Master Mix and an incubation for 1h at 16°C as well as sample warming to RT. The double strand (ds) complementary DNA (cDNA) was immobilized for 15min at RT using 90µl of well-mixed AMPure XP Beads (magnetic). Bead separation was performed at RT as mentioned above. The beads were washed once with 200µl of freshly prepared 80% ethanol, the supernatant completely removed and the beads air-dried for 15min. The DNA elution was achieved with 52.5µl of Resuspension Buffer, an incubation for 2min at RT and repeated magnetic separation. The end repair was prepared with 50µl of the supernatant, 10µl of Resuspension Buffer and 40µl of End Repair Mix and the reaction performed for 30min at 30°C. AMPure XP Beads (160µl) were again used for purification and the ds cDNA eluted in 17.5µl of Resuspension Buffer as described above. Afterwards, 15µl of the elution were transferred to a clean reaction tube and mixed with 2.5µl of Resuspension Buffer as well as 12.5µl of A-Tailing Mix. The 3' attachment of an adenine was performed for 30min at 37°C and followed by the ligation of the sequencing adapters. Therefore, 2.5µl of DNA Ligase Mix, 2.5µl of Resuspension Buffer and 2.5µl of each RNA Adapter Index were added to the mixture and incubated for 10min at 30°C until the reaction was abrogated with 5µl of Stop Ligase Mix. After mixing the adapter ligated ds cDNA solution with 42µl of AMPure XP Beads and subsequent purification, the elution was performed with 52.5µl of Resuspension Buffer. The entire supernatant was again mixed with 50 µl of fresh AMPure XP Beads and the purification round performed for a second time. Eluted was in 22.5µl of Resuspension Buffer and 20µl of the supernatant were transferred to a clean reaction tube for library amplification. The pipetting scheme and PCR cycling conditions were followed as seen in table 17. A final cleaning procedure was performed with 50µl of AMPure XP Beads and 32.5µl of Resuspension Buffer. In the end, 30µl of the prepared cDNA library were aliquoted and stored at -20°C until Next Generation Sequencing. The concentration of the library was measured using the Qubit fluorometer.

Next Generation Sequencing of the library was performed on the Illumina HighSeq.

Table 17: Pipetting scheme and PCR cycling conditions for cDNA library amplification. The PCR reaction was prepared as presented and performed following the displayed denaturing, annealing and elongation steps.

	volume	step	duration	temperature
cDNA library	20µl	**1.**	30sec	98°C
PCR Primer Cocktail	5µl		**15 cycles of steps 2-4**	
PCR Master Mix	25µl	**2.**	10sec	98°C
total	**50µl**	**3.**	30sec	60°C
		4.	30sec	72°C
		5.	5min	72°C
		6.	hold at	10°C

3.2.18.3 Ingenuity Pathway Analysis (IPA)

Ingenuity Pathway Analysis (IPA) is a software tool (Ingenuity) which provides a platform for life science researchers to explore, interpret and analyze complex biological systems such as large expression data-sets derived from mRNA sequencings. The Ingenuity Knowledge Base builds the fundament of the product which comprises of reported experimental facts with links to the original articles and contains additional information from other sources such as protein-protein interactions from "BIOGRID", microRNA-mRNA target interactions from "TARBASE", metabolic pathway information from "KEGG" and enzyme/substrate reactions from "LIGAND".

The analyses in this thesis were performed using the unique symbol of a differentially expressed gene and its corresponding binary logarithm of the fold change (log2 FC). The core analyses were carried out following the guidelines of the company (Ingenuity) and the obtained results were extracted in diagrams and visualized in pathway maps.

3.2.18.4 ConsensusPathDB (CPDB)

The ConsensusPathDB (CPDB) analysis tool is designed by researchers at the Max Planck Institute for Molecular Genetics in Berlin and integrates interaction networks in *Homo sapiens*. It also combines the information from 30 other databases (e.g., "Reactome", "KEGG", "PID") and therefore covers further biologically relevant correlations like protein-protein interactions, signaling reactions, gene regulations and biochemical pathways. CPDB is freely available on the Internet and serviceable without additional software tools.

The unique symbol of a gene presented the basis for the performed analyses. The list of differentially expressed genes after mRNA sequencing experiments, the list of total ChIP Seq targets as well as all continuative overlap analyses were analyzed using the CPDB gene set over-representation path. The most significantly affected pathways in the data-sets were selected with a minimum cut-off of two candidates overlapping with the submitted gene lists and p-values below 0.01. The same criteria were chosen for the identification of affected protein-protein complexes. The results were extracted in table form.

3.2.19 Protein extraction from cultured cells

Diverse panels of cultured cells and experimental set-ups provide the ability of investigating cellular mechanisms and functional dependencies under varying conditions. Whole protein extraction is performed to capture the entire events occurring in the tested cells. These can be analyzed in Western Blot experiments for specific protein conditions and furthermore permit biological relevant conclusions.

Material:

- cultured cells
- PBS
- cell scraper
- lysis buffer A
- 5M NaCl
- centrifuge 5417C
- lysis buffer B
- head-over-heel-rotator Type REAX2
- thermomixer compact 5350

Protocol: The cultured cells were washed once with PBS and harvested on ice in buffer A. Therefore, 300µl of buffer A were added to a 60mm dish and the cells scraped off with a cell scraper. The applied volume of buffer A was adjusted for different culturing plates according to their growth area. The cells were transferred to a clean reaction tube and incubated for 10min on ice. Afterwards, they were lysed mechanically by pipetting up and down, mixed with 500mM NaCl for high salt extraction of nuclear proteins and rocked for 20min at 4°C. A centrifugation step was performed next for 5min at 2500*g and 4°C. The supernatant was transferred to a clean reaction tube on ice and the pellet resuspended in an equal volume of buffer B to buffer A. DNase I digestion was carried out for 30min at 37°C and subsequently followed by another centrifugation step for 5min at 2500*g and

4°C. The supernatant was pooled with the first one on ice and the concentration of total proteins determined by a Bradford assay (see section 3.2.20).

3.2.20 Bradford assay

The Bradford assay is a method used for the determination of protein concentrations. It is performed with the Coomassie Brilliant Blue R250 containing Bradford reagent. This dye binds to proteins in an unspecific manner, appears red in color when unbound and converts blue when protein complexes are formed. The extinction of the solution can be measured at 595nm using a spectrophotometer and the resulting value allows conclusions about the starting amount of proteins in comparison to a standard curve of known protein concentration.

Material:

- BSA standard solution (1µg/µl)
- Bradford reagent
- cell lysate
- cuvettes
- nuclease free water
- spectrophotometer Ultraspec 3000

Protocol: A standard curve was prepared in 20µl of nuclease free water using bovine serum albumin (BSA) protein ranges from 0 to 10µg. Afterwards, 2µl cell lysate of unknown protein concentration were mixed with 18µ of nuclease free water. Each sample and the standard curve preparation was mixed with 1ml of Bradford reagent and incubated for 10min at RT. The extinction was measured at 595nm in a spectrophotometer and the resulting values of the standard curve plotted against the contained protein concentration. The amount of protein in the lysate was calculated according to the linear equation of the standard plot.

3.2.21 Western Blotting

Western Blotting is a combined method of sodium dodecyl sulfate polyacrylamide gel electrophoresis (SDS-PAGE) followed by immunoblotting. It is used for the semiquantitative detection of protein levels under different cellular conditions. The specific proteins

are analyzed using corresponding primary and secondary antibodies as well as chemiluminescence detection of the signals. These are further evaluated in comparison to an unchanged loading control, for example, the expression level of a housekeeping gene and allow biological relevant conclusions.

3.2.21.1 Sodium dodecyl sulfate polyacrylamide gel electrophoresis (SDS-PAGE)

The sodium dodecyl sulfate (SDS) polyacrylamide gel electrophoresis (PAGE) (SDS-PAGE) is used for the separation of proteins according to their size. Therefore, varying charges are negatively masked by the detergent SDS prior to analysis. Afterwards, an electric current leads to protein migrations to the positive pole through a network structured polyacrylamide gel. Unlike agarose gels, a polyacrylamide gel comprises of two parts: a stacking gel and a running gel. They gather the proteins in a tested sample and separate them, respectively. The running gel concentration determines the size range accessible to analyses. The stacking gel usually contains half the concentration of polyacrylamide compared to the running gel. The proteins in a sample travel through the gel in various paces according to their size at which smaller proteins pass through faster than larger ones.

Material:

- 10-30µg of total proteins
- 6x SDS loading buffer
- thermomixer compact 5350
- 1.5M Tris-HCl, pH 8.8
- 0.5M Tris-HCl, pH6.8
- 30% acrylamide/bis-acrylamide solution
- nuclease free water
- 10% APS
- TEMED
- pre-stained protein ladder
- 1x SDS running buffer
- Mini-PROTEAN Tetra Electrophoresis System

Protocol: 10-30µg of total proteins were mixed with 1x SDS loading buffer and denatured for 10min at >95°C. The protein sample and 5µl of a pre-stained protein ladder were loaded on a polyacrylamide gel and separation was performed using 90V for the stacking gel and 130V for the running gel migration, respectively. Table 18 gives an overview on

the utilized components for the running gel preparation and table 19 the corresponding stacking gel utensils.

Table 18: Pipetting scheme for polyacrylamide running gels. The pipetting scheme is sufficient for two polyacrylamide running gels. Important is the abidance of the displayed order of components in the mixing process.

percentage of gel [%]	**8**	**10**	**12.5**	**15**
protein range [kDa]	**below 200**	**below 100**	**below 50**	**below 25**
component	**volume [µl]**	**volume [µl]**	**volume [µl]**	**volume [µl]**
nuclease free water	add to 12,000	add to 12,000	add to 12,000	add to 12,000
1.5M Tris-HCl pH 8.8	3,000	3,000	3,000	3,000
acrylamide/bis-acrylamide solution	3,300	3,900	5,010	6,000
10% APS	39	39	39	39
TEMED	8.1	8.1	8.1	8.1

Table 19: Pipetting scheme for polyacrylamide stacking gels. The pipetting scheme is sufficient for two polyacrylamide stacking gels. Important is the abidance of the displayed order of components in the mixing process.

percentage of gel [%]	**4.5**	**5**	**6**	**7.5**
component	**volume [µl]**	**volume [µl]**	**volume [µl]**	**volume [µl]**
nuclease free water	add to 5,000	add to 5,000	add to 5,000	add to 5,000
0.5M Tris-HCl pH 6.8	1,000	1,000	1,000	1,000
acrylamide/bis-acrylamide solution	600	670	800	1,000
10% APS	40	40	40	40
TEMED	4	4	4	4

3.2.21.2 Immunoblotting and detection

Immunoblotting is a specific staining method for proteins after separation by SDS-PAGE. The proteins are transferred to a membrane, at which the separation order is maintained, and detected using specific primary and secondary antibody. The transfer can be achieved with a tank blotting or an semi-dry procedure. The applied secondary antibody is either coupled to a light emitting horseradish peroxidase (HRP), which leads to a chemiluminescence signal, or an alkaline phosphatase (AP), which allows colorimetric signal detection directly on the membrane. In this thesis I exclusively used HRP coupled secondary antibodies and the tank blotting procedure.

Material:

- SDS-PAGE
- PVDF membrane
- transfer buffer
- whatman paper
- Mini-PROTEAN Tetra Electrophoresis System
- western blotting blocking solution
- western blotting BSA blocking solution
- primary and secondary antibodies
- TBS and TBST
- ECL solution
- photographic film
- photographic film developing case
- darkroom
- photographic film developer Curix 60

Protocol: The PVDF membrane was activated in methanol and equilibrated in transfer buffer for 10min at RT. The separated proteins were transferred to the membrane using the tank blotting system with 100V for 1h at 4°C. Afterwards, the membrane was blocked with western blotting blocking solution and gentle agitation for 1h at RT or overnight (12-16h) at 4°C. The primary antibody against an endogenous protein was incubated rotating overnight at 4°C and against an overexpressed protein 1-2h at RT. Three washing steps in TBST for 5min at RT removed unbound antibodies and were repeated following the incubation with the secondary antibody for 1h at RT. Prior to signal detection, the membrane was washed in TBS and the ECL detection solution incubated on the membrane for 1min at RT. The specific light detection was performed with photo films in a darkroom using adjusted detection times for each of the antibodies. The primary and secondary antibodies used in this thesis as well as their dilutions are summarized in table 20.

Table 20: Primary and secondary antibodies and their dilutions. The primary antibodies were diluted in blocking solution with BSA and the secondary antibodies in blocking solution with milk powder.

antibody anti	raised in	dilution	conjugated with
Brd4	rabbit	1:1,000	
STAT1	rabbit	1:1,000	
LGALS3BP	rabbit	1:1,000	
XPRESS	mouse	1:2,000	
GAPDH	mouse	1:10,000	
TUBA	mouse	1:5,000	
mouse IgG	goat	1:10,000	HRP
rabbit IgG	goat	1:10,000	HRP

3.2.22 ImageJ analysis

ImageJ is an open source software tool which can be used to analyze the intensities of immunoblotting signals. Therefore, it is used to normalize a specific protein level to an unchanged loading control, for example, the expression level of a housekeeping gene. The results can be displayed graphically.

3.2.23 Dual-Luciferase Reporter Assay for promoter analysis

The Dual-Luciferase Reporter Assay System ("Promega") enables activity analyses of gene promoters under defined conditions. The promoter region of interest is cloned in front of the *Photinus pyralis* (firefly) luciferase reporter gene which expression is subsequently driven by the promoter fragment. Luciferases are oxidative enzymes with bioluminescence activity. The expression results in a measurable light production after substrate administration which corresponds to the activity of the analyzed promoter. The pGL3-Enhancer vector system was used for the promoter cloning. A vector system expressing the *Renilla reniformis* (sea pansy) luciferase is secondarily used for further normalization. Both vector systems were kindly provided by the collaborating group of Dr. Sylvia Krobitsch.

Material:

- co-transfected Hek293T cells
- Dual-Luciferase Reporter Assay System
- white 96-well plate with clear flat bottom
- luciferase assay machine Glomax Multi

Protocol: Hek293T cells were co-transfected with the *Renilla reniformis* luciferase reporter vector and either the cloned promoter construct or the empty vector control. Also transfected were overexpression or knockdown constructs and the cells harvested 48h and 72h after transfection, respectively. The luciferase reporter assay was performed following the manufacturer's instructions. The cells grown in a 24-well plate were lysed in 100µl of passive lysis buffer with agitation for 20min at RT. Afterwards, 20µl of lysate were transferred to a 96-well plate with clear flat bottom and the Dual-Luciferase Reporter Assay performed using 25µl of LARII substrate (firefly luciferase) and 25µl of Stop&Glo substrate (sea pansy luciferase). The emitted light was detected using the Glomax Multi machine programmed to 20secs delay. Afterwards, the results were extracted as ratios of the firefly luciferase and sea pansy luciferase activity values (firefly divided by sea pansy)

and further normalized to the empty reporter vector control (promoter construct divided by the empty vector control). The final outcome was displayed in bar diagrams.

Calculation of IFNγ stimulation activity:

The efficiency of an IFNγ stimulation (presented in 3.2.24) can be calculated according to the activity of an activated gene promoter. The efficiency is the level of activity in the stimulated sample compared to the level of the corresponding unstimulated control sample (subtraction of the value of the unstimulated control from the value of the stimulated sample).

3.2.24 Stimulation of human cell lines with INFγ

Interferon gamma (IFNγ) is a secreted small protein which triggers intercellular and intracellular signaling (cytokine) cascades. It is produced by numerous cells and plays a crucial role in innate and adaptive immune responses to viral and bacterial infections. Additionally, it is important for tumor growth control and also known to be abnormally expressed in a variety of auto-inflammatory and auto-immune diseases [82]. It is used for the stimulation of Hek293T and SK-BR-3 cells for functional characterizations of the obtained mRNA Seq results after Brd4 knockdown.

Material:

- cultured cells
- human IFNγ solution (150U/µl)
- BSA control solution
- culture medium

Protocol: The cultured cells of interest were seeded as described in table 13. The human IFNγ solution and the corresponding BSA control were diluted as required in pre-warmed culturing medium. Table 14 summarizes the plating formats and necessary medium volume for the stimulation approach.

Table 21: Plating formats and corresponding volume of medium used for IFNγ stimulation. The stimulation mixture was prepared using the specified volume of culturing medium and the required amount of human IFNγ or corresponding BSA control solution.

	plating format				
	60mm	**6-well**	**12-well**	**24-well**	**96-well**
DMEM used for preparation [µl]	4,600	2,000	792	410	66.7

For example, a 100U IFNγ stimulation in a 6-well format was obtained by mixing 1.334µl of IFNγ solution with 2ml of medium. The matching negative control was prepared with the corresponding volume of BSA control solution. The plating medium on the cells was replaced by the prepared stimulation mixtures. Afterwards, the cells were incubated in the incubator until harvest at various time points.

4 Results

4.1 Brd4 knockdown in Hek293T cells

To be able to analyze and characterize cellular transcription mediated by Brd4 molecular tools such as RNA interference - leading to a reduced expression level - present an effective strategy. For this, commercially available naked small interfering RNA oligos (siRNAs) (in most cases a pool of four targeting one gene) or small hairpin RNAs (shRNAs) expressed from a vector, can be used. In both cases, the sequences match the mRNA of the gene of interest. ShRNAs can also be designed to target different transcript variants of the same gene. Brd4 exists in two isoforms differing in the presence or absence of the C-terminal domain (CTD). Figure 13 schematically shows the locations of the shRNAs used for Brd4-silencing which either target both forms ("shC2") or only the long isoform ("shE1").

Figure 13: Location of short hairpin RNAs used for Brd4 isoform specific knockdown. The mRNAs of both *Brd4* isoforms (*short* and *long*) differ in the inclusion or exclusion of a C-terminal region. ShRNA C2 ("shC2") targets the N-terminus, which is present in both Brd4 variants. ShRNA E1 ("shE1") binds to the C-terminus of the mRNA, which is only included in the long isoform.

The small hairpin RNA "shC2" recognizes the N-terminus of Brd4, resulting in a down-regulation of both transcripts. "shE1" on the other hand, attacks specifically the carboxy-terminal region of Brd4, which is only present in the long variant, leading to a knockdown of Brd4-long. As a negative control, a short hairpin RNA against the "green fluorescent protein" ("shGFP") was used.

To determine the knockdown efficiencies of the shRNAs, time curve experiments in Hek293T cells were performed and analyzed for Brd4 mRNA levels. A primer set, "Brd4-both", located at the 5' prime region of *Brd4*, detected the two different transcript variants. Within first experiments, I focused on the "shC2" knockdown because an expression profile after Brd4 knockdown using mRNA sequencing should present the starting point of this thesis.

Three days after transfection (72h) the levels of Brd4 went down to approximately twenty percent in the qPCR analysis. Four and five days after transfection the samples also showed decreased *Brd4* expressions, but not as strong as in the 72h sample set. Longer knockdowns (96-120h) might lead to a loss of the shRNA due to cell divisions or direct effects might be antagonized by evoking cellular rescue mechanisms. Thus, the knockdown after 72 hours - showing the best results in the qPCR performance - were used for Illumina-library preparation and Next Generation Sequencing (NGS).

4.2 mRNA sequencing of Brd4 knockdown in Hek293T cells

Next Generation Sequencing (NGS) technologies provide the opportunity to detect all DNA or RNA species within a tested sample set. It can be used for the detection of novel transcripts, the determination of gene expression levels and to gain information about differential splicing events. In the case of Brd4, we have used these technologies to gain a transcriptome-wide overview on associations and cellular mechanisms Brd4 is involved in. After Brd4 knockdown, RNA was isolated, libraries prepared and sequenced on an Illumina Genome Analyzer IIx. The overall Illumina mRNA sequencing statistics are summarized in table 22.

Table 22: Summary of mRNA sequencing statistics. The raw data of the mRNA sequencings are matched to the human genome version 19 ("hg19") and further analyzed for uniquely mapped fragments and fragments with unique start sites.

sample	raw reads	uniquely aligned	unique starts
shRNA "C2" (Brd4)	36,369,956	21,168,810	9,574,312
shRNA "GFP" (control)	33,446,105	19,443,356	7,975,427

Both samples were sequenced to comparable depths with 33.4 million (mio) raw reads and 19.4 mio uniquely aligned reads in the "shGFP" control and 36.4 mio raw reads and 21.2 mio uniquely aligned reads in the "shC2" Brd4 knockdown. Raw reads were mapped to the golden path version "hg19" (GRCh37) using the BWA 0.5.9 alignment tool with default parameters. Exon-wise coverages (read counts) were calculated by counting all reads which overlapped with exons by at least one nucleotide. Gene expression levels were inferred by aggregating the reads of all exons of a gene. For the total number of differentially expressed genes in the Brd4 knockdown context, the coverage for each transcript of a gene was compared to the corresponding coverage in the knockdown control,

the differences (ratios) displayed as logarithm to the basis two of the fold change (log2FC), and the differentially expressed transcripts extracted for further analysis. The candidate list was selectively narrowed down using the following cut-off criteria:

- reads per transcript of a gene in the knockdown and control sample: > 20
- p-value: ≤ 0.05
- log2 fold change (log2FC): ≥ 0.6 and ≤ -0.6

Expression ratios obtained by RNA sequencing data are usually more extreme than can be explained by a simple binomial distribution of the reads (overdispersed) [83]. To avoid these extreme ratios, we applied a minimal expression level cut-off of twenty reads per transcript. We also applied a significance threshold (p-value) below 0.05 as well as an expression difference to the control below 0.66 and above 1.58 ($|\log2FC| \geq 0.6$). These cut-off criteria assured the identification of authentic expression changes in the mRNA sequencing data. The results after Brd4 knockdown are summarized in Table 23.

Table 23: Summary of differentially expressed genes and corresponding transcripts after Brd4 knockdown mRNA sequencing. Number of differentially expressed transcripts with the following cut-off criteria: reads per transcript > 20, $p \leq 0.05$, $|\log2FC| \geq 0.6$. The genes were subsequently grouped by their orientation of differential expression.

number of transcripts	number of genes	genes down-regulated	genes up-regulated
2493	896	526/896 (59%)	370/896 (41%)

After comparing the expression levels in the knockdown sample to the corresponding control sample as well as stringency filtering of the obtained ratios, we acquired a total number of 2,493 differentially expressed transcripts belonging to 896 genes. Interestingly, 526 of those genes were found decreased and 370 candidates increased. Thus, the chosen cut-off criteria resulted in 59% downregulations and 41% upregulations.

Before performing further pathway analyses on the data set, qPCR validation experiments of the top most significantly differentially expressed genes were carried out.

4.3 Validation of the mRNA sequencing results after Brd4 knockdown

Quantitative real time PCR (qPCR) analyses present a sensitive method to detect expression changes of a gene using specific target gene amplification primers. Normalization can be performed with mRNAs which expression does not change (e.g., a housekeeping gene). QPCRs were used for the experimental validation of the obtained mRNA sequencing results.

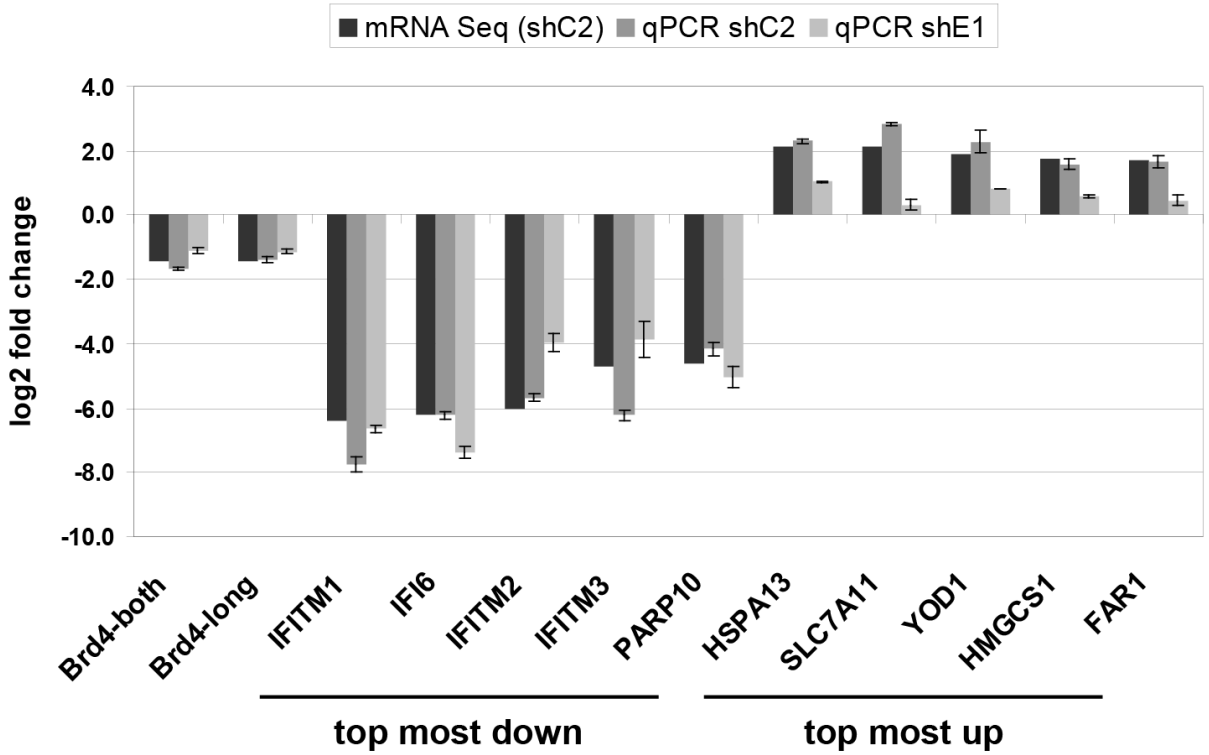

Figure 14: QPCR validations of the five top most significantly downregulated and upregulated genes in the mRNA Seq. QPCR expression analyses of two different Brd4 knockdown experiments ("shC2" and "shE1") in Hek293T cells using primer sets against the most significantly differentially expressed genes identified in the Brd4 knockdown mRNA sequencing. Normalization was performed to the housekeeping gene *HPRT1* and corresponding "shGFP" control. The results are displayed as log2 fold changes. Also displayed in log2 fold changes are the matching mRNA sequencing results. The experiments have been performed three times.

To measure the presence - or in this case the absence - of both Brd4 transcripts and separately the long Brd4 isoform, a primer-set named "Brd4-both" and one called "Brd4-long" was used, respectively. In addition, for the validation of the mRNA Seq data, primers for the top candidates were designed and tested specifically on the same sample

sets (figure 14). As knockdown approaches, shRNAs against both Brd4 isoforms ("shC2") as well as the individual decrease of Brd4-long ("shE1") were used. Taking "shE1" into the set for analysis helps to determine whether the transcriptional deregulation of a gene in "shC2" comes from the combined diminishment of both isoforms or is caused by a specific Brd4-long reduction.

As a validation of the knockdown efficiency, Brd4 was constantly downregulated - as measured by both Brd4-specific primer pairs ("Brd4-both" and "Brd4-long"). For all tested genes we found a very good correlation between the mRNA Seq data and the qPCR results for "shC2" (Spearman correlation coefficient (ρ) = 0.99). The Spearman correlation is presented in figure 15.

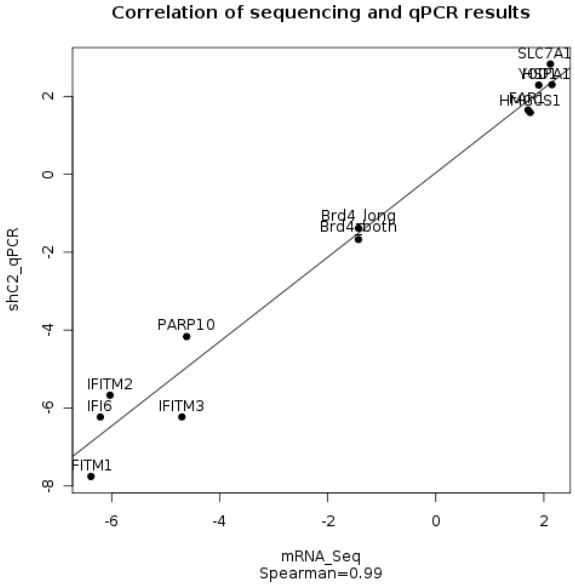

Figure 15: Spearman correlation of the mRNA Seq data and qPCR validations of the most significantly differentially expressed genes after Brd4 knockdown. The Spearman correlation coefficient was calculated using the expression levels of the most significantly differentially expressed genes in the mRNA Seq, determined by qPCR, and the corresponding log2 fold changes in the sequencing data.

Interestingly, "shE1" caused effects like "shC2" on the downregulated genes, but not on the upregulated ones. Here, Brd4 "shE1" knockdown did not result in a corresponding increase of the investigated genes which might indicate an isoform-specific transcriptional regulation. The most significantly downregulated gene detected in the sequencing experiment was interferon induced transmembrane protein 1 (*IFITM1*) with a log2FC of -6.38, corresponding to a 98.8% decreased level. The most significantly upregulated gene was the heat shock protein 70kDa family member 13 (*HSPA13*) with an increase of 4.45 fold (log2FC of 2.15). Besides *HSPA13*, only YOD1 (OTU deubiquinating enzyme 1 homologe (*S. cerevisiae*)) elevated above log2FC > 0.6 in the qPCR validation of the long form knockdown ("shE1") and thus should also be detectable in a mRNA Seq experiment with above mentioned cut-off criteria.

These qPCR analyses validated our generated list of differentially expressed genes identified through Next Generation Sequencing and accentuated some differences between the long and short Brd4 variants.

4.4 Gene expression overlap analysis with Myc target genes and identification of essential genes in Myc-driven cancers

Brd4 is known to regulate Myc expression with subsequent effects on its target genes [54, 61]. A knockdown and inhibition of Brd4 correlates with decreased Myc and target gene levels [22, 23, 24, 66]. Although Myc expression was not significantly impaired in our mRNA sequencing results, its level was still going down approximately twenty percent, compared to the negative control. To screen potential consequences of the expression change of Myc on its target genes, an overlap analysis of the 896 differentially expressed genes after Brd4 knockdown and a list providing 9,234 Myc target genes [84] was performed. The resulting overlap is summarized in table 24.

Table 24: Overlap analysis of Myc targets and deregulated genes after Brd4 knockdown. Identification of differentially expressed Myc target genes in the mRNA sequencing after Brd4 knockdown. The list of Myc targets was extracted from SABioscience [84]. Presented are the overlapping genes, the total number of deregulated genes after Brd4 knockdown as well as the percentage of the overlap.

overlapping genes/ all deregulated genes (% of overlap)	**downregulated all deregulated genes (% of overlap)**	**upregulated all deregulated genes (% of overlap)**
351/896 (39%)	244/351 (70%)	107/351 (30%)

The overlap analysis resulted in 351 Myc target genes which appeared differentially expressed in our Brd4 knockdown sequencing. Approximately 70 percent (244/351) of these genes showed a lower expression level than in the control sample and 107 of the 351 genes in total (30%) an upregulation. Differentially expressed non-Myc targets were distributed equally in either direction. Approximately 50% (282/545) upregulations and 50% (263/545) downregulations. Therefore, the group of down regulated Myc targets was, in comparison to the differentially expressed non-Myc associated genes, significantly enriched in the analyzed sample set (odds ratio (OR) = 2.12, p-value $< 1.3\text{x}10^{-7}$, CI

1.569-2.85). The more than twofold enrichment of decreased Myc target genes confirmed the connection between Brd4, Myc, and Myc target genes.

The oncogene Myc shows an increased expression in a variety of human tumors and presents a central driver of tumor progression [85, 86, 22]. Two independent groups performed siRNA library screens to identify essential tumor growth related genes in Myc-driven cancers. They identified 403 [23] and 101 [24] candidates, respectively, whose knockdown was accompanied by a severe growth reduction of tumor cells. Interestingly, Brd4 was the only gene present in both analyses. Next, we investigated if other essential Myc-driven cancer genes overlapped with our knockdown mRNA sequencing. The results are presented in table 25.

Table 25: Study of essential tumor growth genes in Myc-driven cancers with Brd4 dependency. Overlap analyses of essential tumor growth genes in Myc-driven cancers identified by Kessler *et al.* [23] and Toyoshima *et al.* [24] with the list of decreased genes in the Brd4 knockdown mRNA sequencing. Additional information on Myc affiliation is provided.

Kessler *et al.* 403 candidates		**Toyoshima *et al.* 101 candidates**	
overlap	**Myc target**	**overlap**	**Myc target**
BRD4	no	*BRD4*	no
CORO7	yes	*MATK*	yes
DTD1	yes	*PCBD1*	no
KCNC4	no	*POLR2l*	yes
LHX2	yes		
RTN3	no		

In total, six essential tumor growth related genes from the Kessler *et al.* list and four genes identified by Toyoshima *et al.* were significantly decreased in the Brd4 knockdown situation, presenting a mixture of Myc and non-Myc targets. Loosening the cut-off stringency for the Brd4 knockdown mRNA sequencing data to a p-value below 0.1 (part 4.2) provided us with three additional candidates with positive coupling to the Brd4 level (*ALKBH7*, *FSD1* and *KREMEN1*) from the Kessler *et al.* screen. The identified overlap between both lists of essential tumor growth genes highlights the importance of Brd4 as a potent therapeutic candidate in Myc-driven cancers.

Having approved the validity of our sequencing results, the list of differentially expressed genes after Brd4 knockdown was submitted to general pathway and protein complex analyses using “Ingenuity” and “ConsensusPathDB” software tools.

4.5 Pathway analyses of differentially expressed genes after Brd4 knockdown

4.5.1 Ingenuity pathway analysis (IPA) of Brd4 knockdown mRNA sequencing

Pathway analysis tools present a useful method to gain a general view on connections and enriched pathways in large data sets generated by microarrays and Next Generation Sequencing experiments. They interrelate submitted lists - for example differentially expressed genes and their corresponding fold changes - to already existing data and create information about pathways which are most commonly affected. Ingenuity pathway analysis assigns the identified targets to cellular categories such as "Diseases and Disorders", "Molecular and Cellular Functions" and "Canonical Pathways" and provides the outcome in visualizable form. The top canonical pathways identified in the Brd4 knockdown mRNA Seq are shown in figure 16.

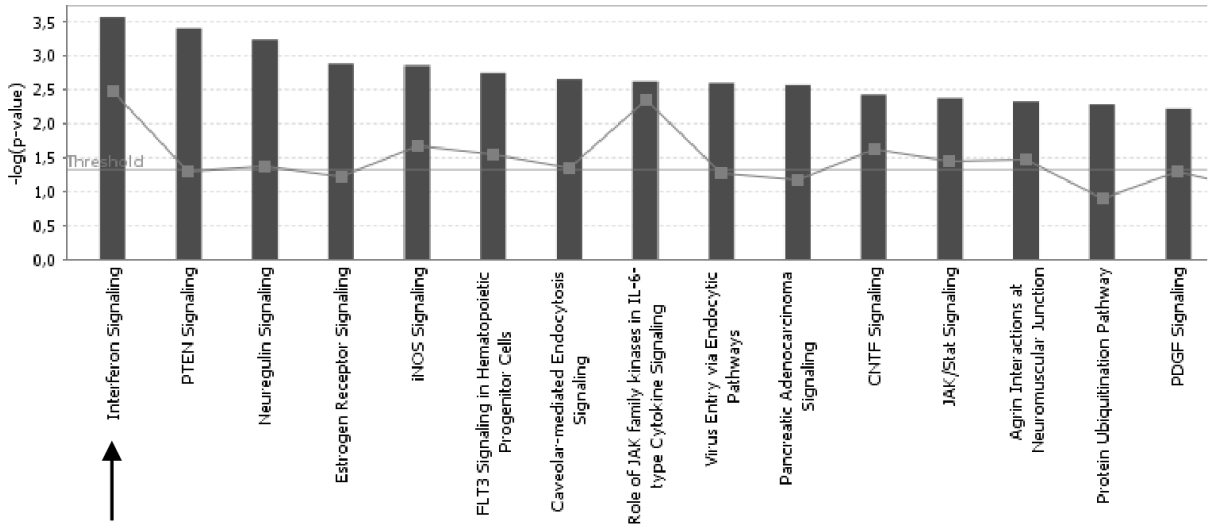

Figure 16: Overview of affected canonical pathways in the Brd4 knockdown mRNA sequencing. The most significantly affected canonical pathways identified by the Ingenuity Pathway Analysis tool (IPA) in the Brd4 knockdown mRNA sequencing are ranked according to the identified number of differentially expressed members in a specific pathway in relation to the total number of genes belonging to that specific pathway (figure generated with IPA).

"Interferon Signaling" was the top most significantly affected pathway in the sample set followed by "PTEN-", "Neuregulin-" and "Estrogen Receptor Signaling". Hence of that

finding Brd4 seems to have an impact on a large number of different signaling events from the cell membrane down to the point of intrinsic transcriptional regulation. Pathway visualizations provided by IPA - such as shown in figure 17 - highlight the involved participants in a color code manner - green for a downregulation and red for an upregulation - plus their cellular location at one glance and help to predict a possible outcome, whether a signaling is turned on or silenced in the analyzed context. The interferon (IFN) pathways (alpha (α), beta (β) and gamma (γ)) and their regulations are shown in figure 17.

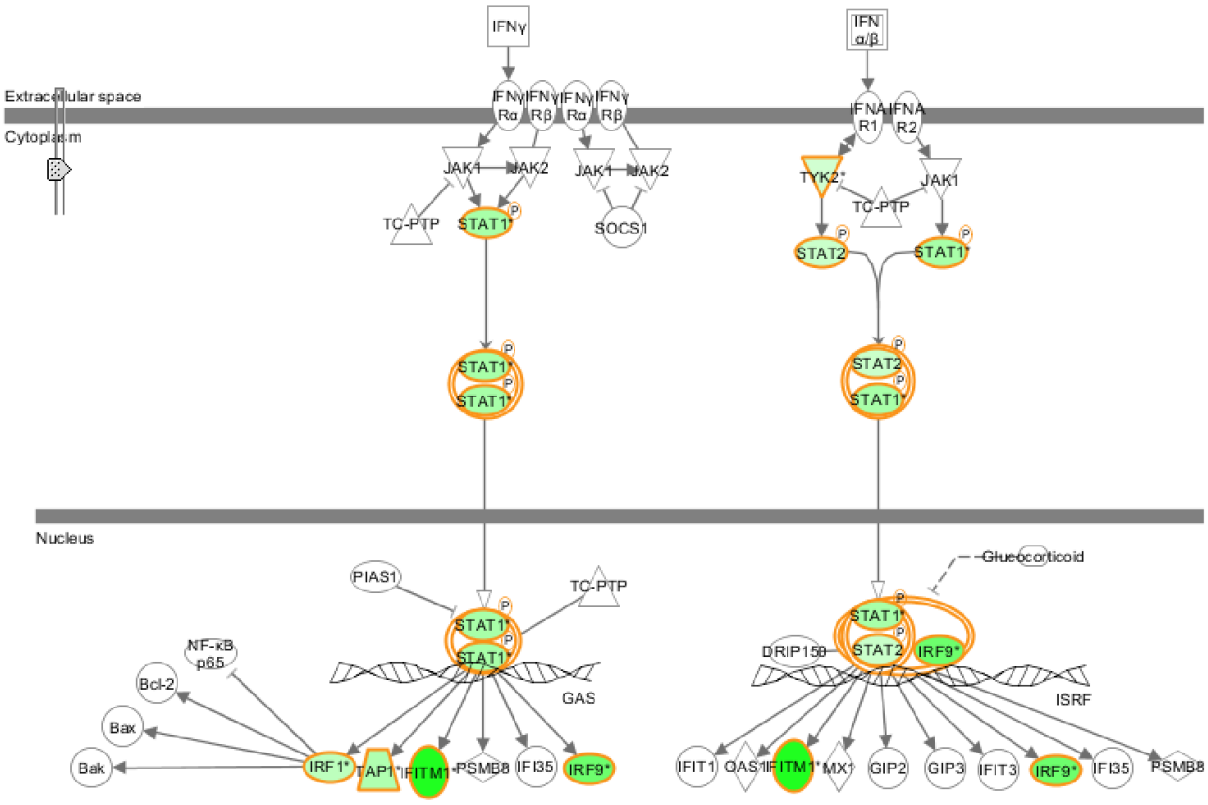

Figure 17: Visualization of the interferon pathways in the mRNA Seq data after Brd4 knockdown. The canonical pathway "Interferon Signaling" is divided in two distinct groups: Interferon alpha and beta signaling (IFNα/β) as well as interferon gamma signaling (IFNγ). IFNα/β is mediated by a hetero-dimer of phosphorylated (p) STAT1 and STAT2, IFNγ by a homo-dimer of phosphorylated STAT1. Both cascades of interferon signaling transcriptionally activate target genes which are partly in common, but also different. The color green highlights downregulations identified in the submitted Brd4 knockdown mRNA sequencing data set (figure generated with Ingenuity Pathway Analysis IPA).

The IPA graphic illustrated that the, through phosphorylation activated signal transducer and activator of transcription 1 (STAT1) homo-dimer - the central complex in interferon gamma (IFNγ) signaling - as well as the hetero-dimer consisting of STAT1 and STAT2 -

being active in interferon alpha and beta (IFNα/β) signaling - were both downregulated in the submitted mRNA Seq after Brd4 knockdown. In addition, also the STAT1/2 target genes (e.g., interferon regulatory factor 1 (*IRF1*) and interferon regulatory factor 9 (*IRF9*)) were decreased, which leads to the assumption of silenced STAT1/2 signaling cascades from the cytoplasm down to the nucleus.

Further down in the list of "Canonical Pathways" summarized in figure 16 one finds additional cascades depending on STAT1 such as "IL-6-type Cytokine Signaling" and "JAK/STAT signaling". They also showed significant downregulations of STAT1 target genes. Signaling events depending on the presence and activation of STAT1 therefore seem to be significantly affected by the low Brd4 levels. To further support the idea of this important Brd4 and STAT1 dependency additional pathway analyses were run using ConsensusPathDB.

4.5.2 ConsensusPathDB (CPDB) pathway analysis of Brd4 knockdown mRNA sequencing

The ConsensusPathDB tool provides, in contrast to the Ingenuity tool, also information on protein complexes and their impairment in a submitted data set. The three top most significantly affected pathways were again "interferon α/β signaling", "type II interferon signaling (IFNγ)" and "interferon signaling" in general, which supported the dependency of these signaling events on the Brd4 level. Table 26 brings together the protein complexes STAT1 is known to be involved in, the number of generally assigned as well as identified members in the specific complex and the source of identification.

Similar to the Ingenuity pathway analysis STAT1 was found complexed with STAT2 and IRF9 - here identified at the *ISG15* promoter - and also with STAT3 in a hetero-duplex in the context of regulating the *IRF1* and *FOS* target genes.

Both pathway analyses stated a profound interconnection of the STAT proteins and the Brd4 expression. Before going into more detailed analyses and the identification of the functional significance in the cell, the reduced STAT1 levels were validated in qPCR and Western Blot experiments.

Table 26: ConsensusPathDB identified impaired STAT1 complexes in the mRNA Seq after Brd4 knockdown. The ConsensusPathDB pathway analysis tool identified affected protein complexes containing the STAT1 protein in the submitted Brd4 knockdown mRNA sequencing data set. The tool combines information from databases such as "InnateDB" and "Reactome". Additionally displayed are the protein complex sizes as well as their identified and differentially expressed complex members (table extracted from CPDB [87]).

complex name	candidates identified in complex size	complex source
STAT1, STAT2 and IRF9 complex with the ISG15 promoter	4/4 (100%)	InnateDB
STAT1 and STAT3 complex with the IRF1 promoter	3/3 (100%)	InnateDB
STAT1 and STAT3 complex with the FOS promoter	3/3 (100%)	InnateDB
p-STAT2:p-STAT1:p-IFNAR1:p-TYK2	3/4 (75%)	Reactome
p-STAT2:p-STAT1	2/2 (100%)	Reactome
p(Y701)-STAT1, p(Y705)-STAT3 dimer	2/2 (100%)	Reactome

4.6 Validation of low STAT1 levels after Brd4 knockdown

As already mentioned in part 4.3, qPCR analyses using primers for specific mRNAs present a reliable validation technique for the obtained mRNA sequencing results. Additionally, they appeared to be very specific (figures 14 and 15). Proteins are the functional signaling molecules in the cell. Therefore, the corresponding STAT1 level was also analyzed on Western Blot. For the validation of its reduction after Brd4 knockdown an antibody was used specifically detecting both known isoforms of STAT1 - STAT1α (750 amino acids, 91kDa) and STAT1β (712 amino acids, 84kDa). The qPCR as well as the Western Blot results are shown in figure 18.

As seen in the mRNA Seq results the *STAT1* level appeared decreased in the qPCR after knocking down Brd4. This held also true for the protein level where less protein was detectable in the knockdown situation in comparison to the corresponding negative control. Due to the small size difference between STAT1α and STAT1β, the two isoforms were not distinguishable.

To capture the entire impact of low STAT1 levels in the Brd4 mRNA sequencing, an overlap analysis of the sequencing data and the known and predicted STAT1 target genes was performed. The list of targets was extracted from SABiosciences [84].

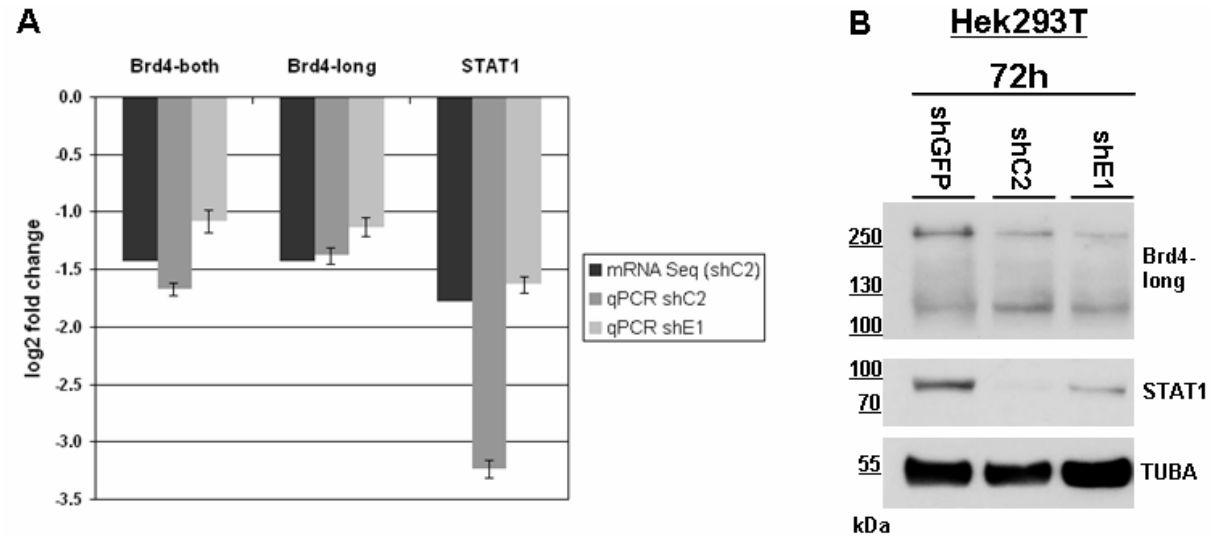

Figure 18: Validation of decreased STAT1 after Brd4 knockdown. (A) QPCR expression analyses of two different Brd4 knockdown experiments ("shC2" and "shE1") after 72h in Hek293T cells using primer sets against *Brd4* and *STAT1*. Normalization was performed to the housekeeping gene *HPRT1* and the corresponding "shGFP" control. The results are displayed as fold changes. (B) Detection of Brd4-long and STAT1 protein levels after knockdown (72h) of both Brd4 variants ("shC2") and the single knockdown of the long isoform ("shE1") as well as the "shGFP" control sample in Hek293T cells. TUBA (tubulin A) was used as a loading control. The experiments have been performed three times and a representative plot is shown.

4.7 Overlap of Brd4 knockdown and STAT1 target gene lists

The web page by SABiosciences (QIAGEN) [84] was used as a reference for the overlap analysis of the transcription factor STAT1 associated genes with the results of the Brd4 knockdown sequencing. The platform provided a list of 8,512 target genes for STAT1. Of those, 322 also appeared in the Brd4 knockdown mRNA Seq which accounted for 3.8% of all known and proposed STAT1 targets. However, here one needs to take into account that not all genes were identified in the sequencing experiment. The calculation of the overlap in relation to the 896 differentially expressed genes identified in the mRNA Seq are depicted in figure 19.

Here, 36% (322/896) of all genes detected by mRNA sequencing were STAT1 target genes. Of these, 219 (68%) were downregulated in the low Brd4 context and 103 (32%) showed a significant increase. The downregulated STAT1 targets presented in comparison to the differentially expressed non-STAT1 target genes a significantly enriched group within the Brd4 knockdown (OR = 1.85, p-value $< 2.2\text{x}10^{-5}$, CI = 1.377 - 2.490). The overlapping

322 genes identified in the mRNA sequencing belonged to pathways such as "Interferon Signaling" with 6 deregulated candidates after Brd4 knockdown out of 36 members in total (6/36), "iNOS Signaling" (7/53) and "Pancreatic Adenocarcinoma Signaling" (8/120). The three mentioned top significant pathways identified by Ingenuity Pathway Analysis rely on the STAT1 protein as a mediator of signaling which itself was found decreased in the tested sample set. Therefore, Brd4 seems to regulate the expression of STAT1 which in turn affects the transcriptional activation of its target genes.

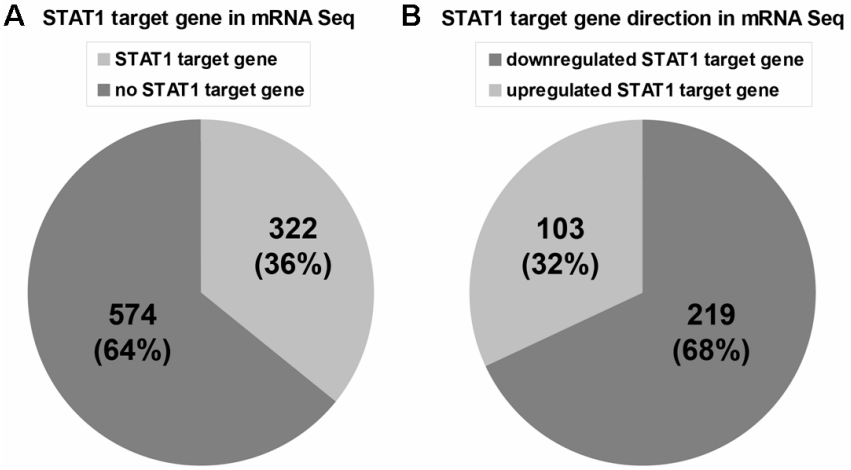

Figure 19: Overlap of STAT1 target genes and the Brd4 knockdown mRNA Seq data. (A) Identification of differentially expressed STAT1 target genes in the mRNA sequencing data after Brd4 knockdown. The list of STAT1 targets was extracted from SABiosciences [91]. (B) Direction of differential expression of STAT1 target genes identified in (A).

Before performing functional characterizations of the novel connection between Brd4 and STAT1 as well as its dependent targets, further STAT1 target genes were validated in the Brd4 knockdown situation.

4.8 Validation of STAT1 target genes in the context of low Brd4 levels

QPCR validations - aiming specifically at the STAT1 target genes - were performed in Hek293T cells using the two different established Brd4 knockdown approaches: "shC2" (against both isoforms of Brd4) and "shE1" (individual decrease of the long Brd4 isoform). Figure 20 gives an overview of the collected results and specifically highlights the interferon stimulated genes (ISGs) within the group of STAT1 targets.

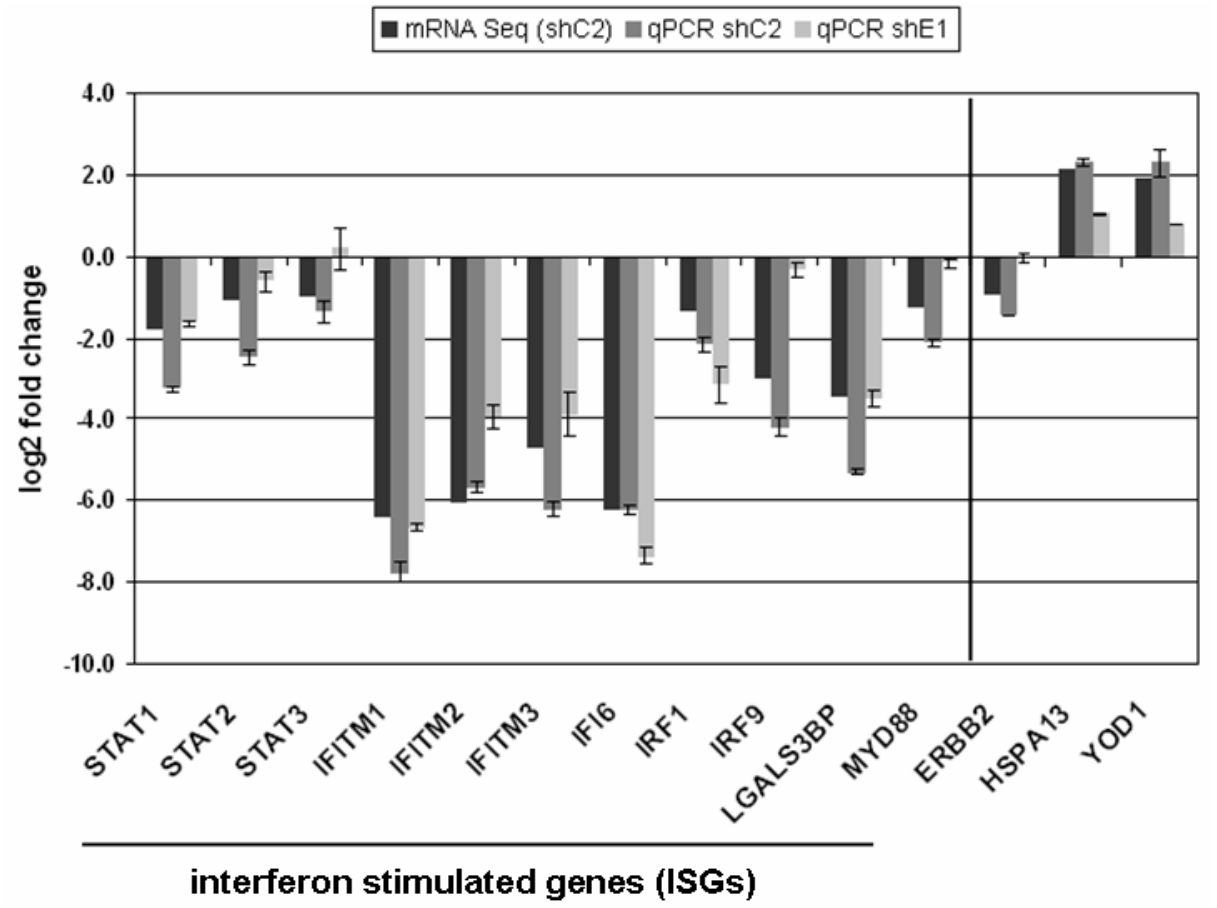

Figure 20: QPCR validation of STAT1 target genes after Brd4 knockdown in Hek293T cells. QPCR expression analyses of STAT1 target genes after two different *Brd4* knockdown experiments ("shC2" and "shE1") in Hek293T cells. Normalization was performed to the corresponding "shGFP" control and the housekeeping gene *HPRT1*. The results are displayed as log2 fold changes. Also displayed as log2 fold changes are the matching mRNA sequencing results. The experiments have been performed three times and a representative plot is shown.

The "shC2" analyses confirmed the mRNA Seq results in Hek293T cells with a high correlation between the two experiments (Spearman correlation coefficient = 0.97). The qPCR results showed a significant deregulation of the tested STAT1 target genes, with accentuation on the downregulated group of interferon stimulated genes (ISGs). The high correlation between the qPCR validations and the mRNA Seq data additionally stated the significance of our obtained data set. The "shE1" knockdown showed, in the majority of the analyzed candidates, the same regulation as the combined "shC2" knockdown. However, for *STAT2*, *STAT3*, *IRF9*, *MYD88* as well as *ERBB2* the results for the "shE1" knockdown were different.

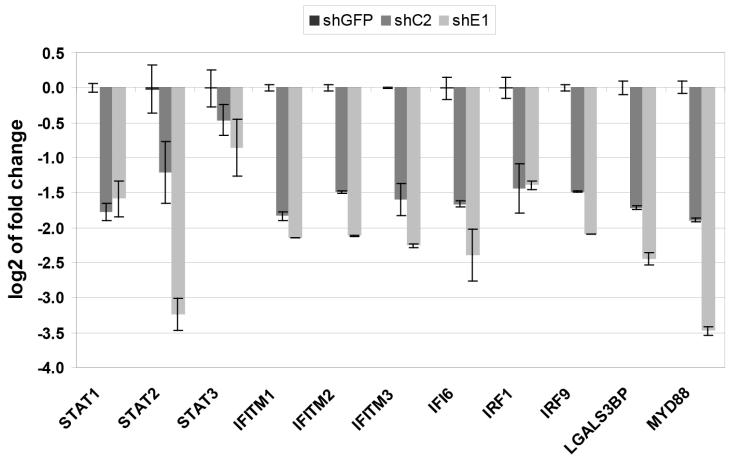

Figure 21: QPCR validations of STAT1 target genes after Brd4 knockdown in Wi38 cells. QPCR expression analyses of interferon stimulated STAT1 target genes in two different Brd4 knockdown experiments ("shC2" and "shE1") performed in Wi38 cells. Normalization was performed to the housekeeping gene *HPRT1*. The results for the "shGFP" control were set to one. The results are displayed as log2 fold changes. The experiments have been performed twice and a representative plot is shown.

The experiment was recapitulated in a second cell line, Wi38 (lung fibroblast cell line), focusing specifically on the interferon stimulated STAT1 target genes. The qPCR results are illustrated in figure 21.

The lung fibroblast cell line Wi38 confirmed in almost all cases the connections identified in the Hek293T cell line. In the presence of a Brd4 knockdown the transcription factor STAT1 repeatedly decreased as well as its target genes.

Having confirmed the mRNA Seq results in different cell lines functional experiments were performed to further characterize the connection between Brd4 and STAT1.

4.9 Analyzing STAT1 and its target genes after Brd4 overexpression

Having identified the connection between low Brd4 levels and decreased STAT1 expression the question arose if STAT1 is increased in a high Brd4 state? Brd4-long overexpression experiments were carried out in Hek293T and Wi38 cells. The results of the corresponding Western Blots and qPCR analyses are shown in figure 22.

Both, STAT1 mRNA as well as protein levels were upregulated after an increased Brd4 expression as shown by the approximately threefold elevation in both experiments.

An upregulation of STAT1 would also implicate an increase of its target genes. Their expression levels were therefore tested by qPCR analyses and presented in figure 23.

In Hek293T and Wi38 cells an elevation of the expression levels of the interferon stimulated STAT1 target genes was detectable. These findings furthermore approved the transcriptional dependency of STAT1 on Brd4.

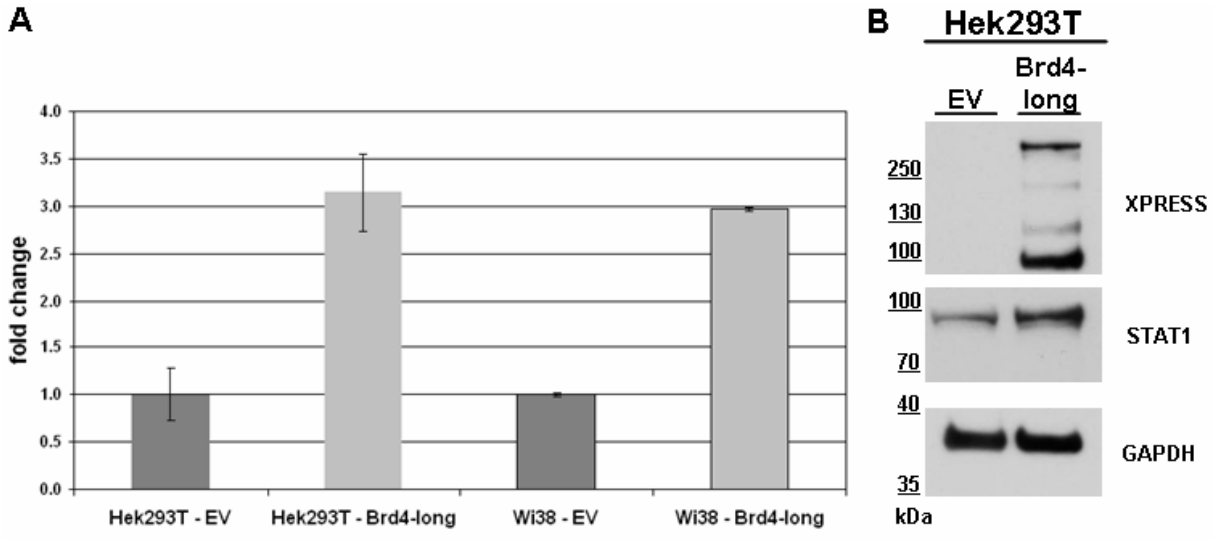

Figure 22: STAT1 expression analyses after Brd4-long overexpression. (A) QPCR expression analyses of *STAT1* after Brd4-long overexpression in Hek293T and Wi38 cells for 48h. As control an empty vector ("EV") was used. Normalization was performed to the housekeeping gene *HPRT1*. The results for the "EV" control were set to one. The results are displayed as fold changes. (B) Detection of Brd4-long and STAT1 protein levels in Hek293T cells overexpressing Brd4-long or the empty vector control ("EV") for 48h. Brd4 was detected using an antibody against the fused XPRESS tag and STAT1 using an antibody recognizing both isoforms (α and β). GAPDH (glyceraldehyde-3-phosphate dehydrogenase) was analyzed as a loading control. The experiments have been performed three times and representative plots are shown.

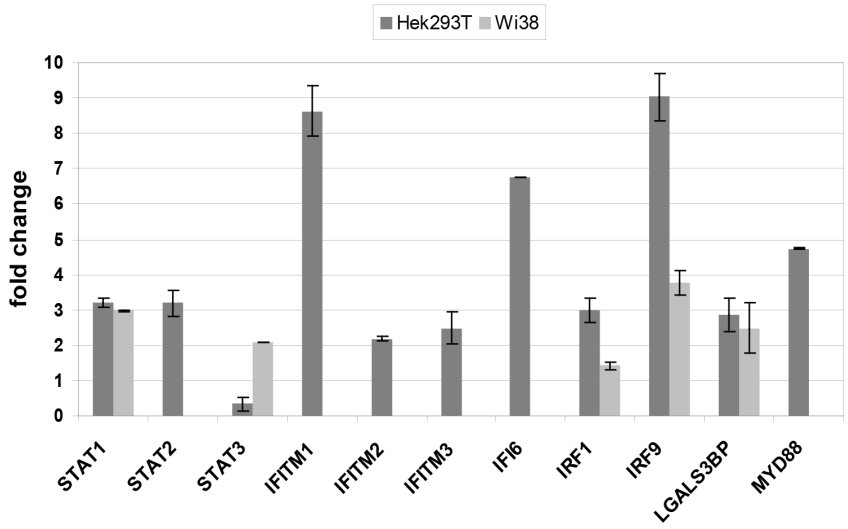

Figure 23: STAT1 target gene expressions after Brd4-long overexpression. QPCR analyses of Brd4-long overexpression for 48h in Hek293T and Wi38 cells. Normalization was performed to the housekeeping gene *HPRT1* and the corresponding empty vector ("EV") control. The results are displayed as fold changes. The experiments have been performed three times and a representative plot is shown.

So far it was possible to show that the expression of Brd4 and STAT1 correlated. The question now remained if Brd4 transcriptionally regulated STAT1. For this luciferase reporter assays of the STAT1 promoter were carried out in the cell culture system.

4.10 *STAT1* promoter analyses

Luciferase reporter assays present an established method to analyze promoter activities. The UCSC Genome Browser helps to define the promoter region of a gene by extracting the DNA sequence. It additionally shows already existing tracks of performed transcription factor chromatin immunoprecipitations which illustrate whether a specific binding site is included in the region of interest or not. For the analyses of the *STAT1* promoter two constructs, differing in their size and the inclusion of specific binding sites, were created. An overview on the size ranges is illustrated in figure 24.

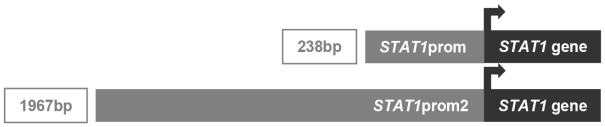

Figure 24: *STAT1* promoter constructs. Illustration of the two cloned fragments of the *STAT1* promoter. The arrows indicate the transcription start site (TSS) of the gene, dark gray indicates the gene itself and light gray the corresponding promoter fragment cloned for luciferase reporter analyses.

The experiments were performed in Hek293T cells and followed the questions whether the STAT1 promoter is less active in the Brd4 knockdown situation and shows enhanced transcription with Brd4-long being overexpressed. The results for the knockdown are shown in figure 25.

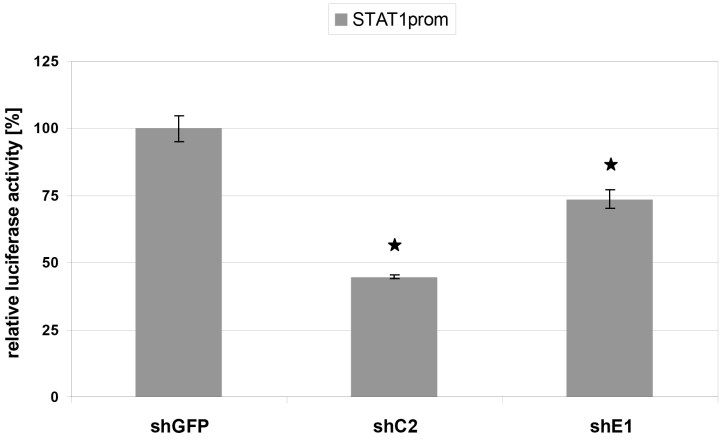

Figure 25: *STAT1* promoter activity after Brd4 knockdown. *STAT1* promoter activity reporter assays of the 238bp construct ("*STAT1*prom") in two different Brd4 knockdowns ("shC2" and "shE1", both for 72h) in Hek293T cells. Normalization was performed to the co-expressed *Renilla reniformis* luciferase and the corresponding empty reporter vector. The *STAT1* promoter activity level of the knockdown control "shGFP" was set to 100%. Stars indicate p-values < 0.05. The experiments have been performed three times and a representative plot is shown.

Using the short *STAT1* promoter construct (STAT1prom), the *STAT1* promoter activity was significantly decreased in the two Brd4-both ("shC2") and Brd4-long ("shE1") knockdown experiments. This correlates with the corresponding STAT1 qPCR and Western Blot results which showed a decrease in the STAT1 expression (figure 18).

For the experimental set-up of the Brd4-long overexpression also the short STAT1 promoter construct was used in Hek293T cells. Due to the contradictory results of this fragment, the long promoter region (STAT1prom2) was additionally applied for testing. The results are depicted in figure 26.

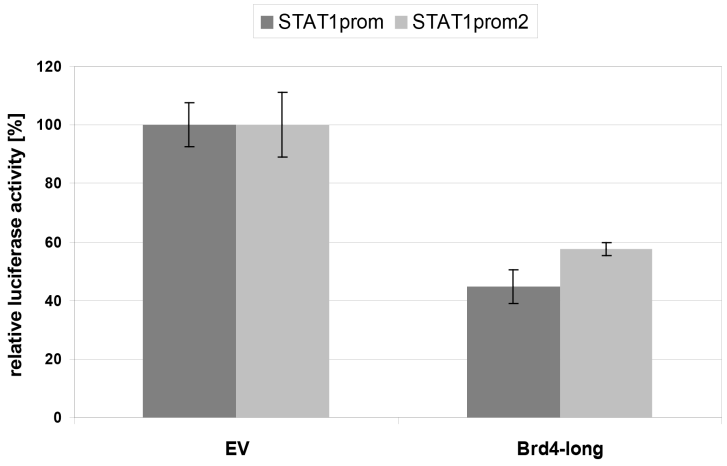

Figure 26: *STAT1* promoter activity after Brd4-long overexpression. *STAT1* promoter activity reporter assays of two generated constructs ("*STAT1*prom" and "*STAT1*prom2") after Brd4-long overexpression for 48h in Hek293T cells. Normalization was performed to the co-expressed *Renilla reniformis* luciferase and the corresponding empty reporter vector. The *STAT1* promoter activity level of the overexpression control "EV" was set to 100%. The experiments have been performed three times.

The activity of the short and also the long *STAT1* promoter fragment showed a reduction in the Brd4 overexpression experiments in comparison to the corresponding controls. This finding is contrary to the obtained expression results which highlight a positive correlation of STAT1 and the Brd4 level (see figure 22). Finding the *STAT1* promoter differently regulated after Brd4 overexpression could potentially be due to the artificial design of the experimental set-up, where only certain genomic sequences are analyzed for their activity. Surrounding regions, as present in the global genomic context, are not included.

Nevertheless, to answer the question of a directly regulated *STAT1* expression by Brd4 chromatin immunoprecipitation sequencings using Brd4 as a target were performed.

4.11 Chromatin immunoprecipitation (ChIP Seq) of Brd4

Chromatin immunoprecipitation (ChIP) experiments were carried out in Hek293T. The first ChIP Seq was performed using an antibody against the long Brd4 isoform, detecting amino acids (aa) 1347-1362 in the C-terminal domain (CTD) of the protein ("ChIP Seq Brd4 output 1"). As a reference, the "Input" material before chromatin immunoprecipitation was used ("ChIP Seq Input"). In the second ChIP Seq set-up a different Brd4-long antibody was used, this time detecting aa 1100-1200 in the CTD ("ChIP Seq Brd4 output 2"). Also employed were antibodies recognizing the N-terminus of stalled and active RNA polymerase II ("ChIP Seq RNA Pol II output") and rabbit IgG ("ChIP Seq IgG output") as an unspecific enrichment control.

The sequencing runs were performed on the Illumina platform and provided the outcome summarized in table 27.

Table 27: Summary of the ChIP sequencing statistics. The raw data of the ChIP sequencing runs were matched to the human genome version 19 ("hg19") and further analyzed for uniquely mapping reads and unique start sites.

ChIP Seq sample	raw reads	uniquely aligned	unique starts
Input	13,384,584	7,606,296	5,074,437
Brd4 output 1	14,661,117	9,627,955	8,568,641
Brd4 output 2	27,051,029	19,236,244	18,915,640
RNA Pol II output	29,518,530	21,117,248	20,703,534
IgG output	33,337,799	23,009,417	22,575,405

Each ChIP Seq sample was sequenced to similar depths in the corresponding set of two and three, respectively. The first set of sequencings varied between 7.6 to 9.6 million (mio) uniquely aligned reads and the enrichment set of Brd4, RNA Pol II and IgG showed a variation from 19.2 to 23.0 mio unique reads. Further alignments were carried out using the BWA 0.5.9 software tool and the human genome 19 ("hg19") as a mapping reference. The ChIP Seq peaks were called using MACS v1.4 [88] and the ChIP Seq subpeaks with PeakSplitter v1 [89]. A subpeak was associated to a transcription start site (TSS) if at least one base of the peak was within the range of 500bp upstream of a TSS. The results were loaded in the UCSC Genome Browser for the visualization of the read location. In the first experiment the peaks specifically enriched by Brd4-long were normalized to the peaks prior to enrichment; in the second set to the unspecific rabbit IgG control. In detail, local coverage profiles were compared for the Brd4-long ChIP Seqs and the

corresponding controls with a sliding window approach. The resulting coverage ratios were evaluated using a Poisson model to calculate the p-values. Peak candidates with p-values lower than 10^{-5} were further compared to a surrounding 10kb window to correct for the influence of local biases. An overview of the identified and overlapping genomic regions in both Brd4-long ChIP sequencings is shown in table 28.

Table 28: Overlap of two Brd4-long ChIP sequencings. The ChIP sequencings of the long Brd4 isoform revealed specific enrichment in promoter or exonic regions of certain genes, but in the majority of the cases identified both occurrences simultaneously.

ChIP Seq	genes total	in promoter	in exon	in both
Brd4 output 1	1669	176	323	1170
Brd4 output 2	701	57	67	577
overlap	**224**			

In total, 1669 Brd4-long target genes were found in the first set of ChIP sequencings with 176 genes (11%) with exclusive binding in the promoter region, 1170 genes (70%) with promoter as well as exon associations and 323 genes (19%) with locations only in the exonic context.

The list of genes identified in the second set of ChIP Seqs comprised 701 targets with 57 genes (8%) with Brd4 binding sites located in the promoter, 577 (82%) in the promoter and exons and 67 (10%) specifically in the exons. We found an overlap of 224 genes in both Brd4 sequencings, disregarding promoter or exon binding. Thus, these genes were identified twice in independent experimental set-ups and are our most promising candidate target genes of the long Brd4 isoform. The discrepancy of our chromatin immunoprecipitation sequencing data sets might be due to the use of different antibodies against the Brd4-long isoform. They probably vary in their overall functionality in the experimental cross-linked chromatin set-up. In addition, the different normalization strategies used for the identification of target genes possibly also led to the deviating results.

Recently, in August 2012, G. LeRoy and colleagues published a ChIP sequencing of Brd4-long overexpression in Hek293 cells [90]. To identify genes in common and different between our two endogenous (2146 genes in total) and their overexpressed Brd4-long ChIP sequencing (5495 genes in total) overlap analyses were performed using a combined list of our two ChIP sequencings, with the duplex genes only counted once, as well as each ChIP Seq investigated separately. The results are pictured in figure 27.

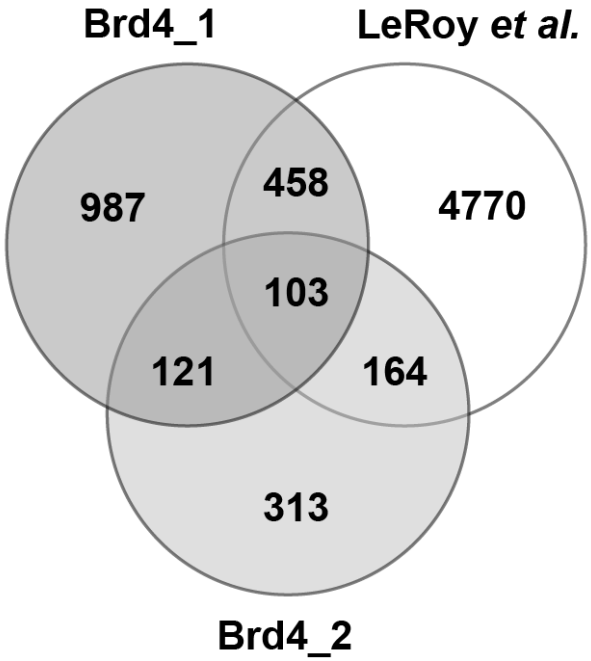

Figure 27: Overlap analyses of two endogenous and one overexpressed Brd4-long ChIP sequencings. Identification of enriched genes in two endogenous ChIP sequencings of Brd4-long in Hek293T cells (Brd4_1 and Brd4_2) and in the ChIP Seq performed by LeRoy *et al.* in 2012 using Hek293 cells with an overexpression of the long variant of Brd4. Brd4_1 indicates our first endogenous ChIP Seq, Brd4_2 the second.

Table 29: Pathway analysis of the overlap of three Brd4 ChIP Seqs. ConsensusPathDB (CPDB) pathway analysis of the overlapping 103 Brd4-long target genes which were identified between our two endogenous and the LeRoy *et. al.* Brd4-long overexpression ChIP Seq. Presented are the top pathways, the number of identified genes in the specific pathway as well as the corresponding gene names.

pathway names			
chromosome maintenance	**mRNA splicing**	**G1/S transition**	**microRNA (miRNA) biogenesis**
HIST2H2BE	*SNRPB*	*CDKN1B*	*DICER*
HIST1H2AK	*SNRPD3*	*MCM5*	*DGCR8*
HIST2H4B	*HNRNPUL1*	*CDC25A*	identified members:
HIST1H4E	*HNRNPH1*	identified members:	**4 out of 12**
HIST2H4A	identified members:	**3 out of 63**	**p = 8.45x10^{-4}**
HIST2H4A	**4 out of 126**	**p = 7.10x10^{-3}**	
HIST1H2BN	**p =5.49x10^{-3}**		
HIST2H2AC			
HIST1H2BJ			
identified members:			
8 out of 115			
p = 6.25x10^{-7}			

Our combined list of 2,146 associated genes showed approximately 34 percent (725 of 2,146) overlap with the data set provided by LeRoy *et al.* The overlap with our first Brd4-long ChIP Seq ("Brd4_1") specifically accounted for 458 of the 725 genes and the

comparison with our second sequencing ("Brd4_2") contributed 164 uniquely identified genes. Most interestingly, 103 target genes were found in all three Brd4-long ChIP sequencings. The results of the ConsensusPathDB pathway analysis of these candidates are presented in table 29.

The ConsensusPathDB analysis of the 103 target genes identified in all three Brd4 ChIP Seqs revealed an affiliation to pathways, such as "chromosome maintenance", "mRNA splicing", "G1/S transition", and "microRNA (miRNA) biogenesis".

Another interesting fact about the data set generated by LeRoy *et al.* was the identification of the *STAT1* gene as Brd4-long target [90] which validated our previous findings. Figure 28 shows the UCSC Genome Browser visualization of the *STAT1* gene in both of our endogenously performed ChIP Seq experiments as well as the data generated by LeRoy *et al.*

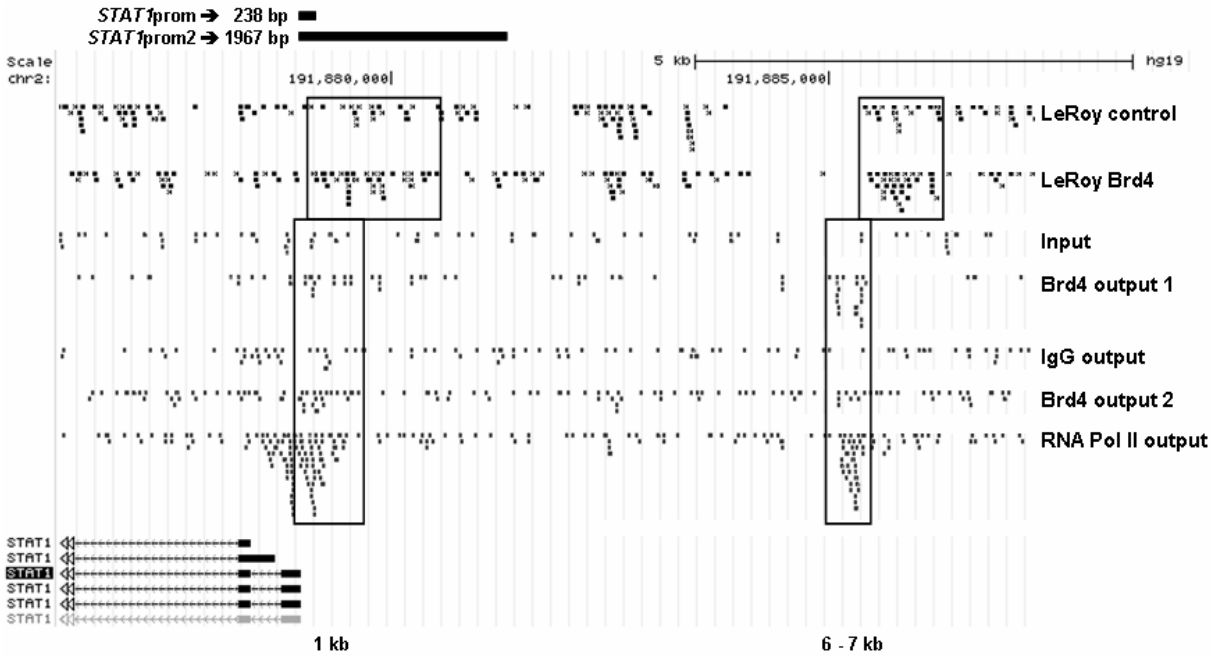

Figure 28: UCSC Genome Browser visualization of the *STAT1* gene in three different ChIP Seq set-ups. The black dots/bars (reads) indicate the enriched sequences identified by ChIP Seq matching the human genome ("hg19"). The solid black boxes at the bottom illustrate the exons of the *STAT1* gene and the dashed lines the intronic regions as well as its orientation. The *STAT1* gene is read out from the reverse strand of the DNA. Specific enrichment by Brd4-long is highlighted by frames and the number below indicates the distance from the transcription start site (TSS) in kilo bases (kb). Additional information on the regions used in the luciferase promoter assay is provided at the top by black bars.

The *STAT1* gene has been identified as a Brd4-long target in both of our ChIP Seq experiments. In our "ChIP Seq Brd4 output 1" it contained significantly more reads in the 1 kb region as well as 6 - 7 kb upstream of the transcription start site (TSS) in comparison to the "ChIP Seq Input" sample. In addition, our "ChIP Seq Brd4 output 2" lane showed more Brd4-long binding in the promoter region close to the first exon than the "ChIP Seq IgG output" negative control. Interestingly, the Brd4-long overexpression ChIP Seq by LeRoy *et al.* also presented specifically more reads in the identified regions, but with a shift to the right. The shift is probably due to the different alignment strategy performed by LeRoy *et al.* They used the reference genome version 18 ("hg18") and not "hg19" as we did. A conversion of their data to a comparable visualization in the UCSC Genome Browser could be the reason for the shift, but nonetheless the enrichments appear in close proximity to our endogenous ChIP sequencings.

Taken together, Brd4-long is specifically associated with the *STAT1* promoter which seems to be a direct target gene. This further supported our obtained luciferase reporter assay results for *STAT1* (figure 25).

4.12 Overlap analysis of the Brd4-long ChIP Seqs and the Brd4 knockdown mRNA Seq

To identify the proportion of deregulated direct Brd4-long target genes, overlap analyses of the mRNA Seq data and the ChIP Seq target genes were performed. Figure 29 gives an overview of the identified ChIP targets in the sequencing after Brd4 knockdown as well as their pattern of differential expression.

In total, 96 genes with direct Brd4-long association were identified deregulated in the Brd4 knockdown mRNA sequencing. The number accounted for 11% (96/896) of all deregulated genes. The other 89% of the differentially expressed genes without direct Brd4 association probably present indirect transcriptional regulations of Brd4. Interestingly, 46% (44/96) of the direct targets with differential expression were decreased and 54% (52/96) showed an upregulation. The analyses accentuate the direct and indirect transcriptional influences of Brd4 and that it can act both as repressor and activator.

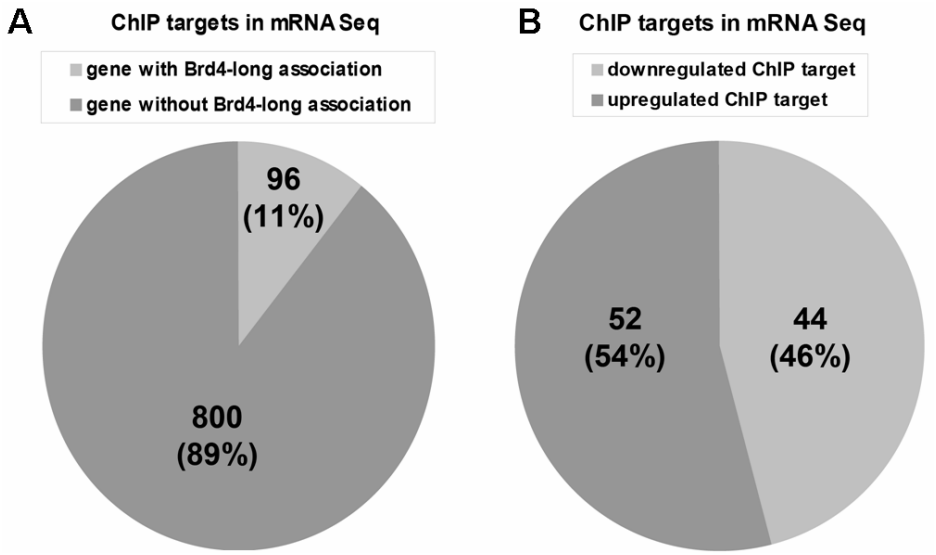

Figure 29: Overlap of differentially expressed mRNA Seq genes with Brd4-long ChIP Seq targets. (A) Differentially expressed genes with (96) and without (800) a Brd4-long association. (B) Direction of differential expression of Brd4-long target genes from (A).

Having identified *STAT1* as a directly activated target of Brd4 raised the question whether the deregulation of STAT1 target genes is indirectly mediated by STAT1 or directly by Brd4 itself. In total, 322 STAT1 target genes were identified differentially expressed in the Brd4 knockdown mRNA sequencing (recall figure 19). Most of them showed an implication in the interferon signaling pathways. The results of the analysis of a direct regulation, which might be resembled by a binding of Brd4 to the promoter, is presented in table 30.

Table 30: Overlap of differentially expressed STAT1 targets and the ChIP sequencing list. Identification of STAT1 target genes in the long form Brd4 ChIP sequencings as well as their presence and orientation in the Brd4 knockdown mRNA sequencing. The list of STAT1 targets was extracted from SABiosciences [84].

	overlap with ChIP Seqs	**downregulated**	**upregulated**
differentially expressed STAT1 targets	32/322 (9.9%)	17/32 (53.1%)	15/32 (46.9%)

Interestingly, 32 differentially expressed STAT1 target genes out of 322 targets in total (9.9%) additionally showed direct binding of the long Brd4 isoform. Of these, 17 appeared decreased. Interestingly, none of the 32 genes was related to the interferon alpha, beta or gamma signaling pathways, which supports the idea of Brd4 directly regulating *STAT1* expression which in turn influences the expression of its target genes and thus influences interferon signaling.

The list of direct Brd4-long targets was subjected to further pathway analysis. It was performed to identify overall pathway regulations and known protein complexes which are directly affected by Brd4.

4.13 Pathway analysis of the overlap of Brd4-long ChIP sequencings and the Brd4 knockdown mRNA sequencing

As mentioned before, 96 genes out of 896 differentially expressed genes identified by mRNA sequencing after Brd4 knockdown also showed a direct association of the long Brd4 isoform. The ConsensusPathDB pathway analysis tool assigned them to the pathways summarized in table 31.

Table 31: Pathway analysis of directly regulated and differentially expressed Brd4-long target genes. ConsensusPathDB (CPDB) pathway analysis of the overlapping 96 Brd4-long target genes which showed a differential expression in the Brd4 knockdown mRNA sequencing. Presented are the top pathways, the number of identified genes in the specific pathway as well as the corresponding gene names.

Amino acid transport across the plasma membrane	**IL-9 signaling pathway**	**IL-7 signaling pathway**
SLC3A2	MAPK3	MAPK3
SLC7A11	STAT3	STAT3
SLC38A1	STAT1	STAT1
SLC38A2	identified members:	identified members:
identified members:	**3 out of 17**	**3 out of 25**
4 out of 31	**p = 6.21x10^{-5}**	**p = 2.05x10^{-5}**
p = 1.2x10^{-5}		

The pathway analysis revealed a direct involvement of Brd4-long in pathways such as "Amino acid transport across the plasma membrane" as well as the two signaling pathways of "IL-9" and IL-7". Notable, both of the presented signaling events do show an implication of the STAT1 protein, as it is true for the interferon signaling pathways. These results further reveal novel direct regulatory functions of the long Brd4 form. In contrast to the mRNA sequencing analyses, interferon signaling was not found enriched in the submitted list of overlapping genes. This is most likely due to an indirect effect of Brd4 on the IFNγ activated target genes, which themselves become activated by STAT1.

Taken together, the results revealed that Brd4 directly activates *STAT1* expression and therefore additionally influenced the expression of STAT1 target genes. Having identified this transcriptional dependency we next investigated the involvement of Brd4 in signaling cascades and responses due to the different implications for STAT1 in such cellular pathways.

4.14 Interferon gamma stimulation of Brd4

For further functional analyses interferon gamma (IFNγ) was chosen, because the pathway exclusively gets mediated by phosphorylated STAT1 homo-dimers. The interferon alpha and beta pathways involve the formation of STAT1 hetero-dimers with other STAT proteins [13]. However, the expressions of STAT2 and STAT3 were not constantly and significantly affected after Brd4 knockdown and thus might diminish the outcome.

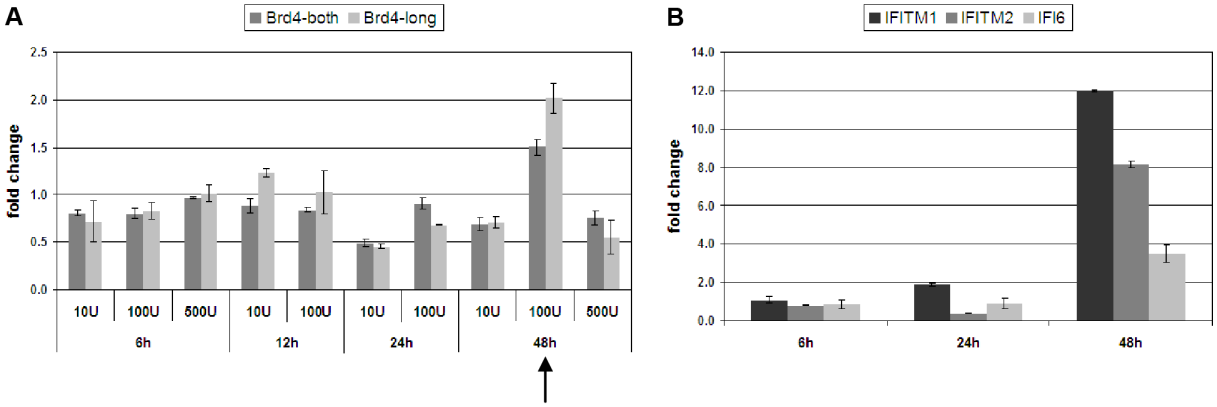

Figure 30: *Brd4* expression analyses after IFNγ stimulation in Hek293T cells. QPCR expression analyses of *Brd4* in IFNγ stimulated Hek293T cells using two primer sets against both isoforms ("Brd4-both") and the long form separately ("Brd4-long"). Stimulation was performed with varying concentrations (U = units) and incubation times (6h - 48h). (B) QPCR expression analyses in IFNγ stimulated Hek293T cells using primer sets against the interferon inducible STAT1 target genes *IFITM1*, *IFITM2* and *IFI6*. Stimulation was performed with 100 units (U) at different time points (6h - 48h). Normalization was carried out to the housekeeping gene *HPRT1* and the corresponding unstimulated control. The results are displayed as fold changes.

The combination of 100 units (U) and 48 hours (h) of IFNγ showed, in comparison to the other conditions, an increase of *Brd4*. Under this condition, three already known ISGs, interferon induced transmembrane proteins 1 and 2 (*IFITM1* and *IFITM2*) as well as interferon induced protein 6 (*IFI6*) were also upregulated. They were significantly higher expressed - *IFI6* at least threefold, *IFITM1* at least twelvefold and *IFITM2* eightfold.

Looking at the qPCR analyses in detail, it seems that particularly the long Brd4 form was increased after stimulation. The increase in *Brd4* could indicate that *Brd4* itself is an interferon inducible gene. The enrichment of the long isoform could be accomplished either by a stabilization of the RNA polymerase II performing Brd4-long specific transcription or by a mRNA stabilization of the long variant under interferon stimulated condition.

Further experiments for the expression analyses of STAT1 and its target genes were performed with 100U and 48h of IFNγ stimulation (figure 31).

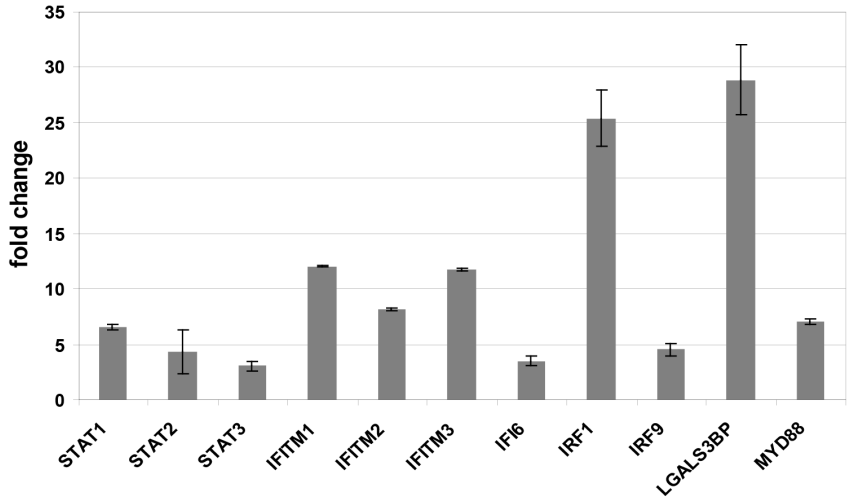

Figure 31: *STAT1* and target gene expression analyses in IFNγ stimulated Hek293T cells QPCR analyses of IFNγ stimulated Hek293T cells. Primer sets against *STAT1* and selected interferon stimulated genes were used. Normalization was performed to the housekeeping gene *HPRT1* and the corresponding unstimulated control. The results are displayed as fold changes.

After IFNγ stimulation the expression of *STAT1* was induced approximately sixfold. Additionally, the expression of all of STAT1's target genes was increased at least twofold. Lectin galactoside-binding soluble 3 binding protein (*LGALS3BP*) and interferon regulatory factor 1 (*IRF1*) presented with approximately 30 and 25 fold enrichment, respectively, the top candidates, and *STAT3* with a two fold upregulation the rear end. So far it was shown that the same IFNγ stimulation condition results in increased *Brd4* and STAT1 target gene levels.

Further experiments were performed to evaluate the IFNγ stimulation after Brd4 knockdown.

4.15 Brd4 knockdown and interferon gamma stimulation

The two different approaches of Brd4 knockdown - "shC2" eliminating both transcription variants and "shE1" specifically the long form - provide the possibility to establish a more

defined participation of Brd4 in the interferon gamma pathway. The expression levels of all so far employed ISGs were analyzed after Brd4 knockdowns and simultaneous IFNγ stimulation in Hek293T cells. The expression results are presented in figure 32.

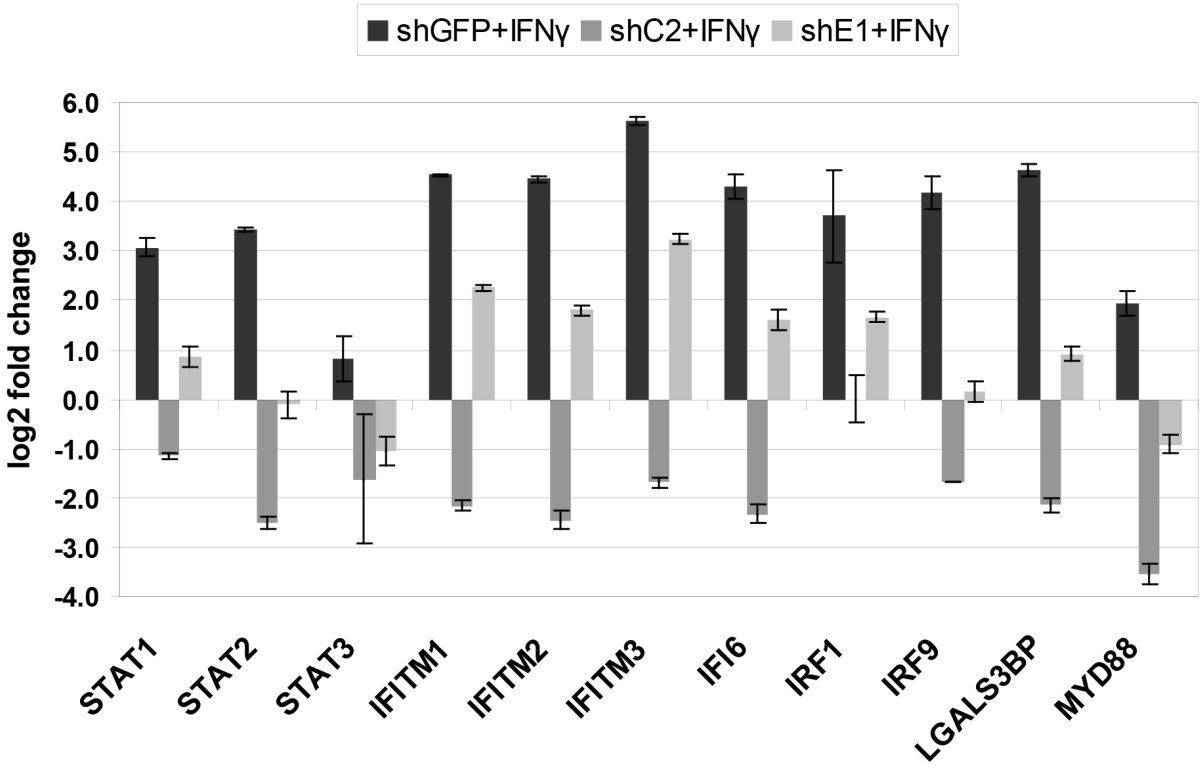

Figure 32: Expression analyses of *STAT1* and ISGs after IFNγ stimulation in Hek293T cells with Brd4 knockdowns. QPCR analyses after IFNγ stimulation in Hek293T cells with simultaneous Brd4 knockdowns. Primer sets against *STAT1* and selected interferon stimulated genes (ISGs) were used. Normalization was carried out to the housekeeping gene *HPRT1* and the unstimulated knockdown control. The results are displayed as log2 fold changes.

The expression of all interferon inducible genes appeared, in comparison to the corresponding control, significantly decreased in the knockdown of both Brd4 variants ("shC2") with IFNγ stimulation. Interestingly, the Brd4-long reduction by "shE1" caused either no change or an upregulation of the genes after treatment. Thus, both Brd4 isoforms seem to be implemented in the interferon signaling pathway, but to different degree. This might be due to different Brd4 knockdown levels, or, since the expression of the Brd4 long isoform was even more increased than the short form after IFNγ stimulation (figure 30), the effect of IFNγ on the Brd4 long isoform might counteract the knockdown efficiency. However, in both cases a knockdown of Brd4 results in a decreased IFNγ response indicating Brd4 as an essential part of this pathway. To support this assumption, further functional analyses were performed.

In addition to the real time PCR experiments STAT1 and LGALS3BP were analyzed on Western Blot after IFNγ stimulation and Brd4 knockdown. The results are shown in figure 33.

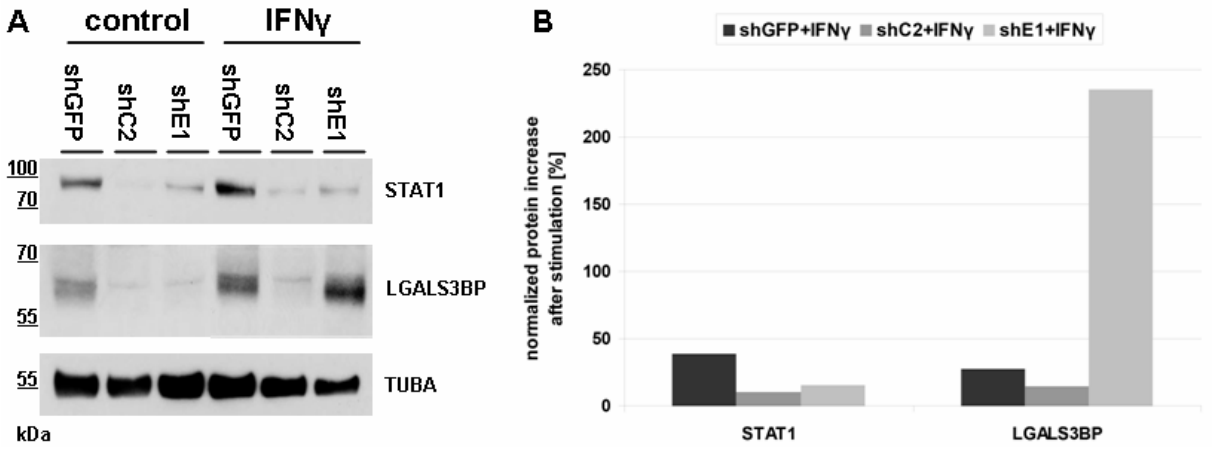

Figure 33: STAT1 and ISG LGALS3BP protein levels in IFNγ stimulated Brd4 knockdowns. (A) Detection of STAT1 and LGALS3BP protein levels in Hek293T cells with IFNγ stimulation and simultaneous Brd4 knockdown. The knockdown was either performed targeting both isoforms of Brd4 ("shC2") or the long form only ("shE1"). TUBA (tubulin A) was used as a loading control. (B) Densitometric analyses (using the ImageJ software) of the protein levels presented in (A). Normalization was performed to the TUBA level.

The induction of STAT1 and LGALS3BP by interferon gamma was present under control conditions ("shGFP") but completely inhibited when both Brd4 forms were missing ("shC2"). In contrast, the sample lacking the long Brd4 variant ("shE1") showed a significant gain of LGALS3BP compared to the knockdown control. Thus, the short Brd4 isoform seems to be essential for the transcriptional activation of LGALS3BP. Brd4-long on the other hand, is differently involved in the interferon gamma pathway. The LGALS3BP protein was upregulated in the stimulated "shE1" knockdown sample, even compared to the stimulated "shGFP" control. Interestingly, the STAT1 level was only slightly increased which was also supported by the qPCR results (figure 32).

Therefore, the long variant seems to play a more complex role in the signaling events mediated by IFNγ. Interestingly, the gain of LGALS3BP protein in the "shE1" IFNγ stimulation sample was even greater than the induction in the "shGFP" control sample. Comparing this strong increase to the obtained expression increase on qPCR level (figure 32) and the increase in promoter activity (figure 34), which never elevated above the control induction, LGALS3BP seems to be stabilized on protein level under IFNγ stimulated conditions.

LGALS3BP has been identified as the top candidate with the highest expression increase after IFNγ stimulation (see figure 31). To further investigate the connection between IFNγ stimulation and Brd4 regulation of STAT1 target genes, an *LGALS3BP* reporter construct was cloned. The *LGALS3BP* promoter activity was tested in presence and absence of IFNγ stimulation and in presence and absence of a Brd4 knockdown in Hek293T cells. The results are presented in figure 34.

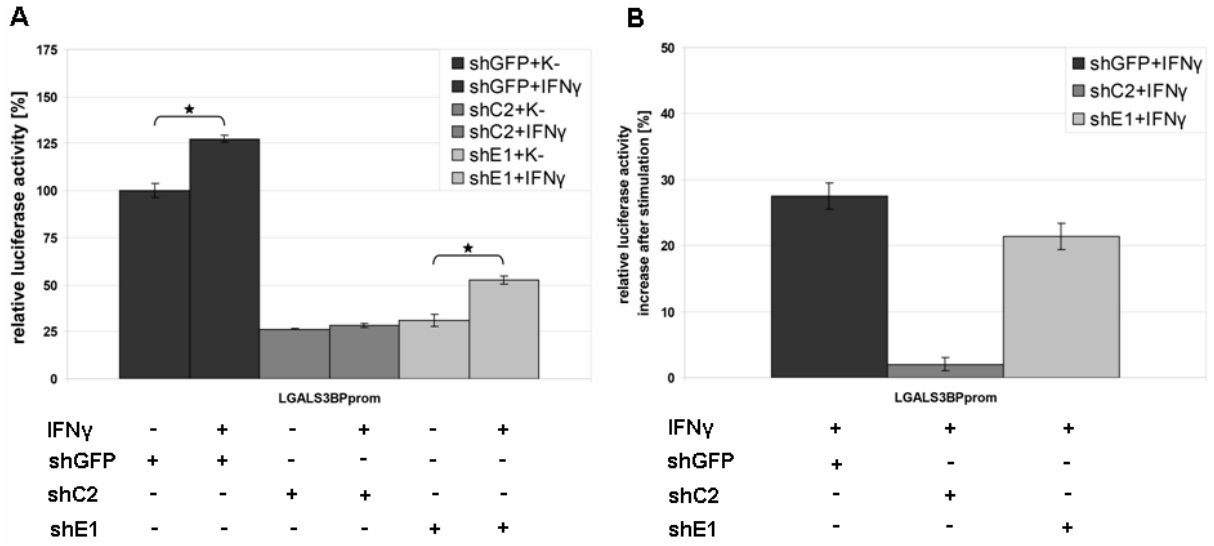

Figure 34: Luciferase reporter assays of the ISG *LGALS3BP* promoter and the calculated enrichment by stimulation. (A) ISG *LGALS3BP* promoter (*LGALS3BP*prom) reporter assays with (+) and without ("K-") (-) IFNγ stimulation, with (+) and without (-) Brd4 knockdown. Two different knockdowns were carried out either by diminishing both forms of Brd4 ("shC2") or the long isoform specifically ("shE1"). Normalization was performed to the co-expressed *Renilla reniformis* luciferase and the corresponding empty reporter vector. The *LGALS3BP* promoter activity level of the "shGFP" control sample was set to 100%. (B) *LGALS3BP* promoter activity increase after IFNγ stimulation with (+) or without (-) Brd4 knockdown. The activity values in (A) served as templates and the calculation was performed to the corresponding unstimulated controls.

Without IFNγ treatment the transcriptional activity of the *LGALS3BP* promoter was decreased in both Brd4 knockdowns. After IFNγ stimulation the promoter activity was significantly increased in the knockdown control and the Brd4-long knockdown "shE1", respectively. Thus, the previously measured increase in *LGALS3BL* expression after "shE1" knockdown (depicted in figures 32 and 33) is most likely due to an elevation of its promoter activity. In contrast, in the Brd4 "shC2" knockdown the promoter activity is only marginally increased after IFNγ stimulation.

In summary, both Brd4 isoforms play different but important roles in the signaling events mediated by interferon gamma. Having established the transcriptional dependency of

STAT1 and its target genes directly on the Brd4 level and having identified two diverging Brd4 implementations in the interferon gamma signaling mediated by the STAT1 protein, the question arose, if this relationship is also valid in the disease context and if so, what conclusion could be drawn from it. To answer these questions, cell culture experiments in breast cancer and reference cells were performed.

4.16 Brd4 and STAT1 expression in breast cancer cells

In 2008 the group of Kent W. Hunter published a study on the correlation between the level of the long Brd4 variant and the disease outcome in breast cancer patients. Low amounts were found associated with a poor prognosis and, vice versa, its activation led to a dramatic reduction of tumor growth [20]. Thus, we asked whether decreased levels of the Brd4 long isoform could be identified also in breast cancer related cell lines (MCF-7 and SK-BR-3) in comparison to a control cell line (MCF10A), and if so, if this would be accompanied by a dependent STAT1 expression. The three chosen cell lines facilitate a direct comparison of metastatic breast tumors (MCF-7 and SK-BR-3) with the corresponding "normal" state (MCF10A). In addition, SK-BR-3 cells have been reported not to respond to IFNγ mediated cell growth inhibition and thus present an ideal model to investigate IFNγ signaling mechanisms. The protein levels of Brd4-long and STAT1 in the three cell lines are presented in figure 35.

Both investigated protein levels, Brd4-long and STAT1, existed to a lower degree in the breast cancer metastasis cell line SK-BR-3 compared to MCF10A and MCF-7 cells. This finding supports the direct transcriptional connected between Brd4 and STAT1. Interestingly, also STAT1 has been already studied in the context of breast cancer and has been identified as an essential mediator of interferon induced anti-proliferative and pro-apoptotic effects on cancer cells [91, 13].

In 2011 the group of Kent W. Hunter published an additional study on the correlation between the Brd4 level and the disease state in breast cancer patients, but this time they investigated the short isoform of Brd4. An increase of the short Brd4 isoform correlated with a higher tumor grade and an increase in metastasis formation [21]. Thus, the long and short isoforms seem to have contrary effects on the outcome of breast cancer.

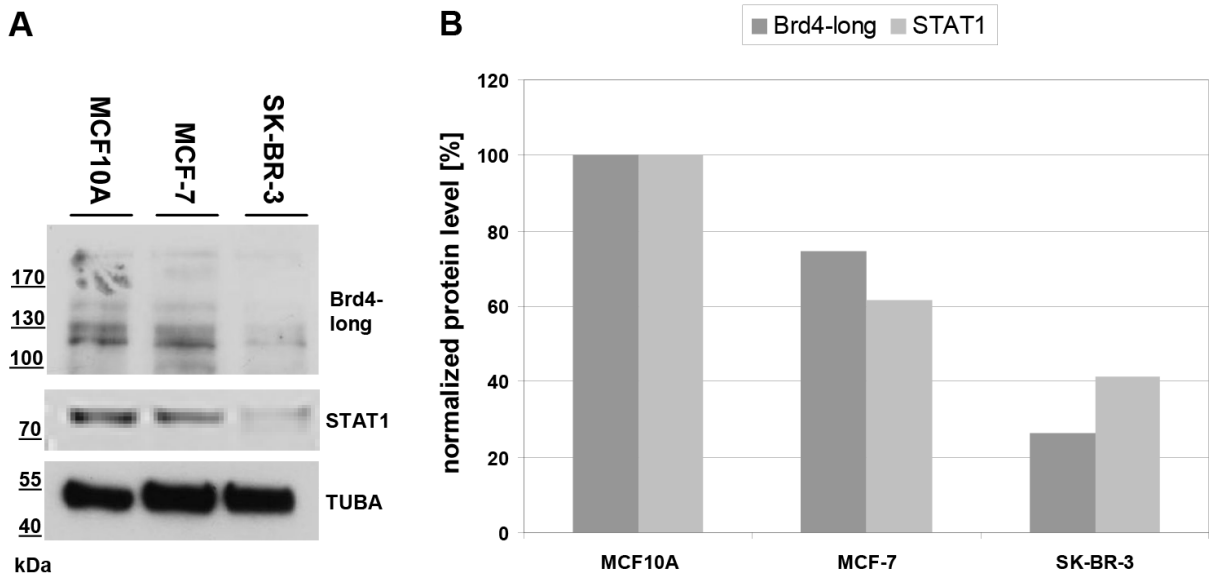

Figure 35: Brd4 and STAT1 levels in breast cancer cell lines. (A) Detection of Brd4-long and STAT1 protein levels in the breast cancer cell lines MCF-7 and SK-BR-3. MCF10A is a "reference" cell line. TUBA was used as a loading control. (B) Densitometric analyses (using the ImageJ software) of the protein levels presented in (A).

We investigated the expression levels of the short and long Brd4 isoforms separately in the breast metastasis cell line SK-BR-3, which showed the strongest decrease in Brd4-long protein level in comparison to the MCF10A normal cells. The expression results are summarized in figure 36.

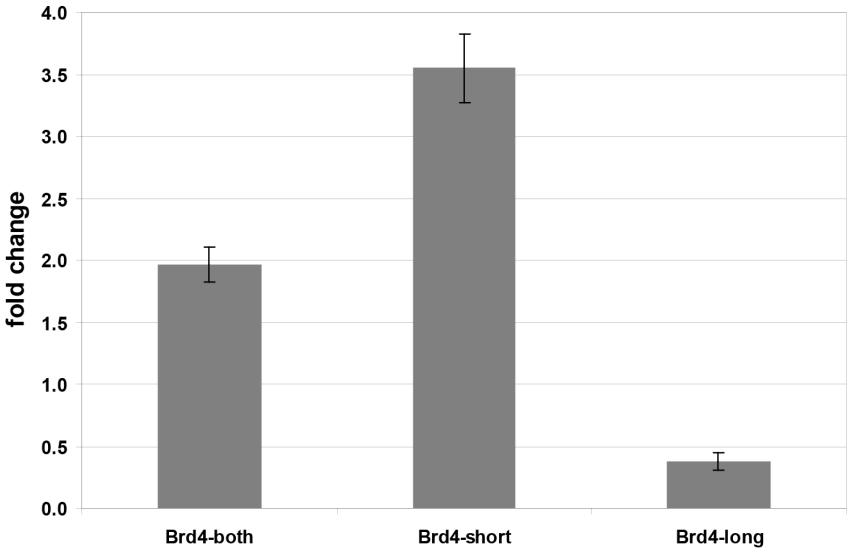

Figure 36: QPCR of *Brd4* variants in SK-BR-3 breast cancer cells. QPCR analyses of the short and long isoform of *Brd4* in SK-BR-3 breast cancer cells. Normalization was performed to the house-keeping gene *HPRT1* and the MCF10A cell line. The results are displayed as fold changes.

The short Brd4 isoform showed an elevated expression of approximately 3.5 fold in the metastatic SK-BR-3 cell line and the long variant a reduction of approximately 60% (fold change 0.4) in comparison to the MCF10A cells. Together with the findings from Hunter *et al.*, where higher Brd4-short levels were associated with greater metastasis formation and lower Brd4-long levels with poor prognosis, SK-BR-3 cells seem to originate from a tumor with a poor prognosis.

Finding STAT1 and the Brd4-long isoform decreased in breast cancer cells further supports the novel direct regulation of STAT1 by Brd4 identified in Hek293T and Wi38 cells. As mentioned previously, the results of the group around Gerard M. Doherty indicated that the SK-BR-3 cell line does not respond to interferon gamma mediated cell growth inhibition. They argue that this was due to the lack of IRF1, a specific STAT1 target gene [92]. Taking into account that the expression of STAT1 as well as its targets was increased in Hek293T cells after Brd4-long overexpression (consider figures 22 and 23), a re-introducing of Brd4 should potentially elevate the *IRF1* level in SK-BR-3 cells via STAT1 increase. This could potentially antagonize the defect in IFNγ mediated cell growth inhibition. We thus performed these experiments and overexpressed Brd4-long in SK-BR-3 cells. The corresponding expression analyses are shown in figure 37.

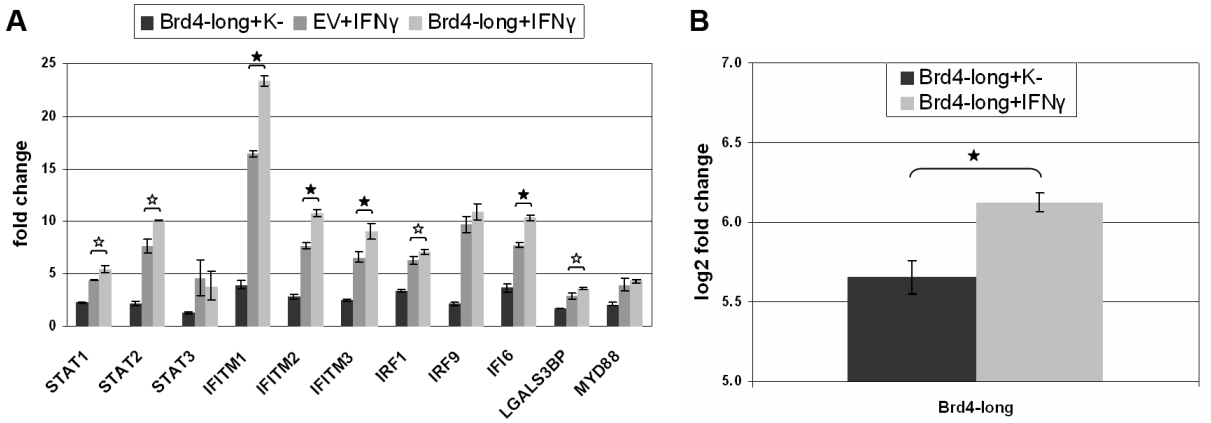

Figure 37: QPCR analyses of Brd4-long overexpression and IFNγ stimulation in SK-BR-3 cells. QPCR analyses of IFNγ stimulated SK-BR-3 cells with simultaneous Brd4-long overexpression. Normalization was carried out to the housekeeping gene *HPRT1* and the unstimulated ("K-") empty vector ("EV") control. The solid stars present significant changes of $p<0.05$ and the blank stars of $p<0.1$, using an one-sided, untailed t-test. (A) Primer sets against *STAT1* and selected interferon stimulated genes were used. The results are displayed as fold changes. (B) A primer pair detecting the long form of *Brd4* was used. The result is displayed as log2 fold change.

Brd4-long elevation alone leads to an increased expression of *STAT1* of more than twofold. Additionally, all of its analyzed target genes were found upregulated in comparison to the

corresponding control. The stimulation with IFNγ also positively influenced the above mentioned expression levels, but the combination of the Brd4-long overexpression and the simultaneous treatment with IFNγ gave rise to the greatest increases. Even the expression of the Brd4-long form - although overexpressed - further increased significantly (by approximately twentyfold) under the stimulation condition. This result supports the assumption of the long form of Brd4 being an interferon stimulated gene itself.

In summary, these results are pointing towards a potential rescue of the non-responsiveness to interferon gamma mediated cell growth inhibition in the metastatic breast cancer cell line SK-BR-3.

5 Discussion

The cellular bromodomain containing protein 4 (Brd4) is a so called "chromatin-reader", which binds to acetylated histone tails via its bromodomains [31] and remains associated with chromosomes during mitosis and interphase [39]. The interest in the protein significantly increased with its identification in the context of papillomavirus (PV) infections, which are the leading cause of different cancer entities, such as cervical and anal cancers [73]. Here, Brd4 directly interacts with the virus encoded protein E2 and tethers the viral genome to host mitotic chromosomes, thereby maintaining the infection in diving cells [19]. Thus, the disruption of the tethering complex is accompanied by a loss of the viral genome and curing of the infection [93]. This implication of Brd4 elevated the interest in its cellular function and presented the starting point for further investigations. The involvement of the bromodomain containing protein in the regulation of gene expression was discovered shortly after. Brd4 directly regulates the transcriptional activity of the papillomaviral E2 protein [47] and was implicated in the cellular transcription as well [57, 59]. A knockdown of Brd4 is associated with global changes in the acetylation patterns of histones after antimicrotubule drug-induced mitotic arrest [37]. This identification shifted Brd4 from a mere "chromatin-ready" to a "chromatin-modulator" which was later on supported by additional analyses. Epigenetic marks on histone tails, for example acetylations and methylations, directly influence the binding, as well as activity, of RNA polymerase II, which subsequently regulates the expression of a gene [42]. Over its extra terminal (ET) domain Brd4 directly interacts with additional "chromatin-modifiers", such as the histone methyltransferase Wolf-Hirschhorn syndrome candidate 1-like 1 (WHSC1L1, also known as NSD3), and the histone demethylase activity inhibiting protein jumonji domain containing 6 (JMJD6) [33]. Depending on the localization of the histone marks produced by NSD3 they are associated with transcriptional activation or repression, respectively [69], and its knockdown is accompanied by differential gene expressions [33].

Brd4 is, next to the mentioned influence on histone modifications, also directly involved in the RNA polymerase II mediated transcriptional process. It phosphorylates RNA polymerase II through its kinase activity and promotes transcriptional elongation [59]. Additionally, the bromodomain protein binds to the positive transcription elongation factor b (pTEFb) which activates the RNA polymerase II via phosphorylation and builds

a bridge to other transcription factors and transcriptional modulators [54, 63]. Two small molecules, "JQ1" and "I-BET", have been developed as specific inhibitors of the BET family of proteins, including Brd4. They target their acetyl-binding bromodomains and prevent the association with histone tails in nucleosomes [79, 18]. Inhibition results in an inhibition of the inflammatory response of macrophages after stimulation with lipopolysaccharides (LPS) [18]. The molecules might therefore be used as potential therapeutics of immune diseases. Furthermore, Zuber *et al.* identified with the BET protein inhibitor "JQ1", as well as with a comparative Brd4 knockdown approach, a significant tumor growth reduction of acute myeloid leukaemia (AML) cells *in vitro* and *in vivo* [22]. Thus, the Brd4 protein as BET family member also seems to be a potent therapeutic target for cancer and other inflammatory diseases. However, a deeper knowledge of its specific regulatory activities - for example genome-wide binding and expression analyses - are required. Thus, we performed expression profiling analyses after Brd4 knockdown (mRNA Seq) and Brd4 chromatin association studies (ChIP Seq) using Next Generation Sequencing technologies. All experiments, validations and functional characterizations were performed in mammalian cell culture systems.

5.1 Brd4 regulates Myc and its target genes

To characterize the transcriptional network of Brd4 we performed mRNA Seq experiments after Brd4 knockdown ("shC2"). We identified 2,493 differentially expressed transcripts which were assigned to 896 genes in total. Of these, 59% showed a decrease and 41% an increase (table 23). The five top most significantly downregulated (*IFITM1*, *IFI6*, *IFITM2*, *IFITM3*, *PARP10*) as well as upregulated (*HSPA13*, *SLC7A11*, *YOD1*, *HMGCS1*, *FAR1*) genes were validated in qPCR analyses, showing a very good correlation ($\rho = 0.99$) to the mRNA sequencing results (figure 14).

One of the best known downstream targets of Brd4 is *Myc* (v-myc myelocytomatosis viral oncogene homolog (avian)). The Myc transcription factor itself was decreased approximately twenty percent in our data set, but overlap investigations with its targets revealed a more than twofold enrichment (OR = 2.12, p-value $< 1.3\text{x}10^{-7}$) of downregulations occurring in Myc associated genes, compared to non-Myc targets (table 24).

The transcription factor Myc is an essential regulator of proliferation and differentiation in normal tissue, but functions also as an oncogene in different types of cancers [94, 95,

96]. Myc amplifications in breast [85], prostate [97] and colon cancer [86] as well as neuroblastoma [98] are associated with poor prognosis. A knockdown of Myc leads to reduced cell proliferation and, in certain cases, also to the induction of apoptosis [99, 100, 101, 102]. Human cancers, as described by Douglas Hanahan and Robert Weinberg, exhibit distinct underlying principles that distinguish them from normal tissues. The researchers proposed a set of eight common traits ("hallmarks of cancer") that govern cancer cell development [1, 2]. The "hallmarks" include for example the uncontrolled growth of tumor cells. Enhanced expression of Myc, leading to enhanced proliferation, would therefore account to one of the identified "hallmarks of cancer". The transcriptional dependency of Myc and its target genes on Brd4 also implicates Brd4 as part of that specific cancer trait and underscores the protein as potential drug target [103, 104].

J. Kessler and colleagues as well as the group around C. Grandori screened Myc-driven cancers for essential tumor growth genes using siRNA libraries. Kessler *et al.* identified 403 genes in total [23] and Toyoshima *et al.* 101 candidates [24] leading to tumor growth reduction. Brd4 presented the only common gene in both sets, which underscores it as key protein in Myc-driven cancers [23, 24]. Overlap analysis of the published lists with our list of differentially expressed genes after Brd4 knockdown resulted in eight genes in common which appeared downregulated after knockdown (table 25). Five of them were Myc target genes [84]. The remaining three were no Myc targets, but of these, *KCNC4* and *RTN3* have already been linked to tumor pathogenesis in the literature before. The ion channel membrane protein Kv3.4 (encoded by the gene *KCNC4*) is found elevated in head and neck cancer [105] as well as oesophageal squamous cell carcinomas [106] and its reduction is associated with a selective cell cycle arrest [105]. RTN3 on the other hand, encoding the endoplasmic reticulum-associated Reticulon 3 protein, is upregulated in astrocytomas [107].

Taken together, the knockdown of Brd4 leads to a reduction of tumor growth in Myc-driven cancers [23, 24] and its downregulation is also associated with the reduction of other genes which are essential for tumor maintenance. Here, it would be interesting to investigate an *in vivo* Brd4 knockdown. However, Brd4 is an essential protein and a knockout in mice is lethal. Thus, a conditional knockout system would be required [28]. On the other hand, mice - injected with acute myeloid leukemia cells with an inducible Brd4 shRNA system - showed a significant tumor growth reduction (as seen for the *in vitro* applications [23, 24]) and a gain in the overall survival [22]. Activation of the shRNA resulted in no serious side effects [22]. These results additionally support a role for Brd4

as potential therapeutic target in tumor therapy.

Having established the validity of our mRNA sequencing data by qPCR analyses and comparisons of known transcriptional connections, we further investigated the most significantly affected cellular pathways after Brd4 knockdown using available pathway analysis tools.

5.2 Brd4 as a member of the IFN signaling cascade

Pathway analysis tools present a useful method to identify connections and enriched pathways in large data sets, such as generated by Next Generation Sequencing experiments. Ingenuity Pathway Analysis (IPA) - being such a software tool - was the method we used for the analysis of the mRNA sequencing data after Brd4 knockdown. The Ingenuity Knowledge Base is the fundament of IPA and comprises reported experimental data with links to original articles, and contains additional information from other sources, such as protein-protein interactions from "BIOGRID", microRNA-mRNA target interactions from "TARBASE", metabolic pathway information from "KEGG" and enzyme/substrate reactions from "LIGAND" [108]. The top pathways most significantly affected by the Brd4 knockdown were identified as "Interferon Signaling" pathways, followed by "PTEN Signaling", "Neuregulin Signaling" and "Estrogen Receptor Signaling" events (figure 16). Signaling processes rely on the transfer of information through the cell to the nucleus, leading to specific gene expression patterns. The "Interferon Signaling" was on position number one (figure 17). These signaling pathways are composed of cascades, triggered by interferon (IFN) cytokines. They stimulate intracellular and intercellular networks with anti-inflammatory (bacterial and viral infections) effects, as well as innate and acquired immune responses [13]. Interestingly, the interferon alpha, beta as well as gamma (IFNα, β and γ) signal mediating proteins, namely signal transducers and activators of transcription 1 and 2 (STAT1 and STAT2) were identified as significantly downregulated in our Brd4 knockdown mRNA sequencing data (figure 17). Next to STAT1 and STAT2, also their specific target genes appeared downregulated. Interestingly, the STAT1 protein is involved in all three IFNα, β and γ mediated signaling processes and appeared even more decreased than STAT2 (figure 17). This leads to the assumption of silenced interferon signaling processes predominantly mediated by STAT1 after knockdown of Brd4. Noteworthy, STAT1 has been identified as a transcriptional activator also in its unphosphorylated state [109], therefore giving an explanation why the interferon signaling pathways

also come up in our unstimulated cellular condition.

As mentioned above, interferon signaling has been associated with inflammatory effects. Brd4 has been implicated in the regulation of inflammatory responses before through its association with the transcription factor complex NFκB (nuclear factor kappa-light-chain-enhancer of activated B cells). Brd4 directly interacts with v-rel reticuloendotheliosis viral oncogene homolog A (avian) (RelA), a subunit of the NFκB complex [17]. NFκB is the transmitting transcription factor in response to a variety of stimuli, including lipopolysaccharides (LPS) and tumor necrosis factor alpha (TNFα) [110, 111]. As such, LPS induce the expression of *TNFa* and interleukin 1 beta (*IL1β*) via activated NFκB. This is a cellular defense mechanism against gram negative bacteria [112]. Nicodeme *et al.* evaluated the BET protein inhibitor "I-BET" in comparison to BET protein knockdowns, including Brd4, and described a suppressive impact on *IL1β*, *IL6* and *TNFa* expression [18]. Interestingly, the *TNFa* gene only showed a decrease after Brd4 knockdown, but not after treatment with the BET protein inhibitor "I-BET" [18]. Huang *et al.* validated the finding by showing that the activation of certain TNFα response genes - namely *TNFa* itself, as well as selectin E (*SELE*) - was diminished after Brd4 knockdown [17]. Taken together, the publications revealed an essential role for the bromodomain protein in the responses to host defense signals [18, 17, 54] most likely over its interaction with the signal mediating transcription factor NFκB. This could similarly hold true for the regulation of the interferon responses mediated by the STAT proteins, which themselves appeared downregulated after Brd4 knockdown (figure 17). Interestingly, STAT1 has also been identified as an interacting partner of RelA, one of the subunits of the NFκB transcription factor [14]. This interaction resulted in the modulation of NFκB activity [14] similar to the interaction between Brd4 and the NFκB subunit [17], indicating that STAT1, RelA and Brd4 might function as a complex. Also of interest is the acetylation of the STAT1 protein, which might present an interaction site for the Brd4 protein, recalling that its bromodomains bind to acetylated proteins [31]. One could therefore imagine a direct binding of Brd4 and STAT1 via its acetylated site. This is supported by the fact that the interaction between Brd4 and RelA is also mediated by an acetylation of RelA. The hypothesis of a direct binding of Brd4 and STAT1 should be tested in future experiments.

In summary, according to the identified "Interferon Signaling" cascades as the most significantly affected pathways after Brd4 knockdown, Brd4 seems to be even deeper involved in the responses to inflammation than previously thought. The TNFα signaling did not appear in the list of affected pathways after Brd4 knockdown. This was probably due

to the unstimulated cellular state which was used for the mRNA sequencing after knockdown. The "Interferon Signaling" cascades most likely came up in the data set because of the action of STAT1 as transcription factor also in an unstimulated condition. To validate the role of Brd4 in the interferon signaling pathways further analyses in cell culture systems were performed which focused specifically on the central protein in each of the interferon pathways, the signal transducer and activator of transcription 1 (STAT1).

5.3 Transcriptional dependency of STAT1 and its target genes on Brd4

Based on our mRNA Seq results which showed a decreased expression of STAT1 as well as its specific target genes in type I and type II interferon signaling (figure 17), we further functionally analyzed the reduced transcriptional activity after Brd4 knockdown. We confirmed the downregulation of STAT1 on mRNA and also on protein level (figure 18) after knockdown of both Brd4 isoforms ("shC2") and the long Brd4 form ("shE1"). Further on, we investigated STAT1 dependent target genes in relation to the Brd4 knockdown. The website by SABiosciences provided a list of known and predicted targets for the STAT1 transcription factor [84]. Overlap analysis of this list with the entire list of differentially expressed genes after Brd4 knockdown resulted in the identification of 36% differentially expressed STAT1 target genes in total. With 68%, the majority of them showed a decrease after Brd4 knockdown which were validated in real time PCR experiments (figure 19). Thus, Brd4 seems to play an important role in the regulation of STAT1 as well as STAT1 dependent target genes in a similar way as seen for the regulation of Brd4 and Myc as well as Myc dependent genes [54, 61, 22, 24, 66]. STAT1 regulates the expression of a distinct group of genes - including certain interferon stimulated genes (ISGs) - even without activation by phosphorylation (no phosphorylation at tyrosine 701 and serine 727 residues) [109]. This fact supports the connection between Brd4, STAT1 and its target genes in our unstimulated cellular system for expression profiling after Brd4 knockdown.

Whether the identified transcriptional dependency could also be transferred to an elevated level of Brd4 was analyzed next. Overexpressions of the long form of Brd4 in two different cell lines was followed by an increase of STAT1 and its target genes on mRNA as well as on protein level (figure 22 and 23). The decrease of STAT1 expression after Brd4 knockdown was shown to be due to a decrease of *STAT1* promoter activity in luciferase reporter assays

(figure 25). Interestingly, the region 250bp upstream of the transcription start site (TSS) seems to be important for the transcriptional regulation by Brd4 (figure 24). Here, on the other hand, an overexpression of Brd4 did not lead to an increased promoter activity in the reporter system (figure 26). This could be due to the experimental set-up, where only certain genomic sequences were analyzed and upstream regulatory regions were missing. In addition, the plasmids were missing epigenetic organizations such as nucleosomes. The overexpression of Brd4 could also lead to a depletion of factors required for transcriptional activity of the reporter plasmid. Interestingly, the first intron of the *STAT1* gene itself was identified to exhibit an enhancer sequence that displayed IFN-regulated activity after IFNα and IFNγ stimulations. This was experimentally approached by luciferase reporter assays and further validated by electromobility shift assays (EMSAs) [113]. This enhancer sequence in the first intron of the *STAT1* promoter could potentially also be necessary for the activation under Brd4 overexpressed conditions and should be investigated in further experiments.

Taken together, the expression of the transcription factor STAT1 is associated to Brd4. In addition, the majority of the STAT1 target genes were regulated in the same direction as STAT1 itself, suggesting that Brd4 regulates them over STAT1. However, to determine whether Brd4 directly or indirectly mediates the regulation of STAT1 and its target genes Brd4 chromatin immunoprecipitations followed by Next Generation Sequencings were performed.

5.4 Brd4 binds and activates the *STAT1* promoter

Brd4 is associated with DNA through its binding to acetyl-lysine residues on histone tails [31] - with preferences for lysine 14 on histone H3 (H3K14) and lysines 5 and 12 on histone H4 (H4K5 and H4K12) [37]. In addition, Brd4 is directly involved in transcriptional regulation by its binding to different transcription factors [54, 17]. This has been first shown for Brd4 by the regulation of the transcriptional activity of the human papillomaviral protein E2 [47]. First indications for Brd4-binding regions have been given by chromatin immunoprecipitations followed by semi-quantitative PCR with particular gene promoters [54, 61, 17, 18]. To extend these studies, we performed two endogenous chromatin immunoprecipitations for Brd4 followed by Next Generation Sequencing.

With these experiments we identified 2,370 target genes in total with 224 candidates present in both ChIP Seqs (table 28). Notably, Brd4 binding was not only found within specific gene promoters, but also identified on exons (table 28). This finding is supported by the results of Rahman *et al.* who described significant Brd4 binding to the promoter as well as the coding region of the serine/threonine protein kinase pim-2 (*PIM2*) target gene [33]. Interestingly, this enrichment pattern on exons was also seen for histone H3 trimethylation at lysine 36 (H3K36me3) [114] which is associated with transcribed regions [42]. Noteworthy, a knockdown of Brd4 has been found to be associated with reduced H3K36 trimethylation levels especially within the gene body [33]. Furthermore, the knockdown of its direct interaction partner Wolf-Hirschhorn syndrome candidate 1-like 1 (WHSC1L1 - also known as NSD3), which is a known histone methyltransferase, also led to a reduction of that specific chromatin mark [33]. Consequently, a siRNA downregulation of NSD3 is accompanied by a decrease in transcription of certain Brd4 target genes, such as *PIM2* and cyclin D1 (*CCND1*).

The trimethylation of lysine 36 on histone H3, identified specifically at exonic regions, additionally correlated with mRNA splicing. High levels of H3K36me3 were found on constitutively included exons and reduced signals led to alternative splicing [114]. A coupling of the cellular processes of transcription and splicing is already discussed in the literature. It is known that some promoter proximal introns are eliminated while the transcriptional process is still ongoing [115]. Therefore, the identification of Brd4 at exonic regions as well as its connection to certain chromatin marks, which are associated with transcription and splicing, could directly imply an involvement of the protein in the simultaneously occurring processes of transcription and splicing. This could potentially be evoked by the recruitment of chromatin modulators as well as the direct blocking of the RNA polymerase II during transcription elongation at specific splice sites at once. An association of Brd4 with the splicing process should therefore be further investigated in the future.

During my work, LeRoy *et al.* published in August 2012 a Brd4 ChIP Seq experiment using an overexpressed Brd4 protein in Hek293 cells [90]. A comparison of their target genes with our two endogenously performed ChIP Seqs revealed a total overlap of 725 genes in at least two of the data sets and 103 target genes present in all three enrichment analyses (figure 27). Pathway analysis of the 103 target genes revealed cellular processes such as “chromosome maintenance”, “mRNA splicing”, “G1/S transition” and “microRNA biogenesis” (table 29). Some of these pathways, such as “chromosome maintenance” and

"G1/S transition", have already been reported in connection to Brd4 [39, 61, 52, 62, 41]. Furthermore, approximately 11% of the deregulated genes identified in the mRNA Seq experiment after Brd4 knockdown also showed an enrichment in Brd4 binding (figure 29). Nevertheless, besides a Brd4 binding to activated gene promoters we also found Brd4 bound to genes which appeared upregulated after Brd4 knockdown (figure 29), indicating a potential function of Brd4 as a repressor in addition. This could possibly be accomplished by, as yet, undiscovered protein-protein interactions to repressors and complexes or via recruitment of chromatin modulating factors [33, 78], leading to altered accessibility of certain gene promoters. The differentially expressed genes with Brd4 association belonged to pathways including "amino acid transport across the plasma membrane", "IL-9 signaling" as well as "IL-7 signaling". The obtained data on gene regulation and binding will provide a platform for future functional studies.

Most notably, the Brd4 chromatin immunoprecipitations, performed by us and also LeRoy *et al.*, identified an association of Brd4 with the *STAT1* promoter (figure 28). To investigate whether the influence of Brd4 on the STAT1 target genes was only mediated by the regulation of the transcription factor itself or was due to a direct binding of Brd4 to the target gene promoters, comparative analyses of the differentially expressed STAT1 targets with the identified Brd4 ChIP targets were performed. The results showed that only a small proportion of the differentially expressed STAT1 targets was also associated with Brd4 and non of them was an interferon stimulated gene (ISG) (table 30). Therefore, Brd4 does not directly regulate the expression of ISGs but regulates STAT1 through promoter activation which in turn modulates its target genes. Next, it would be interesting to identify regulatory elements within the *STAT1* gene promoter or the gene itself, which are subject to the direct regulation by Brd4. This could be performed similarly to Wong *et al.* who identified IFN regulatory sequences by luciferase reporter experiments and electromobility shift assays [113].

In general, we have established the interplay of Brd4, STAT1 and the STAT1 target genes under non-stimulated cellular conditions. Further analyses under interferon stimulated conditions as well as a potential impact of changing Brd4 levels will show the role of Brd4 in the IFNγ signaling process.

5.5 Different functions of the two Brd4 isoforms in the IFNγ response

Interferon gamma (IFNγ) is a glycosylated protein of 140 amino acids which is produced predominantly by natural killer (NK) cells or activated T cells and mediates innate and adaptive immune responses to bacterial and viral infections [116, 82]. Due to its low amino acid sequence homology with the type I interferons (IFNα/β) it is categorized separately as type II interferon. The interferon gamma response requires two interferon gamma receptor proteins in the cell membrane (IFNGR1 and IFNGR2), the tyrosine kinases janus kinase 1 and 2 (JAK1 and JAK2) and the signal transducer and activator of transcription 1 (STAT1) (figure 17). IFNγ binding to IFNGR1 leads to a conformational change of the receptor and the recruitment of IFNGR2. The receptor bound JAK1 and 2 proteins also undergo conformational changes upon stimulation, which is accompanied by their auto- and trans-phosphorylation and subsequent increase in activity. This results in the phosphorylation of STAT1 at tyrosine 701 and serine 727 [117]. The activation by phosphorylation is necessary for its homo-dimerization over the SH2 domains and phosphorylated tyrosines 701 [118, 119, 120]. The activated transcription factor dimer (nutcracker-like structure) translocates to the nucleus and initiates IFNγ stimulated gene (ISG) transcription via gamma activated sequence (GAS) elements in the DNA [121, 122, 123]. Interferon stimulated genes (ISGs) are a diverse group of more than 300 genes, including pro-apoptotic genes (e.g., APO2L/TRAIL, FAS, XIAP) as well as anti-angiogenetics like CXCL9, CXCL10, CXCL11 [12, 7, 13]. Interestingly, STAT1 knockout mice are viable, but show an enhanced susceptibility to bacterial and viral infections due to their loss of responsiveness to type I and type II IFNs [124, 125]. They also develop chemically induced and spontaneous tumors more frequently than their corresponding controls [126]. For STAT1 knockout human cells a decrease in apoptosis and an increase in proliferation has been reported in response to IFNα or IFNγ [127, 91].

Having identified the regulation of STAT1 through Brd4 we wondered whether Brd4 itself is regulated by IFNγ signaling. Indeed, Brd4 increased after IFNγ stimulation (figure 30). The same stimulation composition also led to an upregulation of *STAT1* as well as further known ISGs (figure 31). This implicates Brd4 to be an interferon stimulated gene. The consequences of two different knockdown approaches of Brd4 ("shC2" and "shE1") in combination with an IFNγ stimulation were tested subsequently. As expected, the diminishment of both Brd4 isoforms ("shC2") led to an inhibition of *STAT1* expression

as well as its target genes (figure 32). Unexpected was the elevation of most of the tested mRNA levels, including *STAT1*, after Brd4-long knockdown ("shE1") (figure 32). This finding was supported by a promoter reporter assay of the strongest induced ISG, lectin galactoside-binding soluble 3 binding protein (*LGALS3BP*) (figure 31). The activity in the single knockdown of Brd4-long ("shE1") with IFNγ treatment was increased to a comparable level with the corresponding control, but specifically suppressed when both Brd4 forms were missing under stimulated conditions ("shC2") (figure 34). Another indication of different functions of the long Brd4 isoform came from a Western Blot performed after Brd4 ("shC2" and "shE1") knockdown and IFNγ treatment. The STAT1 and LGALS3BP protein levels were decreased in the "shC2" knockdown. However, LGALS3BP was increased in the "shE1" knockdown (figure 33). This increase was not seen for the STAT1 protein level in the same sample. This difference in the protein levels might be due to the antibody used for STAT1 detection, which potentially did not recognize the phosphorylated variant of STAT1.

In summary, the IFNγ pathway is inhibited when both Brd4 isoforms are missing. In contrast, the long form of *Brd4* presents an interferon stimulated gene itself. Its specific knockdown ("shE1"), on the other hand, leads to an enhanced stimulation response. These diverging IFNγ signaling outcomes could potentially be traced back to the different Brd4 knockdown situations used for the analyses which varied in the presence ("shE1") or absence ("shC2") of the short Brd4 isoform. The induction of specifically the long Brd4 form by IFNγ might be, in general, based on the presence of the short form. The knockdown approach of "shE1" under IFNγ stimulation could have been driven by the presence of the short Brd4 isoform leading to an even greater induction of Brd4-long or the stabilization of its remaining parts and thus enhancing the IFNγ responses. Therefore, the short form of Brd4 seems to be essential for the signaling itself, but the long isoform responsible for the amount of the responses. The greater increase in LGALS3BP protein, specifically in the "shE1" Brd4 knockdown, could also support this hypothesis of an enhanced signaling. One could additionally think of further protein stabilizations produced by Brd4-long, which has already been seen in regard to the papillomavirus E2 protein, where Brd4 inhibits its ubiquitination and thus degradation via the proteasome [128, 129]. Figure 38 displays a potential model for the regulation of the signaling process for the different Brd4 knockdown approaches with simultaneous IFNγ stimulation.

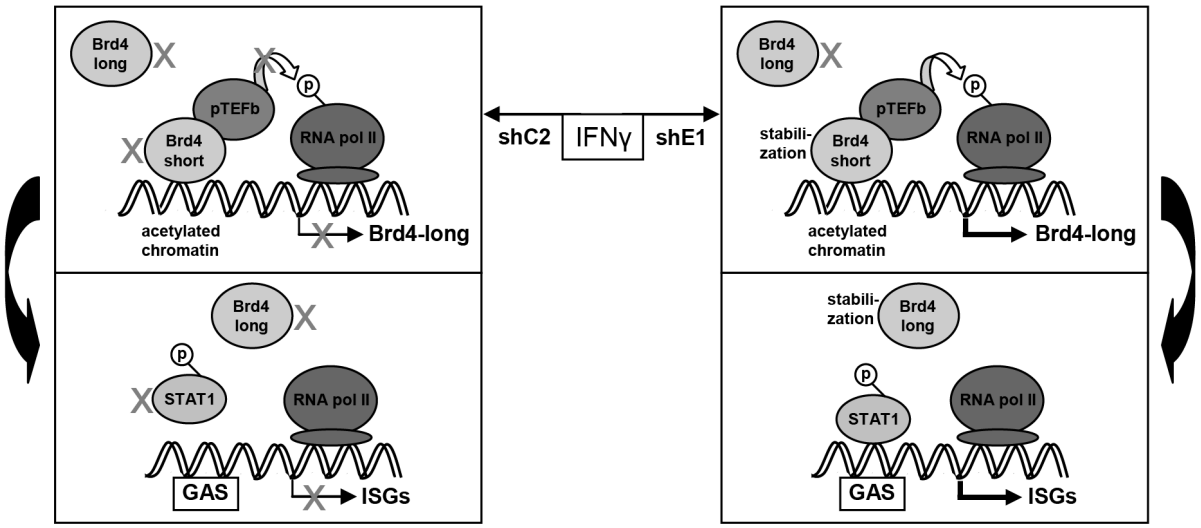

Figure 38: Model of the regulation mechanisms for the IFNγ responses after Brd4 knockdown. The knockdown of both Brd4 isoforms ("shC2") and simultaneous interferon gamma (IFNγ) stimulation potentially results in less transcriptional activation of the long *Brd4* isoform, which might rely on the support of Brd4-short. This would further affect *STAT1* expression and its activation of the interferon stimulated target genes (ISGs), leading to diminished IFNγ responses. On the other hand, after knockdown of Brd4-long ("shE1") the short Brd4 form is still present in the cell and potentially activates *Brd4-long* transcription under IFNγ stimulated conditions, thereby reverting the Brd4 "shE1" effect. This would in turn result in an activation of the expression of *STAT1* and its target genes, leading to an enhanced IFNγ signaling. The regulatory mechanism on the transcriptional level could otherwise also be supported by a posttranscriptional stabilization of the Brd4 proteins after knockdown and IFNγ stimulation.

However, to support the hypothesis of an enhanced IFNγ signaling after a knockdown of the long Brd4 isoform ("shE1") additional experiments are needed. These should include the specific detection of phosphorylated STAT1 under "shE1" and IFNγ stimulated conditions as well as the cloning of a *STAT1* promoter construct which responds to the IFNγ stimulation (following the results of Wong *et al.* [113]). Also necessary will be the validation of additional STAT1 target genes on protein level as well as a more detailed analysis of the regulation of both Brd4 isoforms. Besides a transcriptional regulation through Brd4 of STAT1, one could imagine an impact of Brd4 on STAT1 phosphorylation. This could be facilitated by the kinase activity of the Brd4 protein [59]. Further experimental set-ups in this direction should also be established in the future.

In summary, Brd4 directly regulates the expression of STAT1 and its target genes under unstimulated as well as IFNγ stimulated cellular conditions. This connection is similar to the identified NFκB interaction and activity modulation with consequences for the regulation of *TNFa* as well as further cytokine expressions and subsequent suppression of

inflammatory responses [17, 18]. The regulation through Brd4 will most likely also be seen for IFNα and β triggered inflammatory gene expression patterns due to the involvement of STAT1. To identify the function of Brd4, STAT1 and its target genes in the disease state, further experiments were performed.

5.6 Brd4, STAT1, and interferon gamma in breast cancer cells

Brd4 is implicated in DNA-tumor virus mediated tumors such as cervical cancer, Kaposi's sarcoma and Burkitt's lymphoma. You *et al.* have found that Brd4 directly interacts with the papillomavirus E2 protein and thus tethers the viral genome to host mitotic chromosome with the consequence of the maintenance of the viral infection in dividing cells (figure 3) [43, 44, 45]. Based on these results Brd4 has been found in diverse other tumor entities (breast cancer, acute myeloid leukemia) and identified as a potential target in tumor therapy. Its knockdown as well as inhibition by the BET protein inhibitor "JQ1" is accompanied by tumor growth reduction *in vitro* and *in vivo*, mainly discussed in matters of Myc and Myc target gene repression [23, 24, 20, 21].

In 2008 Crawford *et al.* found a negative correlation between Brd4 protein levels and the disease outcome in breast cancer patients [20]. Higher Brd4-long levels correlated with a better prognosis, possibly indicating a prognostic potential for the expression level of the long Brd4 isoform. An overexpression of Brd4-long in breast cancer cells with low Brd4 levels led to significant tumor growth reduction as well as a diminished metastatic potential [20]. This finding was also validated in colon cancers. Reduced expression of *Brd4* was explained by an aberrant promoter hypermethylation, leading to, at least in part, a silenced gene. Again, a re-introduction of Brd4-long resulted *in vitro* and *in vivo* in a marked reduction of tumor growth and tumor size [78]. Taken together, these publications implicate Brd4 as a potential tumor suppressor in breast and colon cancers. Most interestingly, the STAT1 protein was also identified in connection to breast cancers. Patients with higher levels of phosphorylated and DNA-bound STAT1 showed a better prognosis and lived longer [130]. Due to the prognostic effects for Brd4 and STAT1 in breast tumors, we chose this cancer entity for further functional studies. We found significantly decreased levels of the long Brd4 protein in one metastatic breast cancer cell line (SK-BR-3 cells). This finding was accompanied by a simultaneously lower expression of STAT1 (figure 35). The SK-BR-3 cell line was derived from a pleural effusion (metastatic site) of a patient with a breast adenocarcinoma [80].

Interestingly, experiments in breast cancers investigating the level of the short Brd4 isoform revealed that its expression level correlated with a poor disease outcome and an overexpression of Brd4-short resulted in a greater metastasis forming capacity of the cells [21]. Having these results in mind we measured the expression levels of both Brd4 isoforms in the SK-BR-3 cells separately. We identified a condition of notable lower *Brd4-long* expression which corresponds to the analyzed protein level (figure 35), but also a more than threefold increased expression of *Brd4-short*, in comparison to the normal cells (figure 36). Our findings, as well as the results from Crawford *et al.* and Alsarraj *et al.* would indicate a poor prognosis for the donator of those cells. In addition to our findings, Yim *et al.* indicated that especially the SK-BR-3 cell line showed a non-response to interferon gamma (IFNγ) mediated cell growth inhibition [92]. They argue that the missing response of SK-BR-3 cells to IFNγ was due to the lack of interferon regulatory factor 1 (*IRF1*) expression, one of the best known STAT1 target genes [92]. Following their path, we investigated the overexpression of Brd4-long in that specific cell line as well as the expression profile after overexpression and simultaneous IFNγ stimulation. As expected from other previous results, the expression of *STAT1* increased after Brd4-long overexpression and so did the expression of *IRF1* and STAT1's other target genes. The analyzed levels also elevated under interferon gamma stimulation alone, but the greatest increase was produced on *STAT1* and the targets in the combination of the overexpression and the IFNγ stimulation (figure 37). Interestingly, although Brd4-long was overexpressed in the unstimulated as well as INFγ stimulated sample, its mRNA level after stimulation was upregulated approximately twentyfold (figure 37). This additional result validated the detected elevation of *Brd4-long* mRNA after interferon gamma stimulation in Hek293T cells (figure 30). Based on these findings in the stimulated and unstimulated SK-BR-3 cells with Brd4-long overexpression, there could be a rescue of the described IFNγ non-responsiveness of the cell line. This should be detectable by a cell growth inhibition through activated STAT1 expression. Further analyses should be performed for the validation of this hypothesis. Also, the increase in STAT1 expression as well as its target genes after Brd4-long overexpression with simultaneous IFNγ stimulation should be analyzed on protein levels for additional validations.

Taken together, it seems that the missing response of the metastatic breast cancer cell line SK-BR-3 to IFNγ could be antagonized by an overexpression of the long Brd4 isoform.

5.7 The bottom line conclusion

The mRNA sequencing after Brd4 knockdown provided us with an expression profile which consisted of known and unknown cellular targets of Brd4. The most significant alterations after Brd4 knockdown were in the interferon signaling cascades through the regulation of STAT proteins, and in particular STAT1. The regulation of *STAT1* expression was further validated using Brd4-long ChIP sequencings and was shown to be directly due to the association of Brd4 with the *STAT1* promoter. This connection between Brd4, STAT1 and its targets was additionally confirmed under IFNγ stimulated conditions, which showed important implications for both of the Brd4 isoforms in the signaling process. Their presence regulated the outcome of the stimulation response and highlighted yet another role for Brd4-long in the process as an interferon inducible gene itself. The established regulation in the unstimulated as well as stimulated cellular state was transferred to the breast cancer cell system and supported the proposed prognostic potential for the long Brd4 form. The regulation of the interferon pathway by Brd4 might be used as a new therapeutic strategy for the treatment of inflammatory diseases and cancer.

Besides the above mentioned involvement of Brd4 in the interferon signaling pathways, our mRNA Seq data after Brd4 knockdown uncovered even further pathways dependent on the Brd4 level. For example the phosphatase and tensin homolog (PTEN) signaling (figure 16) was the second most significantly affected pathway identified. This connection is highly interesting, because PTEN signaling is often lost or suppressed in tumor cells due to its opposing actions on proliferative signaling cascades [1, 2]. Also noteworthy is the possible link between the long form of Brd4 and mRNA splicing, which was hypothesized in matters of the ChIP sequencing results and the identification of Brd4-specific preferences to exon sequences. Taken together, our data obtained by Next Generation Sequencing present known as well as unknown cellular processes depending on the bromodomain containing protein 4, provide an extensive set of information on transcriptional and genomic associations for Brd4 and hold the potential for further analyses in the future concerning Brd4's function in the cell.

6 Summary

The cellular bromodomain protein 4 (Brd4) is a transcriptional regulator. It binds to transcription factors, the positive transcriptional elongation complex and acetylated histone residues. Furthermore, it has been shown to function as a master regulator in diverse cancer entities such as breast cancer, acute myeloid leukemia (AML) and specific midline carcinomas. Within my thesis I investigated the gene expression profile after Brd4 knockdown obtained by mRNA Next Generation Sequencing. I was able to validate the regulation of Myc and its target genes through Brd4 and I identified a so far unknown role of Brd4 in the interferon (IFN) signaling pathways. Here, I specifically found that Brd4 regulates STAT1, a key protein in IFNα, β and γ processes. With endogenous Brd4 chromatin immunoprecipitations (ChIP Seqs) and luciferase reporter assays I further characterized STAT1 as a direct Brd4 target gene.

The signal transducer and activator of transcription 1 (STAT1) is the exclusive mediator of interferon gamma (IFNy) signaling, an inflammatory mechanism for the protection against infections which is also required for the control of tumor growth. STAT1 showed a significant decrease after Brd4 knockdown and an increase after Brd4 elevation. I was also able to show an impact of Brd4 on STAT1 target gene expressions, specifically on the group of interferon stimulated genes (ISGs), such as the interferon inducible transmembrane proteins 1, 2 and 3 (IFITM1-3) and the lectin galactoside-binding soluble 3 binding protein (LGALS3BP). These genes are activated in response to IFNγ triggered phosphorylation of STAT1. Since inflammation is discussed not only as a major cause for but also a defense mechanism against cancers, I further investigated breast cancer cells with a known diminished IFNγ response. Here, I found a reduced level of Brd4 accompanied by a STAT1 reduction. A re-introduction of Brd4 resulted in a STAT1 upregulation. In addition, its target genes - such as interferon regulatory factors 1 (IRF1) and interferon alpha-inducible protein 6 (IFI6) - increased. These findings indicate a possible rescue mechanism and counteraction for interferon independent growth of tumor cells. Taken together, I was able to uncover a novel function of Brd4 in the regulation of the interferon gamma response. This has important implications in regard to the anti-proliferative and pro-apoptotic effects of IFNγ in tumors and suggests potential novel strategies for cancer therapies in the future.

7 Zusammenfassung

Das zelluläre Bromodomänen Protein 4 (Brd4) ist ein transkriptioneller Regulator. Es bindet an Transkriptionsfaktoren, den positiven Transkriptionselongationskomplex und azetylierte Histon-Reste. Des weiteren konnte gezeigt werden, dass es als übergeordneter Regulator in verschiedenen Tumorarten, wie zum Beispiel dem Brustkrebs und der akuten myeloischen Leukämie (AML), eine wichtige Rolle spielt. Als wesentlichen Bestandteil meiner Doktorarbeit habe ich das Genexpressionsprofil nach der Brd4-Reduktion untersucht, welches ich mit Hilfe von mRNA-Sequenzierung erstellt habe. Hierbei war es mir möglich, die transkriptionellen Abhängigkeiten von Myc und seinen Zielgenen zu bestätigen und einen bisher unbekannten Zusammenhang zu den Interferon (IFN) Signalwegen herzustellen. Hierbei fiel besonders die Regulation von STAT1 auf, welches das Schlüssel-Protein der IFNα, β and γ Prozesse darstellt. Anhand von endogenen Brd4-Chromatin-Immunpräzipitationen und Luziferase-Reporter-Experimenten konnte ich STAT1 weiterführend als direktes Zielgen von Brd4 identifizieren.

Der Signalüberträger und Transkriptionsaktivator 1 (STAT1) ist der einzige Vermittler des Interferon gamma Signalweges, ein Bekämpfungsmechanismus gegen Virusinfektionen, der zusätzlich bei der Wachstumskontrolle von Tumoren eine wichtige Rolle spielt. STAT1 zeigte eine signifikante Herabregulierung nach der Brd4-Reduktion und einen Anstieg bei Brd4-Erhöhung. Des weiteren war es mir möglich zu zeigen, dass auch die STAT1-Zielgene, speziell die Subgruppe der Interferon stimulierten Gene (ISGs), wie zum Beispiel die Interferon induzierten Transmembranproteine 1, 2 und 3 (IFITM1-3), von der Brd4-Menge abhängig waren. Diese Gene werden durch die IFNγ angestoßene Phosphorylierung von STAT1 aktiviert und vermitteln die weiterführende Immun-Antwort.

Entzündungsprozesse werden als bedeutende Auslöser von Krebs diskutiert, auf der anderen Seite jedoch auch als seine Bekämpfungsmechanismen. Mit diesem Hintergrund untersuchte ich Brustkrebszellen, welche sich durch ein bekanntes Fehlen der IFNγ-Antwort auszeichneten. In diesen identifizierte ich ein reduziertes Brd4-Level, das von einer ebenfalls reduzierten STAT1-Menge begleitet war. Eine Wiedereinführung von Brd4 resultierte in einem Anstieg von STAT1. Zusätzlich stieg auch die Expression seiner Zielgene an, unter anderem des Interferon regulierenden Faktors 1 (IRF1) und des Interferon al-

pha induzierbaren Proteins 6 (IFI6). Diese Ergebnisse lassen vermuten, dass es hierbei möglicherweise zu einer Umkehrung des zuvor bekannten Interferon unabhängigen Tumorwachstums kommt.

Zusammenfassend konnte ich eine neue Funktion von Brd4 in der Regulation der Interferon gamma Antwort aufdecken. Diese hat eine besondere Bedeutung für die anti-proliferativen und pro-apoptotischen Effekte in Tumoren, die durch IFNγ vermittelt werden, welche potentiell neue Behandlungsstrategien für Krebs in der Zukunft nach sich ziehen könnte.

8 References

[1] D. Hanahan and R. A. Weinberg. The hallmarks of cancer. *Cell*, 100(1):57–70, Jan 2000.

[2] D. Hanahan and R. A. Weinberg. Hallmarks of cancer: the next generation. *Cell*, 144(5):646–674, Mar 2011.

[3] T. D. Gilmore. Introduction to NF-kappaB: players, pathways, perspectives. *Oncogene*, 25(51):6680–6684, Oct 2006.

[4] A. R. Brasier. The NF-kappaB regulatory network. *Cardiovasc. Toxicol.*, 6(2): 111–130, 2006.

[5] A. Mantovani, P. Allavena, A. Sica, and F. Balkwill. Cancer-related inflammation. *Nature*, 454(7203):436–444, Jul 2008.

[6] M. Karin. NF-kappaB as a critical link between inflammation and cancer. *Cold Spring Harb Perspect Biol*, 1(5):a000141, Nov 2009.

[7] M. J. de Veer, M. Holko, M. Frevel, E. Walker, S. Der, J. M. Paranjape, R. H. Silverman, and B. R. Williams. Functional classification of interferon-stimulated genes identified using microarrays. *J. Leukoc. Biol.*, 69(6):912–920, Jun 2001.

[8] G. Germano, P. Allavena, and A. Mantovani. Cytokines as a key component of cancer-related inflammation. *Cytokine*, 43(3):374–379, Sep 2008.

[9] H. Yu, M. Kortylewski, and D. Pardoll. Crosstalk between cancer and immune cells: role of STAT3 in the tumour microenvironment. *Nat. Rev. Immunol.*, 7(1):41–51, Jan 2007.

[10] H. Yu, D. Pardoll, and R. Jove. STATs in cancer inflammation and immunity: a leading role for STAT3. *Nat. Rev. Cancer*, 9(11):798–809, Nov 2009.

[11] V. Baud and M. Karin. Is NF-kappaB a good target for cancer therapy? Hopes and pitfalls. *Nat Rev Drug Discov*, 8(1):33–40, Jan 2009.

[12] S. D. Der, A. Zhou, B. R. Williams, and R. H. Silverman. Identification of genes differentially regulated by interferon alpha, beta, or gamma using oligonucleotide arrays. *Proc. Natl. Acad. Sci. U.S.A.*, 95(26):15623–15628, Dec 1998.

[13] E. C. Borden, G. C. Sen, G. Uze, R. H. Silverman, R. M. Ransohoff, G. R. Foster, and G. R. Stark. Interferons at age 50: past, current and future impact on biomedicine. *Nat Rev Drug Discov*, 6(12):975–990, Dec 2007.

[14] O. H. Kramer, D. Baus, S. K. Knauer, S. Stein, E. Jager, R. H. Stauber, M. Grez, E. Pfitzner, and T. Heinzel. Acetylation of Stat1 modulates NF-kappaB activity. *Genes Dev.*, 20(4):473–485, Feb 2006.

[15] A. Garg and B. B. Aggarwal. Nuclear transcription factor-kappaB as a target for cancer drug development. *Leukemia*, 16(6):1053–1068, Jun 2002.

[16] G. Sethi, B. Sung, and B. B. Aggarwal. Nuclear factor-kappaB activation: from bench to bedside. *Exp. Biol. Med. (Maywood)*, 233(1):21–31, Jan 2008.

[17] B. Huang, X. D. Yang, M. M. Zhou, K. Ozato, and L. F. Chen. Brd4 coactivates transcriptional activation of NF-kappaB via specific binding to acetylated RelA. *Mol. Cell. Biol.*, 29(5):1375–1387, Mar 2009.

[18] E. Nicodeme, K. L. Jeffrey, U. Schaefer, S. Beinke, S. Dewell, C. W. Chung, R. Chandwani, I. Marazzi, P. Wilson, H. Coste, J. White, J. Kirilovsky, C. M. Rice, J. M. Lora, R. K. Prinjha, K. Lee, and A. Tarakhovsky. Suppression of inflammation by a synthetic histone mimic. *Nature*, 468(7327):1119–1123, Dec 2010.

[19] J. You, J. L. Croyle, A. Nishimura, K. Ozato, and P. M. Howley. Interaction of the bovine papillomavirus E2 protein with Brd4 tethers the viral DNA to host mitotic chromosomes. *Cell*, 117(3):349–360, Apr 2004.

[20] N. P. Crawford, J. Alsarraj, L. Lukes, R. C. Walker, J. S. Officewala, H. H. Yang, M. P. Lee, K. Ozato, and K. W. Hunter. Bromodomain 4 activation predicts breast cancer survival. *Proc. Natl. Acad. Sci. U.S.A.*, 105(17):6380–6385, Apr 2008.

[21] J. Alsarraj, R. C. Walker, J. D. Webster, T. R. Geiger, N. P. Crawford, R. M. Simpson, K. Ozato, and K. W. Hunter. Deletion of the proline-rich region of the murine metastasis susceptibility gene Brd4 promotes epithelial-to-mesenchymal transition- and stem cell-like conversion. *Cancer Res.*, 71(8):3121–3131, Apr 2011.

[22] J. Zuber, J. Shi, E. Wang, A. R. Rappaport, H. Herrmann, E. A. Sison, D. Magoon, J. Qi, K. Blatt, M. Wunderlich, M. J. Taylor, C. Johns, A. Chicas, J. C. Mulloy, S. C. Kogan, P. Brown, P. Valent, J. E. Bradner, S. W. Lowe, and C. R. Vakoc. RNAi screen identifies Brd4 as a therapeutic target in acute myeloid leukaemia. *Nature*, 478(7370):524–528, Oct 2011.

[23] J. D. Kessler, K. T. Kahle, T. Sun, K. L. Meerbrey, M. R. Schlabach, E. M. Schmitt, S. O. Skinner, Q. Xu, M. Z. Li, Z. C. Hartman, M. Rao, P. Yu, R. Dominguez-Vidana, A. C. Liang, N. L. Solimini, R. J. Bernardi, B. Yu, T. Hsu, I. Golding, J. Luo, C. K. Osborne, C. J. Creighton, S. G. Hilsenbeck, R. Schiff, C. A. Shaw, S. J. Elledge, and T. F. Westbrook. A SUMOylation-dependent transcriptional subprogram is required for Myc-driven tumorigenesis. *Science*, 335(6066):348–353, Jan 2012.

[24] M. Toyoshima, H. L. Howie, M. Imakura, R. M. Walsh, J. E. Annis, A. N. Chang, J. Frazier, B. N. Chau, A. Loboda, P. S. Linsley, M. A. Cleary, J. R. Park, and C. Grandori. Functional genomics identifies therapeutic targets for MYC-driven cancer. *Proc. Natl. Acad. Sci. U.S.A.*, 109(24):9545–9550, Jun 2012.

[25] E. Shang, G. Salazar, T. E. Crowley, X. Wang, R. A. Lopez, X. Wang, and D. J. Wolgemuth. Identification of unique, differentiation stage-specific patterns of expression of the bromodomain-containing genes Brd2, Brd3, Brd4, and Brdt in the mouse testis. *Gene Expr. Patterns*, 4(5):513–519, Sep 2004.

[26] A. Paillisson, A. Levasseur, P. Gouret, I. Callebaut, M. Bontoux, P. Pontarotti, and P. Monget. Bromodomain testis-specific protein is expressed in mouse oocyte and evolves faster than its ubiquitously expressed paralogs BRD2, -3, and -4. *Genomics*, 89(2):215–223, Feb 2007.

[27] M. Kasahara. Genome dynamics of the major histocompatibility complex: insights from genome paralogy. *Immunogenetics*, 50(3-4):134–145, Nov 1999.

[28] D. Houzelstein, S. L. Bullock, D. E. Lynch, E. F. Grigorieva, V. A. Wilson, and R. S. Beddington. Growth and early postimplantation defects in mice deficient for the bromodomain-containing protein Brd4. *Mol. Cell. Biol.*, 22(11):3794–3802, Jun 2002.

[29] F. Jeanmougin, J. M. Wurtz, B. Le Douarin, P. Chambon, and R. Losson. The

bromodomain revisited. *Trends Biochem. Sci.*, 22(5):151–153, May 1997.

[30] S. Y. Wu and C. M. Chiang. The double bromodomain-containing chromatin adaptor Brd4 and transcriptional regulation. *J. Biol. Chem.*, 282(18):13141–13145, May 2007.

[31] L. Zeng and M. M. Zhou. Bromodomain: an acetyl-lysine binding domain. *FEBS Lett.*, 513(1):124–128, Feb 2002.

[32] Y. Nakamura, T. Umehara, K. Nakano, M. K. Jang, M. Shirouzu, S. Morita, H. Uda-Tochio, H. Hamana, T. Terada, N. Adachi, T. Matsumoto, A. Tanaka, M. Horikoshi, K. Ozato, B. Padmanabhan, and S. Yokoyama. Crystal structure of the human BRD2 bromodomain: insights into dimerization and recognition of acetylated histone H4. *J. Biol. Chem.*, 282(6):4193–4201, Feb 2007.

[33] S. Rahman, M. E. Sowa, M. Ottinger, J. A. Smith, Y. Shi, J. W. Harper, and P. M. Howley. The Brd4 extraterminal domain confers transcription activation independent of pTEFb by recruiting multiple proteins, including NSD3. *Mol. Cell. Biol.*, 31(13):2641–2652, Jul 2011.

[34] H. Fukazawa and A. Masumi. The conserved 12-amino acid stretch in the inter-bromodomain region of BET family proteins functions as a nuclear localization signal. *Biol. Pharm. Bull.*, Sep 2012.

[35] A. Dey, J. Ellenberg, A. Farina, A. E. Coleman, T. Maruyama, S. Sciortino, J. Lippincott-Schwartz, and K. Ozato. A bromodomain protein, MCAP, associates with mitotic chromosomes and affects G(2)-to-M transition. *Mol. Cell. Biol.*, 20 (17):6537–6549, Sep 2000.

[36] UniProt. http://www.uniprot.org/uniprot/o60885, November 2012. URL `http://www.uniprot.org/uniprot/O60885`.

[37] A. Nishiyama, A. Dey, J. Miyazaki, and K. Ozato. Brd4 is required for recovery from antimicrotubule drug-induced mitotic arrest: preservation of acetylated chromatin. *Mol. Biol. Cell*, 17(2):814–823, Feb 2006.

[38] S. Y. Wu, A. Y. Lee, S. Y. Hou, J. K. Kemper, H. Erdjument-Bromage, P. Tempst, and C. M. Chiang. Brd4 links chromatin targeting to HPV transcriptional silencing. *Genes Dev.*, 20(17):2383–2396, Sep 2006.

[39] A. Dey, F. Chitsaz, A. Abbasi, T. Misteli, and K. Ozato. The double bromodomain protein Brd4 binds to acetylated chromatin during interphase and mitosis. *Proc. Natl. Acad. Sci. U.S.A.*, 100(15):8758–8763, Jul 2003.

[40] C. Muchardt, J. C. Reyes, B. Bourachot, E. Leguoy, and M. Yaniv. The hbrm and BRG-1 proteins, components of the human SNF/SWI complex, are phosphorylated and excluded from the condensed chromosomes during mitosis. *EMBO J.*, 15(13): 3394–3402, Jul 1996.

[41] R. Wang, Q. Li, C. M. Helfer, J. Jiao, and J. You. Bromodomain protein Brd4 associated with acetylated chromatin is important for maintenance of higher-order chromatin structure. *J. Biol. Chem.*, 287(14):10738–10752, Mar 2012.

[42] T. Kouzarides. Chromatin modifications and their function. *Cell*, 128(4):693–705, Feb 2007.

[43] J. You, V. Srinivasan, G. V. Denis, W. J. Harrington, M. E. Ballestas, K. M. Kaye, and P. M. Howley. Kaposi's sarcoma-associated herpesvirus latency-associated nuclear antigen interacts with bromodomain protein Brd4 on host mitotic chromosomes. *J. Virol.*, 80(18):8909–8919, Sep 2006.

[44] A. Lin, S. Wang, T. Nguyen, K. Shire, and L. Frappier. The EBNA1 protein of Epstein-Barr virus functionally interacts with Brd4. *J. Virol.*, 82(24):12009–12019, Dec 2008.

[45] T. Silla, A. Mannik, and M. Ustav. Effective formation of the segregation-competent complex determines successful partitioning of the bovine papillomavirus genome during cell division. *J. Virol.*, 84(21):11175–11188, Nov 2010.

[46] H. Feng, M. Shuda, Y. Chang, and P. S. Moore. Clonal integration of a polyomavirus in human Merkel cell carcinoma. *Science*, 319(5866):1096–1100, Feb 2008.

[47] M. R. Schweiger, J. You, and P. M. Howley. Bromodomain protein 4 mediates the papillomavirus E2 transcriptional activation function. *J. Virol.*, 80(9):4276–4285, May 2006.

[48] J. A. Smith, E. A. White, M. E. Sowa, M. L. Powell, M. Ottinger, J. W. Harper, and P. M. Howley. Genome-wide siRNA screen identifies SMCX, EP400, and Brd4 as E2-dependent regulators of human papillomavirus oncogene expression. *Proc.*

Natl. Acad. Sci. U.S.A., 107(8):3752–3757, Feb 2010.

[49] H. Kurachi, Y. Wada, N. Tsukamoto, M. Maeda, H. Kubota, M. Hattori, K. Iwai, and N. Minato. Human SPA-1 gene product selectively expressed in lymphoid tissues is a specific GTPase-activating protein for Rap1 and Rap2. Segregate expression profiles from a rap1GAP gene product. *J. Biol. Chem.*, 272(44):28081–28088, Oct 1997.

[50] K. Kometani, D. Ishida, M. Hattori, and N. Minato. Rap1 and SPA-1 in hematologic malignancy. *Trends Mol Med*, 10(8):401–408, Aug 2004.

[51] A. Farina, M. Hattori, J. Qin, Y. Nakatani, N. Minato, and K. Ozato. Bromodomain protein Brd4 binds to GTPase-activating SPA-1, modulating its activity and subcellular localization. *Mol. Cell. Biol.*, 24(20):9059–9069, Oct 2004.

[52] K. Mochizuki, A. Nishiyama, M. K. Jang, A. Dey, A. Ghosh, T. Tamura, H. Natsume, H. Yao, and K. Ozato. The bromodomain protein Brd4 stimulates G1 gene transcription and promotes progression to S phase. *J. Biol. Chem.*, 283(14):9040–9048, Apr 2008.

[53] H. Ishii, T. Inageta, K. Mimori, T. Saito, H. Sasaki, M. Isobe, M. Mori, C. M. Croce, K. Huebner, K. Ozawa, and Y. Furukawa. Frag1, a homolog of alternative replication factor C subunits, links replication stress surveillance with apoptosis. *Proc. Natl. Acad. Sci. U.S.A.*, 102(27):9655–9660, Jul 2005.

[54] M. K. Jang, K. Mochizuki, M. Zhou, H. S. Jeong, J. N. Brady, and K. Ozato. The bromodomain protein Brd4 is a positive regulatory component of P-TEFb and stimulates RNA polymerase II-dependent transcription. *Mol. Cell*, 19(4):523–534, Aug 2005.

[55] J. Peng, N. F. Marshall, and D. H. Price. Identification of a cyclin subunit required for the function of Drosophila P-TEFb. *J. Biol. Chem.*, 273(22):13855–13860, May 1998.

[56] D. H. Price. P-TEFb, a cyclin-dependent kinase controlling elongation by RNA polymerase II. *Mol. Cell. Biol.*, 20(8):2629–2634, Apr 2000.

[57] Z. Yang, J. H. Yik, R. Chen, N. He, M. K. Jang, K. Ozato, and Q. Zhou. Recruitment of P-TEFb for stimulation of transcriptional elongation by the bromodomain protein

Brd4. *Mol. Cell*, 19(4):535–545, Aug 2005.

[58] M. Zhou, M. A. Halanski, M. F. Radonovich, F. Kashanchi, J. Peng, D. H. Price, and J. N. Brady. Tat modifies the activity of CDK9 to phosphorylate serine 5 of the RNA polymerase II carboxyl-terminal domain during human immunodeficiency virus type 1 transcription. *Mol. Cell. Biol.*, 20(14):5077–5086, Jul 2000.

[59] B. N. Devaiah, B. A. Lewis, N. Cherman, M. C. Hewitt, B. K. Albrecht, P. G. Robey, K. Ozato, R. J. Sims, and D. S. Singer. BRD4 is an atypical kinase that phosphorylates serine2 of the RNA polymerase II carboxy-terminal domain. *Proc. Natl. Acad. Sci. U.S.A.*, 109(18):6927–6932, May 2012.

[60] J. You, Q. Li, C. Wu, J. Kim, M. Ottinger, and P. M. Howley. Regulation of aurora B expression by the bromodomain protein Brd4. *Mol. Cell. Biol.*, 29(18):5094–5103, Sep 2009.

[61] Z. Yang, N. He, and Q. Zhou. Brd4 recruits P-TEFb to chromosomes at late mitosis to promote G1 gene expression and cell cycle progression. *Mol. Cell. Biol.*, 28(3): 967–976, Feb 2008.

[62] A. Dey, A. Nishiyama, T. Karpova, J. McNally, and K. Ozato. Brd4 marks select genes on mitotic chromatin and directs postmitotic transcription. *Mol. Biol. Cell*, 20(23):4899–4909, Dec 2009.

[63] M. Barboric, R. M. Nissen, S. Kanazawa, N. Jabrane-Ferrat, and B. M. Peterlin. NF-kappaB binds P-TEFb to stimulate transcriptional elongation by RNA polymerase II. *Mol. Cell*, 8(2):327–337, Aug 2001.

[64] S. Kanazawa, L. Soucek, G. Evan, T. Okamoto, and B. M. Peterlin. c-Myc recruits P-TEFb for transcription, cellular proliferation and apoptosis. *Oncogene*, 22(36): 5707–5711, Aug 2003.

[65] C. Simone, L. Bagella, C. Bellan, and A. Giordano. Physical interaction between pRb and cdk9/cyclinT2 complex. *Oncogene*, 21(26):4158–4165, Jun 2002.

[66] C. J. Ott, N. Kopp, L. Bird, R. M. Paranal, J. Qi, T. Bowman, S. J. Rodig, A. L. Kung, J. E. Bradner, and D. M. Weinstock. BET bromodomain inhibition targets both c-MYC and IL7R in high-risk acute lymphoblastic leukemia. *Blood*, Aug 2012.

[67] D. C. Hargreaves, T. Horng, and R. Medzhitov. Control of inducible gene expression by signal-dependent transcriptional elongation. *Cell*, 138(1):129–145, Jul 2009.

[68] J. S. Byun, M. M. Wong, W. Cui, G. Idelman, Q. Li, A. De Siervi, S. Bilke, C. M. Haggerty, A. Player, Y. H. Wang, M. J. Thirman, J. J. Kaberlein, C. Petrovas, R. A. Koup, D. Longo, K. Ozato, and K. Gardner. Dynamic bookmarking of primary response genes by p300 and RNA polymerase II complexes. *Proc. Natl. Acad. Sci. U.S.A.*, 106(46):19286–19291, Nov 2009.

[69] S. M. Kim, H. J. Kee, G. H. Eom, N. W. Choe, J. Y. Kim, Y. S. Kim, S. K. Kim, H. Kook, H. Kook, and S. B. Seo. Characterization of a novel WHSC1-associated SET domain protein with H3K4 and H3K27 methyltransferase activity. *Biochem. Biophys. Res. Commun.*, 345(1):318–323, Jun 2006.

[70] B. Chang, Y. Chen, Y. Zhao, and R. K. Bruick. JMJD6 is a histone arginine demethylase. *Science*, 318(5849):444–447, Oct 2007.

[71] C. J. Webby, A. Wolf, N. Gromak, M. Dreger, H. Kramer, B. Kessler, M. L. Nielsen, C. Schmitz, D. S. Butler, J. R. Yates, C. M. Delahunty, P. Hahn, A. Lengeling, M. Mann, N. J. Proudfoot, C. J. Schofield, and A. Bottger. Jmjd6 catalyses lysyl-hydroxylation of U2AF65, a protein associated with RNA splicing. *Science*, 325 (5936):90–93, Jul 2009.

[72] X. Hong, J. Zang, J. White, C. Wang, C. H. Pan, R. Zhao, R. C. Murphy, S. Dai, P. Henson, J. W. Kappler, J. Hagman, and G. Zhang. Interaction of JMJD6 with single-stranded RNA. *Proc. Natl. Acad. Sci. U.S.A.*, 107(33):14568–14572, Aug 2010.

[73] D. M. Parkin and F. Bray. Chapter 2: The burden of HPV-related cancers. *Vaccine*, 24 Suppl 3:11–25, Aug 2006.

[74] C. A. French, C. L. Ramirez, J. Kolmakova, T. T. Hickman, M. J. Cameron, M. E. Thyne, J. L. Kutok, J. A. Toretsky, A. K. Tadavarthy, U. R. Kees, J. A. Fletcher, and J. C. Aster. BRD-NUT oncoproteins: a family of closely related nuclear proteins that block epithelial differentiation and maintain the growth of carcinoma cells. *Oncogene*, 27(15):2237–2242, Apr 2008.

[75] C. A. French, I. Miyoshi, J. C. Aster, I. Kubonishi, T. G. Kroll, P. Dal Cin, S. O. Vargas, A. R. Perez-Atayde, and J. A. Fletcher. BRD4 bromodomain gene rear-

rangement in aggressive carcinoma with translocation t(15;19). *Am. J. Pathol.*, 159 (6):1987–1992, Dec 2001.

[76] C. A. French, I. Miyoshi, I. Kubonishi, H. E. Grier, A. R. Perez-Atayde, and J. A. Fletcher. BRD4-NUT fusion oncogene: a novel mechanism in aggressive carcinoma. *Cancer Res.*, 63(2):304–307, Jan 2003.

[77] M. A. den Bakker, B. H. Beverloo, M. M. van den Heuvel-Eibrink, C. A. Meeuwis, L. M. Tan, L. A. Johnson, C. A. French, and G. J. van Leenders. NUT midline carcinoma of the parotid gland with mesenchymal differentiation. *Am. J. Surg. Pathol.*, 33(8):1253–1258, Aug 2009.

[78] R. M. Rodriguez, C. Huidobro, R. G. Urdinguio, C. Mangas, B. Soldevilla, G. Dominguez, F. Bonilla, A. F. Fernandez, and M. F. Fraga. Aberrant epigenetic regulation of bromodomain BRD4 in human colon cancer. *J. Mol. Med.*, 90 (5):587–595, May 2012.

[79] P. Filippakopoulos, J. Qi, S. Picaud, Y. Shen, W. B. Smith, O. Fedorov, E. M. Morse, T. Keates, T. T. Hickman, I. Felletar, M. Philpott, S. Munro, M. R. McKeown, Y. Wang, A. L. Christie, N. West, M. J. Cameron, B. Schwartz, T. D. Heightman, N. La Thangue, C. A. French, O. Wiest, A. L. Kung, S. Knapp, and J. E. Bradner. Selective inhibition of BET bromodomains. *Nature*, 468(7327):1067–1073, Dec 2010.

[80] LGC Standards and ATCC. http://www.lgcstandards-atcc.org/, November 2012. URL `http://www.lgcstandards-atcc.org/`.

[81] S. Rozen and H. Skaletsky. http://frodo.wi.mit.edu/, November 2008-2012. URL `http://frodo.wi.mit.edu/`.

[82] J. R. Schoenborn and C. B. Wilson. Regulation of interferon-gamma during innate and adaptive immune responses. *Adv. Immunol.*, 96:41–101, 2007.

[83] M. D. Robinson, D. J. McCarthy, and G. K. Smyth. edgeR: a Bioconductor package for differential expression analysis of digital gene expression data. *Bioinformatics*, 26(1):139–140, Jan 2010.

[84] SABiosciences. http://www.sabiosciences.com/chipqpcrsearch.php?app=tfbs, May 2012. URL `http://www.sabiosciences.com/chipqpcrsearch.php?`

app=TFBS.

[85] J. Blancato, B. Singh, A. Liu, D. J. Liao, and R. B. Dickson. Correlation of amplification and overexpression of the c-myc oncogene in high-grade breast cancer: FISH, in situ hybridisation and immunohistochemical analyses. *Br. J. Cancer*, 90 (8):1612–1619, Apr 2004.

[86] L. Kozma, I. Kiss, S. Szakall, and I. Ember. Investigation of c-myc oncogene amplification in colorectal cancer. *Cancer Lett.*, 81(2):165–169, Jun 1994.

[87] ConsensusPathDB. http://cpdb.molgen.mpg.de/, November 2012. URL `http://cpdb.molgen.mpg.de/`.

[88] Y. Zhang, T. Liu, C. A. Meyer, J. Eeckhoute, D. S. Johnson, B. E. Bernstein, C. Nusbaum, R. M. Myers, M. Brown, W. Li, and X. S. Liu. Model-based analysis of ChIP-Seq (MACS). *Genome Biol.*, 9(9):R137, 2008.

[89] M. Salmon-Divon, H. Dvinge, K. Tammoja, and P. Bertone. PeakAnalyzer: genome-wide annotation of chromatin binding and modification loci. *BMC Bioinformatics*, 11:415, 2010.

[90] G. Leroy, I. Chepelev, P. A. Dimaggio, M. A. Blanco, B. M. Zee, K. Zhao, and B. A. Garcia. Proteo-Genomic characterization and mapping of nucleosomes decoded by Brd and HP1 proteins. *Genome Biol.*, 13(8):R68, Aug 2012.

[91] C. K. Lee, E. Smith, R. Gimeno, R. Gertner, and D. E. Levy. STAT1 affects lymphocyte survival and proliferation partially independent of its role downstream of IFN-gamma. *J. Immunol.*, 164(3):1286–1292, Feb 2000.

[92] J. H. Yim, S. H. Ro, J. K. Lowney, S. J. Wu, J. Connett, and G. M. Doherty. The role of interferon regulatory factor-1 and interferon regulatory factor-2 in IFN-gamma growth inhibition of human breast carcinoma cell lines. *J. Interferon Cytokine Res.*, 23(9):501–511, Sep 2003.

[93] J. You, M. R. Schweiger, and P. M. Howley. Inhibition of E2 binding to Brd4 enhances viral genome loss and phenotypic reversion of bovine papillomavirus-transformed cells. *J. Virol.*, 79(23):14956–14961, Dec 2005.

[94] C. Arvanitis and D. W. Felsher. Conditionally MYC: insights from novel transgenic

models. *Cancer Lett.*, 226(2):95–99, Aug 2005.

[95] D. W. Felsher and J. M. Bishop. Reversible tumorigenesis by MYC in hematopoietic lineages. *Mol. Cell*, 4(2):199–207, Aug 1999.

[96] S. Pelengaris, M. Khan, and G. I. Evan. Suppression of Myc-induced apoptosis in beta cells exposes multiple oncogenic properties of Myc and triggers carcinogenic progression. *Cell*, 109(3):321–334, May 2002.

[97] H. Sato, S. Minei, T. Hachiya, T. Yoshida, and Y. Takimoto. Fluorescence in situ hybridization analysis of c-myc amplification in stage TNM prostate cancer in Japanese patients. *Int. J. Urol.*, 13(6):761–766, Jun 2006.

[98] J. R. Park, A. Eggert, and H. Caron. Neuroblastoma: biology, prognosis, and treatment. *Pediatr. Clin. North Am.*, 55(1):97–120, Feb 2008.

[99] D. Cappellen, T. Schlange, M. Bauer, F. Maurer, and N. E. Hynes. Novel c-MYC target genes mediate differential effects on cell proliferation and migration. *EMBO Rep.*, 8(1):70–76, Jan 2007.

[100] C. M. Koh, B. Gurel, S. Sutcliffe, M. J. Aryee, D. Schultz, T. Iwata, M. Uemura, K. I. Zeller, U. Anele, Q. Zheng, J. L. Hicks, W. G. Nelson, C. V. Dang, S. Yegnasubramanian, and A. M. De Marzo. Alterations in nucleolar structure and gene expression programs in prostatic neoplasia are driven by the MYC oncogene. *Am. J. Pathol.*, 178(4):1824–1834, Apr 2011.

[101] H. Wang, S. Mannava, V. Grachtchouk, D. Zhuang, M. S. Soengas, A. V. Gudkov, E. V. Prochownik, and M. A. Nikiforov. c-Myc depletion inhibits proliferation of human tumor cells at various stages of the cell cycle. *Oncogene*, 27(13):1905–1915, Mar 2008.

[102] C. V. Dang. MYC on the path to cancer. *Cell*, 149(1):22–35, Mar 2012.

[103] L. Soucek, J. Whitfield, C. P. Martins, A. J. Finch, D. J. Murphy, N. M. Sodir, A. N. Karnezis, L. B. Swigart, S. Nasi, and G. I. Evan. Modelling Myc inhibition as a cancer therapy. *Nature*, 455(7213):679–683, Oct 2008.

[104] A. R. Wasylishen and L. Z. Penn. Myc: the beauty and the beast. *Genes Cancer*, 1(6):532–541, Jun 2010.

[105] S. T. Menendez, J. P. Rodrigo, E. Allonca, D. Garcia-Carracedo, G. Alvarez-Alija, S. Casado-Zapico, M. F. Fresno, C. Rodriguez, C. Suarez, and J. M. Garcia-Pedrero. Expression and clinical significance of the Kv3.4 potassium channel subunit in the development and progression of head and neck squamous cell carcinomas. *J. Pathol.*, 221(4):402–410, Aug 2010.

[106] K. W. Chang, T. C. Yuan, K. P. Fang, F. S. Yang, C. J. Liu, C. S. Chang, and S. C. Lin. The increase of voltage-gated potassium channel Kv3.4 mRNA expression in oral squamous cell carcinoma. *J. Oral Pathol. Med.*, 32(10):606–611, Nov 2003.

[107] X. Huang, H. Yang, Y. Zhou, J. Liu, B. Yin, X. Peng, B. Qiang, and J. Yuan. Overexpression of human reticulon 3 (hRTN3) in astrocytoma. *Clin. Neuropathol.*, 23(1):1–7, 2004.

[108] Ingenuity Systems. http://www.ingenuity.com/, November 2012. URL `http://www.ingenuity.com/`.

[109] H. Cheon and G. R. Stark. Unphosphorylated STAT1 prolongs the expression of interferon-induced immune regulatory genes. *Proc. Natl. Acad. Sci. U.S.A.*, 106 (23):9373–9378, Jun 2009.

[110] S. Ghosh, M. J. May, and E. B. Kopp. NF-kappa B and Rel proteins: evolutionarily conserved mediators of immune responses. *Annu. Rev. Immunol.*, 16:225–260, 1998.

[111] T. Hehlgans and K. Pfeffer. The intriguing biology of the tumour necrosis factor/tumour necrosis factor receptor superfamily: players, rules and the games. *Immunology*, 115(1):1–20, May 2005.

[112] D. Heumann and T. Roger. Initial responses to endotoxins and Gram-negative bacteria. *Clin. Chim. Acta*, 323(1-2):59–72, Sep 2002.

[113] L. H. Wong, H. Sim, M. Chatterjee-Kishore, I. Hatzinisiriou, R. J. Devenish, G. Stark, and S. J. Ralph. Isolation and characterization of a human STAT1 gene regulatory element. Inducibility by interferon (IFN) types I and II and role of IFN regulatory factor-1. *J. Biol. Chem.*, 277(22):19408–19417, May 2002.

[114] P. Kolasinska-Zwierz, T. Down, I. Latorre, T. Liu, X. S. Liu, and J. Ahringer. Differential chromatin marking of introns and expressed exons by H3K36me3. *Nat. Genet.*, 41(3):376–381, Mar 2009.

[115] F. Carrillo Oesterreich, N. Bieberstein, and K. M. Neugebauer. Pause locally, splice globally. *Trends Cell Biol.*, 21(6):328–335, Jun 2011.

[116] F. D. Shi and L. Van Kaer. Reciprocal regulation between natural killer cells and autoreactive T cells. *Nat. Rev. Immunol.*, 6(10):751–760, Oct 2006.

[117] Z. Wen, Z. Zhong, and J. E. Darnell. Maximal activation of transcription by Stat1 and Stat3 requires both tyrosine and serine phosphorylation. *Cell*, 82(2):241–250, Jul 1995.

[118] K. Shuai, A. Ziemiecki, A. F. Wilks, A. G. Harpur, H. B. Sadowski, M. Z. Gilman, and J. E. Darnell. Polypeptide signalling to the nucleus through tyrosine phosphorylation of Jak and Stat proteins. *Nature*, 366(6455):580–583, Dec 1993.

[119] K. Shuai, C. M. Horvath, L. H. Huang, S. A. Qureshi, D. Cowburn, and J. E. Darnell. Interferon activation of the transcription factor Stat91 involves dimerization through SH2-phosphotyrosyl peptide interactions. *Cell*, 76(5):821–828, Mar 1994.

[120] M. H. Heim, I. M. Kerr, G. R. Stark, and J. E. Darnell. Contribution of STAT SH2 groups to specific interferon signaling by the Jak-STAT pathway. *Science*, 267 (5202):1347–1349, Mar 1995.

[121] K. Shuai, C. Schindler, V. R. Prezioso, and J. E. Darnell. Activation of transcription by IFN-gamma: tyrosine phosphorylation of a 91-kD DNA binding protein. *Science*, 258(5089):1808–1812, Dec 1992.

[122] G. R. Stark, I. M. Kerr, B. R. Williams, R. H. Silverman, and R. D. Schreiber. How cells respond to interferons. *Annu. Rev. Biochem.*, 67:227–264, 1998.

[123] X. Chen, U. Vinkemeier, Y. Zhao, D. Jeruzalmi, J. E. Darnell, and J. Kuriyan. Crystal structure of a tyrosine phosphorylated STAT-1 dimer bound to DNA. *Cell*, 93(5):827–839, May 1998.

[124] J. E. Durbin, R. Hackenmiller, M. C. Simon, and D. E. Levy. Targeted disruption of the mouse Stat1 gene results in compromised innate immunity to viral disease. *Cell*, 84(3):443–450, Feb 1996.

[125] M. A. Meraz, J. M. White, K. C. Sheehan, E. A. Bach, S. J. Rodig, A. S. Dighe, D. H. Kaplan, J. K. Riley, A. C. Greenlund, D. Campbell, K. Carver-Moore, R. N.

DuBois, R. Clark, M. Aguet, and R. D. Schreiber. Targeted disruption of the Stat1 gene in mice reveals unexpected physiologic specificity in the JAK-STAT signaling pathway. *Cell*, 84(3):431–442, Feb 1996.

[126] D. H. Kaplan, V. Shankaran, A. S. Dighe, E. Stockert, M. Aguet, L. J. Old, and R. D. Schreiber. Demonstration of an interferon gamma-dependent tumor surveillance system in immunocompetent mice. *Proc. Natl. Acad. Sci. U.S.A.*, 95(13): 7556–7561, Jun 1998.

[127] R. McKendry, J. John, D. Flavell, M. Muller, I. M. Kerr, and G. R. Stark. High-frequency mutagenesis of human cells and characterization of a mutant unresponsive to both alpha and gamma interferons. *Proc. Natl. Acad. Sci. U.S.A.*, 88(24):11455–11459, Dec 1991.

[128] D. Gagnon, S. Joubert, H. Senechal, A. Fradet-Turcotte, S. Torre, and J. Archambault. Proteasomal degradation of the papillomavirus E2 protein is inhibited by overexpression of bromodomain-containing protein 4. *J. Virol.*, 83(9):4127–4139, May 2009.

[129] G. Zheng, M. R. Schweiger, G. Martinez-Noel, L. Zheng, J. A. Smith, J. W. Harper, and P. M. Howley. Brd4 regulation of papillomavirus protein E2 stability. *J. Virol.*, 83(17):8683–8692, Sep 2009.

[130] A. Widschwendter, S. Tonko-Geymayer, T. Welte, G. Daxenbichler, C. Marth, and W. Doppler. Prognostic significance of signal transducer and activator of transcription 1 activation in breast cancer. *Clin. Cancer Res.*, 8(10):3065–3074, Oct 2002.

9 Publication record

1. **A. Wunderlich**, M. Hussong, M. Kerick, A. Fischer, B. Timmermann, H. Lehrach, and M. R. Schweiger. **Brd4 directly regulates interferon gamma signaling via STAT1.** 2012, in preparation.

2. M. Hussong (equally contributed), **A. Wunderlich** (equally contributed), M. Hirsch-Kauffmann, H. Lehrach, and M. R. Schweiger. **The bromodomain protein 4 regulates oxidative stress responses.** 2012, in preparation.

3. F. Bröcker, **A. Wunderlich**, M. R. Schweiger, H. Lehrach, and K. Mölling. **Comparative expression profiling of mutant and wildtype proto-oncogene c-Src.** 2012, in preparation.

4. C. Röhr, M. Kerick, A. Fischer, A. Kühn, K. Kashofer, B. Timmermann, T. Meinel, D. Drichel, S. T. Börno, A. Nowka, S. Krobitsch, T. Becker, **A. Wunderlich**, C. Barmeyer, C. Viertler, K. Zatloukal, C. Wierling, H. Lehrach, M. R. Schweiger. **Identification of miRNA-1 as tumor suppressor and modeling of its therapeutic functions.** Molecular Cancer Therapies, 2012, under review.

5. H. Bu, M. R. Schweiger, T. Manke, **A. Wunderlich**, B. Timmermann, M. Kerick, L. Pasqualini, E. Shehu , C. Fuchsberger, A. Cato, and H. Klocker. **Anterior gradient 2 and 3: two prototype androgen responsive genes transcriptionally upregulated by androgens and by estrogens in prostate cancer cells.** FEBSJ, 2012, accepted.

6. S. T. Börno, A. Fischer, M. Kerick, M. Falth, M. Laible, J. C. Brase, R. Kuner, A. Dahl, C. Grimm, B. Sayanjali, M. Isau, C. Röhr, **A. Wunderlich**, B. Timmermann, R. Claus, C. Plass, M. Graefen, R. Simon, F. Demichelis, M. A. Rubin, G. Sauter, T. Schlomm, H. Sultmann, H. Lehrach, and M. R. Schweiger. **Genome-wide DNA methylation events in TMPRSS2:ERG fusion negative prostate cancers implicate an EZH2 dependent mechanism with miRNA-26a hypermethylation.** Cancer Discovery, 2(11):1024-1035, 2012.

7. B. Timmermann, M. Kerick, C. Röhr, A. Fischer, M. Isau, S. T. Börno, **A. Wunderlich**, C. Barmeyer, P. Seemann, J. Koenig, M. Lappe, A. W. Kuss, M. Garshasbi, L. Bertram, K. Trappe, M. Werber, B. G. Herrmann, K. Zatloukal, H. Lehrach, and M. R. Schweiger. **Somatic mutation profiles of MSI and MSS colorectal cancer identified by whole exome next generation sequencing and bioinformatics analysis.** PLoS ONE, 5(12):e15661, 2010.

10 Curriculum vitae

Der Lebenslauf ist in der Online-Version aus Gründen des Datenschutzes nicht enthalten.

11 Acknowledgement

First of all, I would like to thank Prof. Dr. Hans Lehrach for having given me the opportunity to complete my PhD thesis in his department. In particular the multitude of technologies made my work feasible. I am also grateful to Prof. Dr. Rupert Mutzel who supported me throughout my whole time at the university, even in despite of his spare time. I owe the greatest gratitude to my supervisor Dr. Dr. Michal-Ruth Schweiger who made this venture happen and introduced me to an extraordinary interesting research field. She always believed in me, supported me and taught me independent scientific work. Furthermore, I specifically want to thank Dr. Bodo Lange and Dr. Sylvia Krobitsch as well as all the members of their work groups for the inspiring and fruitful collaborations. For their great work I also want to say thanks to the sequencing core facility around Dr. Bernd Timmermann.

Starting with the members of the lab, I am very thankful to Anna Kosiura for her excellent technical support in NGS-library preparation and Dr. Martin Kerick and Axel Fischer who provided the sequencing data in manageable form, even for a "wet-lab" scientist. Furthermore, I want to express my thanks to my student Michelle Hussong, with whom work became extremely enjoyable. Alongside, I also thank the rest of the members of the group, namely Christina Röhr, Melanie Isau, Nada Kumer and Dr. Stefan Börno as well as the entire "Schweiger brigade" for the pleasant working climate, the supportive discussions and courtesies as well as the numerous days with nice little chats and a lot of laughter.

To bring up Melanie Isau again, I am especially grateful to have such a good friend in and outside of work and who is always at my side since university. Additionally, I am thankful for all of my other dearest friends whose names would blast this acknowledgement but who know who they are. Last but not least I am more than happy to have my supporting and loving partner with me. You are just the best.

12 Abbreviations

°C degree centigrade

% percent

BDI bromodomain I

BDII bromodomain II

bp base pairs

Brd4 bromodomain containing protein 4

Brd4-long long isoform of Brd4

Brd4-short short isoform of Brd4

BSA bovine serum albumin

C cytosine

cDNA complementary DNA

ChIP Seq Chromatin immunoprecipitation sequencing

CO_2 carbon dioxide

CPDB ConsensusPathDB

CTD carboxy-terminal domain

Da dalton

DNA deoxyribonucleic acid

DMEM Dulbecco's Modified Eagle's Medium

dNTP deoxyribonucleotide

DPBS Dulbecco's phosphate buffered saline

ds double strand

E.coli *Escherichia coli*

ERBB2 v-erb-b2 erythroblastic leukemia viral oncogene homolog 2

ET extra terminal domain

FBS fetal bovine serum

FC fold change

G guanine

GAPDH glyceraldehyde-3-phosphate dehydrogenase

GFP green fluorescent protein

h hour

Hek293T human embryonic kidney cells

HPRT1 hypoxanthine guanine phosphoribosyl transferase

IFI6 interferon, alpha-inducible protein 6

IFITM1 interferon induced transmembrane protein 1

IFITM2 interferon induced transmembrane protein 2

IFITM3 interferon induced transmembrane protein 3

IFN interferon

IFNα interferon alpha

IFNβ interferon beta

IFNγ interferon gamma

IPA Ingenuity Pathway Analysis

IRF1 interferon regulatory factor 1

IRF7 interferon regulatory factor 9

ISG interferon stimulated gene

kb kilo base

kd knockdown

K- negative control

l liter

LB Luria Bertani

LGALS3BP lectin galactoside-binding soluble 3 binding protein

log2 logarithm to the base 2

M molar

mA milli ampere

MEM Modified Eagle's Medium

mg milli gram

min minute

mio million

ml milli liter

mM milli molar

mRNA messenger ribonucleic acid

mRNA Seq messenger ribonucleic acid sequencing

ng nano gram

NLS nuclear localization signal

nM nano molar

PARP10 poly (ADP-ribose) polymerase family member 10

PBS Phosphate buffered saline

PCR polymerase chain reaction

Pen/Strep penicillin and streptomycin

prom promoter fragment of a gene

qPCR quantitative polymerase chain reaction

RNA ribonucleic acid

rpm rounds per minute

RT room temperature

SDS sodium dodecyle sulfate

sec second

SEED serine/glutamine/asparagine-rich region

shGFP short hairpin RNA against GFP

shC2 short hairpin RNA against both Brd4 isoforms

shE1 short-hairpin RNA against the long Brd4 isoform

STAT1 signal transducer and activator of transcription 1

STAT2 signal transducer and activator of transcription 2

STAT3 signal transducer and activator of transcription 3

STDEV standard deviation error

T large T antigen

TAE Tris/glacial acetic acid/EDTA buffer

Taq thermostable DNA polymerase named after the bacterium *Thermus aquaticus*

TBS Tris buffered saline

TBST Tris buffered saline with Tween20

TE Tris/EDTA buffer

TSS transcription start site

TUBA tubulin alpha

U units

UV ultra violet light

V volt

v volume

w weight

µg micro gram

µl micro liter

µM micro molar

13 Supplement

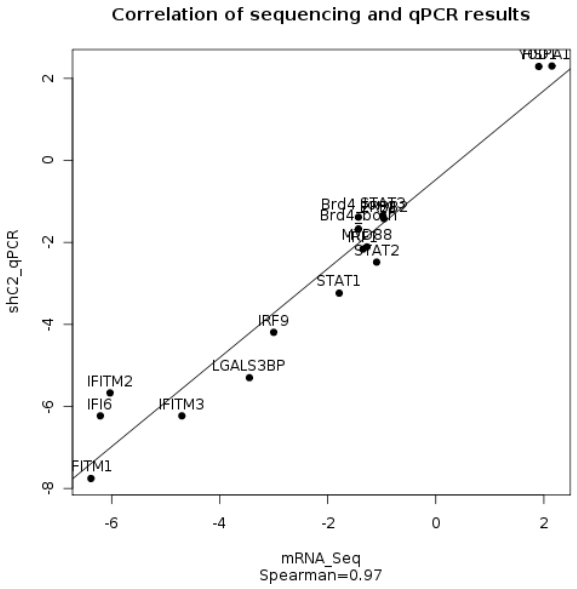

Figure 39: Spearman correlation of the mRNA Seq data and qPCR validations of selected STAT1 target genes. The Spearman correlation coefficient was calculated using the expression levels of selected STAT1 target genes, determined by qPCR, and the corresponding log2 fold changes in the mRNA Seq data.

Table 32: Downregulated Myc targets in the mRNA sequencing after Brd4 knockdown. Identification of downregulated Myc target genes in the mRNA sequencing after Brd4 knockdown.

downregulated Myc target genes after Brd4 knockdown						
ABCA2	BAMBI	CAMK2N2	DDAH2	EPB41L1	GNAI2	IGFBP5
ABHD14A	BCAM	CD151	DDR1	EPPK1	GPS2	IL17RC
ABHD14B	BCKDK	CELSR2	DERL3	ERBB2	GRINA	INPP5J
ABHD4	BCL7C	CIZ1	DHRS11	F11R	HAND1	IRF7
ABTB1	BLOC1S1	CNP	DHRS3	FABP3	HDAC3	IRF9
ACCN2	BMF	COL2A1	DLG4	FARP1	HDDC3	ISG15
ACP2	BTG2	COL6A1	DLGAP4	FCHSD1	HLA-B	ISOC2
AMOT	C14orf132	COPS7A	DLL1	FDXR	HOXC10	ISYNA1
ANO8	C16orf53	COQ10A	DLX4	FGFR2	HOXC4	JUP
APEH	C17orf61	CORO7	DNPEP	FGFRL1	HOXC6	KCNJ4
APH1B	C18orf56	CPT1B	DPF1	FHOD1	IDUA	KHK
ARAP1	C19orf22	CRAT	DPP3	FIBP	IFI6	KIAA0895L
ARMC6	C19orf50	CSDA	DPY30	FLT1	IFITM1	KIF17
ARRB2	C22orf40	CTF1	DTD1	G6PC3	IFITM2	LGALS1
ATG7	C5orf4	CUL9	EFNA3	GABARAP	IFITM3	LHPP
ATP13A2	C8orf82	CYB5R1	EIF4EBP1	GALK1	IGDCC3	LHX2
B4GALNT1	CALM3	CYBA	EML2	GDF11	IGF2	LTBP4

downregulated Myc target genes after Brd4 knockdown						
LYPD1	NCDN	PEX16	PORCN	SAMD10	SLC7A8	TMEM132A
MANEAL	NEFL	PFKFB4	PPOX	SEMA3F	SLITRK3	TMEM132E
MAPK3	NEO1	PFKL	PRDM16	SERPINH1	SMARCD1	TMEM145
MAPKAPK3	NMB	PFKP	PSME1	SEZ6L2	SMOC1	TRIM62
MATK	NME4	PGC	PTEN	SHISA5	SNORD15B	TTYH3
MDK	NR1D1	PIGT	PTGES2	SHKBP1	SREBF1	TYMS
MED12	NUDT22	PIK3R2	QARS	SIPA1	ST3GAL1	UCK2
MED16	NUDT8	PIP4K2C	RABEP2	SIRT2	STAT1	UNC93B1
MFAP2	NXPH4	PLCD3	RBCK1	SLC1A3	STAT3	USP11
MFSD10	OGDH	PLK3	REC8	SLC1A5	SYNGR3	VAMP1
MFSD3	OGG1	PLOD1	REEP6	SLC25A1	SYP	VEGFB
MKNK1	PABPC4	PLP2	RELL2	SLC25A11	TAPBP	WNK2
MOSPD3	PACS1	PLSCR3	RMRP	SLC25A23	TBC1D10A	ZMIZ2
MOV10	PARP10	PMF1	RNF208	SLC26A6	TCTA	ZNF358
MTG1	PATZ1	PNPLA2	ROBO3	SLC27A3	TFAP2C	ZNF385A
MXI1	PBXIP1	POLD2	ROGDI	SLC2A8	TGFB1	ZNF76
MYH9	PDK2	POLR2I	RTN2	SLC35F1	TGFB1I1	ZNF784
NAT6	PDLIM7	POLR2J2	RUSC1	SLC5A6	TM7SF2	

Table 33: Upregulated Myc targets in the mRNA sequencing after Brd4 knockdown. Identification of upregulated Myc target genes in the mRNA sequencing after Brd4 knockdown.

upregulated Myc target genes after Brd4 knockdown						
ADAM9	CHSY3	HERPUD1	MFSD1	PRPF38B	SCML1	UROS
APOLD1	CPEB1	HMGCS1	MGEA5	PRTFDC1	SEC23IP	USP38
ARFGEF2	CTH	HSPA4	MIS12	PSD3	SEC63	USP9X
ARHGAP4	CYP2E1	IFT57	MTF1	PTPN11	SLC38A2	VCPIP1
ARL5B	DIDO1	IPO7	MTX3	RAB11FIP2	SNX18	VKORC1L1
ARRDC4	E2F6	ITGA6	NHLRC2	RAB21	SOAT1	WDR36
ATP2C1	ELOVL4	KBTBD2	NUCB2	RFK	STAG2	XPO1
ATP6V1A	FBXO33	KBTBD8	NUFIP2	RHBDF1	SUPT16H	XPOT
AURKA	FMR1	KIF5B	OGT	RINT1	SYT11	YJEFN3
BNIP2	FOS	KIF5C	OTUD1	RNF103	TBCEL	ZBTB10
C10orf46	FOXD4L1	LIN28B	PAPD5	RNF6	TBK1	
C1GALT1	G3BP2	LRP2	PIBF1	RPIA	TRIB3	
C5orf41	GALNT4	LRPPRC	PLEKHA3	RPL27A	TROVE2	
C5orf51	GCLC	LTV1	POLR1B	RSPRY1	TTC33	
CCND2	GLO1	LYSMD1	PPP1R15B	SAMD8	TWISTNB	
CCNG2	GLS	MEX3C	PPWD1	SAR1B	UBA6	

Table 34: Downregulated STAT1 target genes in the mRNA Seq after Brd4 knockdown. Identification of downregulated STAT1 target genes in the mRNA sequencing after Brd4 knockdown.

downregulated STAT1 target genes after Brd4 knockdown						
ABHD14B	COL4A2	FGFR2	IRAK2	MUSTN1	PNPLA2	STAT1
ACP2	COQ10A	FGFRL1	IRF1	MXI1	POLR2I	STAT3
AGRN	CORO7	FHOD1	IRF7	MYD88	PPOX	SYNGR3
ALDH16A1	CPT1B	FIBP	IRF9	NCDN	PRR14	SYP
AMOT	CRAT	FLT1	ISG15	NEO1	PSME1	TAP1
ANO8	CTF1	FZD10	ISOC2	NMB	PTEN	TAPBP
APEH	CTNNBIP1	G6PC3	ITGA3	NPNT	RABEP2	TCTA
ARAP1	CUL9	G6PD	ITGA5	NR1D1	RBCK1	TFAP2C
ARHGAP10	CYB5R1	GABARAP	ITIH4	NUDT22	REC8	TGFB1I1
ARPC1B	DAP	GANAB	KCNC4	NXPH4	RMRP	TM7SF2
ATG7	DDAH2	GCAT	KCNJ4	OGG1	ROBO3	TMEM132A
ATP13A2	DDR1	GDF11	KHK	PACS1	ROGDI	TMEM145
B2M	DHRS3	GNAI2	KIAA0895L	PACSIN3	RTN2	TP53I11
B4GALNT1	DLG4	GP1BB	LGALS1	PARP9	SAMD10	TSHZ2
BAMBI	DLGAP4	GPR124	LHFP	PATZ1	SELENBP1	TYK2
BCKDK	DLL1	GPR137	LHX2	PBXIP1	SEMA3F	UBE2L6
BCL7C	DLX4	GPS2	LLGL2	PCBD1	SERPINH1	UCK2
BLOC1S1	DNPEP	HAND1	LPCAT3	PDK2	SEZ6L2	UNC93B1
BMF	DPF1	HDAC6	LRCH3	PDLIM7	SHISA5	USP11
BTG2	DTD1	HDDC3	LTBP4	PEX19	SHKBP1	USP18
C16orf53	DTX3L	HOXB13	LYPD1	PFKP	SIPA1	WDR54
C17orf61	ECE1	HOXC10	MAPKAPK3	PGC	SLC1A5	WDR54
C19orf50	EFHD1	HOXC4	MAST3	PIGT	SLC25A11	ZDHHC12
C22orf40	EIF2AK2	HOXC6	MDK	PIK3R2	SLC25A23	ZMIZ2
C9orf16	EPB41L1	IFI6	MED12	PIP4K2C	SLC26A6	ZNF385A
CALM3	EPPK1	IFIT5	MFAP2	PLCD3	SLC35F1	ZNF76
CAMK2N2	ERBB2	IFITM1	MKNK1	PLD2	SLC5A6	ZNF784
CD151	EXOSC1	IFITM2	MKNK2	PLK3	SLITRK3	
CDK2AP1	FABP3	IFITM3	MMP15	PLP2	SMARCD1	
CERCAM	FAM125A	IGDCC3	MOSPD3	PLSCR1	SNX15	
CNP	FBLIM1	IGF2	MOV10	PLSCR3	SREBF1	
COL2A1	FDXR	INPP5J	MPI	PML	ST3GAL1	

Table 35: Upregulated STAT1 target genes in the mRNA Seq after Brd4 knockdown. Identification of upregulated STAT1 target genes in the mRNA sequencing after Brd4 knockdown.

upregulated STAT1 target genes after Brd4 knockdown						
ADAM9	APOLD1	ATP2C1	BICC1	C13orf23	CBX6	CCND2
ALKBH8	ARID2	ATP6V1A	C10orf137	C5orf28	CCDC132	CCT8
ANKRD1	ARMC9	BET1	C11orf58	C5orf41	CCNC	CHSY3

upregulated STAT1 target genes after Brd4 knockdown						
COQ10B	GLS	LRP2	POLR1B	RSPRY1	TMEM33	WDR35
CYLD	HSP90B1	LRPPRC	POLR2B	SCML1	TROVE2	WDR36
CYP2E1	HSPA13	LYSMD1	PPP1R15B	SEC23IP	TRUB1	XPO1
DIDO1	HSPA4	MRS2	PPP2R1B	SLC30A1	TTC33	YJEFN3
FAM171B	HSPA7	MTF1	PRPF38B	SLC30A7	TWISTNB	YOD1
FAM46C	IBTK	MTRR	PTCD3	SLC38A1	UBA6	ZBTB37
FAM91A1	IFT57	NHLRC2	QPCT	SMCR7L	UGCG	ZDHHC20
FOS	KAT2B	NUPL1	RHBDF1	SOAT1	UHMK1	ZNF277
FRS2	KBTBD2	OSBPL11	RNF11	STX16	USP33	ZNF420
FZD6	KBTBD8	PDE12	RNF6	SUMF1	USP9X	ZNF800
GEN1	KRBA1	PHF6	RPIA	SUPT16H	VCPIP1	
GLO1	LRP12	PIBF1	RRAGD	TCAP	VEZT	

Table 36: Identification of overlapping target genes in two Brd4-long ChIP sequencings. Identification of target genes present in two endogenous Brd4-long ChIP sequencings, disregarding promoter or exon binding.

overlapping genes of two Brd4-long ChIP Seqs					
AC002310.7	ARHGDIA	CTA-286B10.7	GABPB2	HIST2H2AA3	HSPA8
AC006486.1	ARID1B	CTD-2184C24.2	GNB1L	HIST2H2AA4	IGFBP5
AC007383.3	ATF4	CTD-2201E18.3	GTF2A1	HIST2H2AB	IMPACT
AC007563.5	B4GALT6	DACH1	GTF2I	HIST2H2AC	INO80D
AC084018.1	BCLAF1	DDX3X	HCG14	HIST2H2BC	JUN
AC090421.1	BOLA1	DDX6	HIAT1	HIST2H2BD	KB-1995A5.13
AC091609.1	BRD2	DGCR8	HIATL2	HIST2H2BE	KIAA0368
AC091736.5	BRD4	DICER1	HIST1H1C	HIST2H3A	LIN9
AC092171.2	BRWD1	DIS3L	HIST1H1E	HIST2H4A	LUC7L2
AC136007.2	C10orf95	DLX2	HIST1H2AG	HIST2H4B	MALAT1
ACAD9	C12orf61	DNAJB12	HIST1H2AH	HNRNPD	MAT2A
ADSS	C20orf72	DOCK3	HIST1H2AK	HNRNPH1	MAZ
AGBL3	C22orf13	EGLN1	HIST1H2AM	HNRNPH3	MCM5
AK2	C22orf29	EIF4G2	HIST1H2BJ	HNRNPUL1	MDM2
AKAP7	CAMK2D	EWSR1	HIST1H2BK	HOTAIR	MIR1292
AL034548.2	CCNL1	FAIM	HIST1H2BN	HOXA10	MIR1469
AL121928.1	CDC25A	FAM35B2	HIST1H2BO	HOXA11	MIR148A
AL136040.2	CDC42BPA	FAM36A	HIST1H3B	HOXA11-AS1	MSH5
AL356017.3	CDKN1B	FBXL17	HIST1H3J	HOXA4	MTAP
AMD1	CIRBP	FBXW4	HIST1H4C	HOXB8	MTF2
ANP32B	CLIC1	FOXC1	HIST1H4E	HOXC4	NAPEPLD
APOLD1	CPSF6	FOXP2	HIST1H4K	HOXD11	NCOA7

overlapping genes of two Brd4-long ChIP Seqs					
NCRNA00245	PTPRG	RP11-501C14.5	SATB2	TARS2	ZC3H4
NCRNA00257	PUM1	RP11-527N22.1	SENP6	TFAP2A	ZC3H6
NDUFS7	RASEF	RP11-575L16.2	SERBP1	TMBIM4	ZCCHC3
NFIA	RBM25	RP11-59H1.3	SETD2	TNRC18	ZIC5
NOP56	RBM39	RP11-631N16.2	SLC25A21	TOB2	ZNF398
NR2F1	REPIN1	RP11-685M7.3	SLITRK5	TP53BP2	ZNF503
NR2F2	RHBDD3	RP1-170O19.2	SNRPB	TUT1	ZNF518A
NUF2	RNF125	RP11-864I4.1	SNRPD3	U2	ZNF688
PARP1	RNU1-1	RP1-290C9.2	SNX5	UBE2E1	ZNF689
PHIP	RNU1-4	RP1-290I10.3	SOX4	UBE2R2	ZNF76
PIGL	RNU1-8	RP1-315G1.3	SRCAP	USP24	ZNF775
PPM1A	RP11-150O12.2	RP4-794H19.2	SRSF1	WASH1	ZNF839
PRDM15	RP11-267N12.3	RPL3	SRSF4	WDR34	
PRDM5	RP11-316M1.11	RPTOR	STAG2	YARS	
PRKCE	RP11-347I19.3	RSBN1L	SUV420H1	YTHDF2	
PTMA	RP11-357H14.7	S100PBP	TARBP1	YWHAE	

Table 37: Identification of target genes in two endogenous and one overexpressed Brd4-long ChIP Seqs. Identification of target genes present in all three Brd4-long ChIP sequencings.

overlapping genes of three Brd4-long ChIP Seqs						
AC006486.1	CDC25A	GTF2I	HIST2H2BE	LIN9	RHBDD3	TP53BP2
ACAD9	CDKN1B	HIAT1	HIST2H4A	MAZ	RNF125	UBE2R2
ADSS	CLIC1	HIATL2	HIST2H4B	MCM5	RPL3	USP24
AK2	DDX3X	HIST1H1C	HNRNPH1	MSH5	RSBN1L	WASH1
AMD1	DGCR8	HIST1H1E	HNRNPH3	MTF2	S100PBP	WDR34
ARHGDIA	DICER1	HIST1H2AG	HNRNPUL1	NAPEPLD	SENP6	YARS
ARID1B	DIS3L	HIST1H2AH	HOXA10	NR2F1	SERBP1	YTHDF2
B4GALT6	DOCK3	HIST1H2AK	HOXA11	NR2F2	SNRPB	ZC3H4
BCLAF1	EWSR1	HIST1H2AM	HOXA4	NUF2	SNRPD3	ZNF398
BOLA1	FAM36A	HIST1H2BJ	HOXB8	PARP1	SOX4	ZNF503
BRD2	FBXW4	HIST1H2BN	HOXC4	PHIP	SRCAP	ZNF689
BRD4	FOXC1	HIST1H3B	HOXD11	PIGL	TARBP1	ZNF76
C10orf95	FOXP2	HIST1H4E	IGFBP5	PTMA	TARS2	ZNF839
C22orf29	GABPB2	HIST2H2AB	IMPACT	PUM1	TFAP2A	
CCNL1	GNB1L	HIST2H2AC	JUN	RBM39	TOB2	

Table 38: Identification of downregulated direct Brd4-long target genes. Identification of downregulated Brd4-long target genes in the mRNA Seq after Brd4 knockdown with a binding site in the ChIP Seqs.

downregulated Brd4-long target genes						
5_8S_rRNA	ARL2	DDR1	IGFBP5	PPAP2B	SNX15	ZNF358
5S_rRNA	BLOC1S1	DHRS3	MANEAL	PRSS30P	STAT1	ZNF76
AC005522.1	BRD4	ERBB2	MAPK3	RMRP	STAT3	
AC009108.1	C11orf51	HDAC6	MAPKAPK3	RP11-527N22.1	TMEM143	
ALDH4A1	CIZ1	HOXC10	MFSD1	SAMD11	TRMT11	
AP2A1	COPS7A	HOXC4	MFSD3	SH3GLB2	UCK2	
APEH	DCAF6	HOXC6	PGPEP1	SLC25A11	WDR34	

Table 39: Identification of direct upregulated Brd4-long target genes. Identification of upregulated Brd4-long target genes in the mRNA Seq after Brd4 knockdown with a binding site in the ChIP Seqs.

upregulated Brd4-long target genes						
ABHD5	BROX	CWC27	MED21	RP13-15E13.1	SLC7A11	XPO1
APOLD1	C10orf137	E2F6	MIER3	SAR1B	SSFA2	Y_RNA
ARFGEF2	C5orf28	EXOC8	NAA50	SEC63	STAG2	ZBTB43
ARID2	C5orf51	GLS	NOP58	SENP6	STX16	ZMYM1
ARPP19	C9orf5	GOLPH3	NUCB2	SLC19A2	SUMF1	
ATP6V1A	CBX6	IPO7	PHF6	SLC38A1	TBC1D23	
AURKA	CD46	LCOR	POLR1B	SLC38A2	UBA5	
B3GNT5	CKAP5	LRP2	PRPF38B	SLC3A2	WDR37	